

Doctoral Dissertation

**A STUDY ON THE APPLICATION OF WATER-FILM-FORMING-UNIT (WFFU)  
IN ENHANCING CARBON DIOXIDE REMOVAL EFFECTIVENESS USING  
WATER ABSORPTION METHOD**

(水を吸収媒体に用いた二酸化炭素除去プロセスへの液膜形成装置 (WFFU) の導入によるその効率向上に関する研究)

NGUYEN KIM DIEM MAI

Division of Environmental Science and Engineering

Graduate School of Science and Engineering

Yamaguchi University, Japan

September 2018

博士論文

Doctoral Dissertation

**A STUDY ON THE APPLICATION OF WATER-FILM-FORMING-UNIT (WFFU)  
IN ENHANCING CARBON DIOXIDE REMOVAL EFFECTIVENESS USING  
WATER ABSORPTION METHOD**

(水を吸収媒体に用いた二酸化炭素除去プロセスへの液膜形成装置 (WFFU) の導入によるその効率向上に関する研究)

NGUYEN KIM DIEM MAI

A dissertation submitted to the Division of Environmental Science and Engineering of Yamaguchi University in partial fulfillment of the requirements for the degree of Doctor of Engineering (Dr. Eng.)

Advisor: Professor Dr. Tsuyoshi IMAI  
Division of Environmental Engineering,  
Graduate School of Science and Technology for Innovation,  
Yamaguchi University

Committee Members:

Professor Dr. Tsuyoshi IMAI  
Professor Dr. Masahiko SEKINE  
Professor Dr. Masakazu NIINAE  
Professor Dr. Takashi SAEKI  
Professor Dr. Takaya HIGUCHI

山口大学大学院理工学研究科環境共生系専攻  
Division of Environmental Science and Engineering  
Graduate School of Science and Engineering  
Yamaguchi University, Japan

## ABSTRACT

With increased global attention on the greenhouse effect and climate change, identifying an effective and economical solution to control the release of greenhouses gases, especially carbon dioxide (CO<sub>2</sub>), into the atmosphere has been the subject of much research. Because it does not use chemicals or produce toxic byproducts, water scrubbing is an environmentally friendly method of absorbing CO<sub>2</sub> from exhaust gas and therefore provides a promising means of controlling emissions of CO<sub>2</sub>. However, the great limitation of this method is a low interaction between CO<sub>2</sub> and water, resulting in a low degree of removal and a high-pressure (1.0 to 2.0 MPa) operating requirement. In this study, I employed an apparatus outfitted with one or several water-film-forming-units (WFFU) which can produce a large number of water-films along with fine bubbles to promote the mass transfer and contact between the gas and liquid phases and improve the effectiveness of water scrubbing.

The doctoral dissertation included 6 chapters and its content was presented as the following.

**Chapter 1** introduced the background, the objectives of this study and the structure of the doctoral dissertation.

The literature review related to this research and the summary of the previous study on the CO<sub>2</sub> removal technology were presented in **Chapter 2**.

In **Chapter 3**, the performance of an apparatus outfitted with a water-film generator in removing CO<sub>2</sub> from different concentrations of mixed gases (containing CO<sub>2</sub> and N<sub>2</sub>) while tap water as a physical solvent to absorb CO<sub>2</sub> was assessed through the obtained results of removal efficiency and absorption rate under various conditions of key factors including internal pressure, gas supplying pressure, temperature, gas-to-liquid ratio (G/L), and initial CO<sub>2</sub> content. The internal pressure in the absorption tank and CO<sub>2</sub> initial content, have a significantly direct effect whereas temperature shows an inverse effect on the CO<sub>2</sub> removal efficiency and its absorption rate in water. The results also prove that the good performance of CO<sub>2</sub> removal process can be seen at the low gas supplying pressure of 0.30 MPa. The low value of G/L can increase the removal efficiency but it prevents the economic aspect due to a decrease of CO<sub>2</sub> absorption rate. On varying the experimental conditions – internal pressure (0.06 and 0.10 MPa), gas supplying pressure (0.30 – 0.70 MPa), temperature (10 °C – 30 °C), G/L (0.36

– 1.79), and initial CO<sub>2</sub> content (10% – 100%) – the CO<sub>2</sub> removal ability and absorption rate varied from 22.9% to 90.0% and  $4.5 \times 10^{-4}$  to  $44.5 \times 10^{-4}$  mol s<sup>-1</sup>L<sup>-1</sup>, respectively. For instance, the removal and absorption rates reached approximately 90.0% and  $12.0 \times 10^{-4}$  mol s<sup>-1</sup>L<sup>-1</sup>, respectively, when the experiment was operated at 10°C and 0.30 MPa of gas supplying pressure with 35% CO<sub>2</sub> inlet gas content and 0.71 G/L.

**Chapter 4** discussed about the application of statistical tools in assessing the performance of CO<sub>2</sub> removal process using the advanced water absorption apparatus. The influence of various parameters—pressure, initial CO<sub>2</sub> concentration, G/L, and temperature—on the CO<sub>2</sub> removal efficiency and its absorption rate in water were investigated and estimated thoroughly by statistical polynomial models obtained by the utilization of the response surface method (RSM) with a central composite design (CCD). Based on the analysis of experimental matrix containing 31 trials, a high efficiency of CO<sub>2</sub> capture can be reached in conditions such as low pressure, high CO<sub>2</sub> concentration at the inlet, low gas/liquid ratio, and low temperature. Furthermore, the coefficients of determination,  $R^2$ , were 0.996 for the removal rate and 0.982 for the absorption rate, implying that the predicted values computed by the constructed models correlate strongly and fit well with the experimental values. It evidences that the models can be used as useful tools to predict the CO<sub>2</sub> removal efficiency and absorption rate accurately without carrying out a large number of experiments. Therefore, the utilization of RSM-CCD can provide several benefits such as time saving, reducing of experimental trials and availability for observing the interactions among factors.

As discussed above, the advanced apparatus equipped with one WFFU support for the CO<sub>2</sub> removal performance at low pressure but it still remains the limitation due to the low removal rate under high load of feed gas (low absorption rate at high G/L). So as to assess comprehensively the effect and the benefits of using WFFU in improving CO<sub>2</sub> removal process, I carried out the comparison of the values of CO<sub>2</sub> removal and absorption rate which obtained when conducting experiments in the apparatus equipped with non-, one- and two-WFFUs. The results and discussions for this matter was shown in **Chapter 5**. Based on our results, the WFFU significantly improves CO<sub>2</sub> capture at 0.30 MPa in a water absorption system with two WFFUs. The CO<sub>2</sub> removal rate was 20% greater than for conventional systems without WFFUs. Moreover, statistical data attained by the Taguchi analysis method showed that the

number of WFFUs used in the absorption system has the greatest influence on CO<sub>2</sub> removal efficiency (contribution percentage = 50.65%) compared to gas supplying pressure, initial CO<sub>2</sub> concentration, G/L, and liquid temperature. I also thoroughly investigated the effects of these factors on CO<sub>2</sub> removal performance in the apparatus linked with non- , one- and two-WFFUs. The optimum conditions for CO<sub>2</sub> removal efficiency in a system equipped with two WFFUs are: low temperature, a G/L of 0.71, a gas supplying pressure of 0.30 MPa, and a high inlet CO<sub>2</sub> concentration. Therefore, our research improves on the physical absorption method for removing CO<sub>2</sub> from exhaust gas using tap water, thereby introducing a promising new technology for controlling carbon dioxide emissions in a more environmentally friendly manner.

Finally, **Chapter 6** summarized the findings of this research including the CO<sub>2</sub> removal performance when using WFFU in enhancing the water absorption process, the optimum removal conditions and the benefits of WFFU in the improvement of water absorption method. In this chapter, the suggestions for the further work was revealed.

## 学位論文要旨

近年、温室効果ガスやそれによる気候変動などが世界的に注目される中、効果的で低コストな温室効果ガス、とりわけ二酸化炭素のコントロール手法の開発が望まれ、多くの研究がなされている。化学薬品を用いないこと、有害な副産物を生じないこと等から、水を吸収媒体に用いた二酸化炭素除去プロセスが環境配慮型の二酸化炭素排出制御方法として注目されている。しかしながら、この方法にはまだいくつかの克服すべき大きな課題がある。すなわち、二酸化炭素と水との接触時間（あるいは接触面積）が小さく低い二酸化炭素除去率しか得られていないこと、及び比較的高い装置内圧力（1~2MPa）が必要であることである。本研究では、多数の液膜（水の泡）とファインバブルを同時に形成可能で水中の気体交換効率を加速することが期待できる液膜形成装置を1つないし複数組み込んだ二酸化炭素除去プロセスの開発を行う。

本博士論文は6章で構成されており、その内容は以下の通りである。

第1章では、本研究の背景と目的、本論文の構成について述べている。

第2章では、二酸化炭素除去技術に関する従来の研究についてまとめている。

第3章では、液膜形成装置を組み込んだ二酸化炭素除去プロセスの性能評価（二酸化炭素除去率及び二酸化炭素吸収速度について）を行った。本章では二酸化炭素含有率を変化させた混合ガス（二酸化炭素と窒素）を対象に、二酸化炭素の吸収媒体として水を用いた。具体的には、ガス供給圧力、水温、気液比、二酸化炭素含有率を影響因子として、液膜形成装置を組み込んだ二酸化炭素除去プロセスを用いた水への二酸化炭素溶解によるその除去効率及び吸収速度に関する検討を行った。実験結果より、ガス供給圧力及び二酸化炭素含有率が二酸化炭素除去効率に大きな影響を与えることが明らかとなった。一方で、水温はマイナスの影響を与えることが明らかとなった。ガス供給圧力が0.3MPaの場合に高い二酸化炭素除去効率を得られた。変化させたパラメータは、装置内圧力（0.06, 0.1MPa）、ガス供給圧力（0.30-0.70MPa）、水温（10-30℃）、気液比（0.36-1.79）、二酸化炭素含有量（10-100%）であり、二酸化炭素除去効率は22.9-90.0%、二酸化炭素吸収速度は $4.5 \times 10^{-4}$ —44.5

$\times 10^{-4} \text{ mol s}^{-1} \text{ L}^{-1}$ の間で変化した。最適条件は、水温  $10^{\circ}\text{C}$ 、ガス供給圧力  $0.3\text{MPa}$ 、二酸化炭素含有量  $35\%$ 、気液比  $0.71$  の場合に二酸化炭素除去効率が  $90\%$ 、二酸化炭素吸収速度は  $12.4 \times 10^{-4} \text{ mol s}^{-1} \text{ L}^{-1}$  であった。本プロセスの適用により従来よりもかなり低い圧力下で二酸化炭素の高効率な除去効果が得られた。

第4章では、統計的な手法（Response Surface Method: RSM + Central Composite Design: CCD）を用いて、ガス供給圧力、二酸化炭素含有率、気液比、水温が本プロセスによる二酸化炭素除去効率及び二酸化炭素吸収速度に与える影響について解析を行った。この解析結果から様々な条件下で二酸化炭素除去効率及び二酸化炭素吸収速度を予測できるモデルの構築を行った。31の実験条件を変化させた実験結果を解析した結果、ガス供給圧力は低めで、高い二酸化炭素含有率、低い気液比の場合に高い二酸化炭素除去率が得られることが明らかとなった。さらに、決定係数  $R^2$  値は二酸化炭素除去率に関して  $0.996$ 、二酸化炭素吸収速度に関して  $0.982$  と高い値が得られ、この統計的な手法を用いて得られたモデル式による予測値は実測値をよく再現していることが示された。したがって、このモデル式を用いて様々な予測を行うことができ、その有用性が示された。

第5章では、これまでの章で本プロセスの有用性を示したが、本プロセスの実用化を見据えたスケールアップ時における液膜形成装置の数を増やした場合の効果について検討した。特に本装置の高負荷運転（気液比が高い状態）時における二酸化炭素除去効率の改善について、液膜形成装置の数を  $0$ 、 $1$ 、 $2$  個と変化させた実験を行い、二酸化炭素除去効率に及ぼす影響を検討した。実験結果（ガス供給圧力  $0.3\text{MPa}$ ）から、液膜形成装置の数を増やすことで  $\text{CO}_2$  除去効率が大きく改善する（ $20\%$ 向上）ことが示された。さらに、TAGUCHI METHOD による統計学的解析の結果、ガス供給圧力、二酸化炭素含有率、気液比、水温に比較して、液膜形成装置の数が二酸化炭素除去効率と二酸化炭素吸収速度に顕著（貢献率  $50.65\%$ ）に影響することが示された。したがって、液膜形成装置を  $2$  個設置した場合の最適運転条件は、水温は低く、気液比が  $0.71$ 、ガス供給圧力が  $0.3\text{MPa}$ 、高い二酸化炭素含有率であることが明らかとなった。

第6章では，以上をまとめて，液膜形成装置を組み込んだ二酸化炭素除去プロセスで，水を二酸化炭素の吸収媒体とした場合の装置の最適運転条件を把握し，本法の有用性を示すことができたものと結論し，今後の展望について述べた．



## ACKNOWLEDGEMENTS

First and foremost, I would like to express my sincere thanks to my supervisor Prof. Dr. Tsuyoshi Imai for giving me an opportunity to be his doctoral student. Without his guidance and persistent motivation in ups and down, this dissertation would not have been completed. I extremely appreciate for his kindness, immense knowledge, valuable supervision, supports and encouragement throughout three and a half year that I have studied in Japan.

This dissertation would not have been finished without the supports of the Ministry of Education, Culture, Sports and Technology, Japan (MEXT) (Monbukagakusho Scholarship).

I would like to express my gratitude to the members of my graduate committee, Professor Dr. Tsuyoshi Imai, Professor Dr. Masahiko Sekine, Professor Dr. Masakazu Niinae, Professor Dr. Takashi Saeki, and Professor Dr. Takaya Higuchi, for their expert, constructive and helpful suggestions for improving my dissertation.

It is a great honor for me to express my sincere gratitude to academic staffs in Graduate School of Sciences and Technology for Innovation, Yamaguchi University: Prof. Dr. Masahiko Sekine, Prof. Dr. Takaya Higuchi, Prof. Dr. Koichi Yamamoto, Prof. Dr. Ariyo Kanno and Ms. Toshimi Yamamoto for their expert suggestions and constructive criticism which can improve my research.

Sincere thanks and appreciation are also expressed to members of EISEI laboratory for their helps and warm friendship. Special thanks to Shahira Aly, F. Mella, Y.P. Devia, A. Rivai, D.T.T. Loc, D.T.T. Uyen, J. Wang, G. Yudha, S. Riza, T. Dyah, S. Nishihara, K. Tsukihara, W. Yoshida, Y. Torigoe and other friends for their helps, encouragement and great friendship.

Last, but certainly not least, I would like to express my deepest, sincere and heartfelt gratitude to my beloved parents, brother and sister for their great love, utmost support and encouragement. Their love would always be my great motivation, inspiration and spiritual support throughout of my life.

*Nguyen Kim Diem Mai*

# CONTENT

ABSTRACT .....	i
學位論文要旨 .....	iv
ACKNOWLEDGEMENTS .....	vii
CONTENT.....	viii
LIST OF FIGURES .....	xii
LIST OF TABLES .....	xv
LIST OF ABBREVIATIONS .....	xvi
CHAPTER 1 INTRODUCTION.....	1
1.1 Background and problem statement.....	1
1.2 Dissertation objectives .....	4
1.3 Structure of dissertation .....	5
1.4 References .....	6
CHAPTER 2 LITERATURE REVIEW.....	9
2.1 Environmental issues of greenhouse gases and carbon dioxide .....	9
2.1.1 Global emissions of greenhouse gases and carbon dioxide.....	9
2.2 Carbon dioxide capture and storage (CCS).....	14
2.2.1 Overview of Carbon capture and Storage.....	14
2.2.2 Capture technologies .....	16
2.2.3 CO <sub>2</sub> separation techniques.....	18
2.2.3.1 Absorption.....	18
2.2.3.2 Water scrubbing .....	20
2.2.3.3 Adsorption.....	21
2.2.3.4 Cryogenic distillation.....	23
2.2.3.5 Membrane .....	24
2.2.4 CO <sub>2</sub> transport .....	24
2.2.5 CO <sub>2</sub> storage .....	25
2.2.6 CO <sub>2</sub> utilization .....	26
2.2.6.1 Direct utilization of CO <sub>2</sub> .....	27

2.2.6.2	Conversion of CO <sub>2</sub> into chemicals and fuels .....	27
2.2.6.3	Mineral carbonation .....	27
2.2.6.4	Enhanced oil and coal-bed methane recovery .....	28
2.2.6.5	Microalgae.....	28
2.3	Potential application of microbubble and liquid/water-film in the removal of carbon dioxide using water scrubbing.....	29
2.3.1	Characteristics of microbubble .....	29
2.3.2	Characteristics of liquid-film.....	32
2.3.3	Water scrubbing advanced with the generation of microbubble and liquid-film/water-film in the removal of carbon dioxide .....	34
2.4	References .....	35
CHAPTER 3 PERFORMANCE OF A CARBON DIOXIDE REMOVAL PROCESS USING A WATER SCRUBBER WITH THE AID OF A WATER-FILM-FORMING-UNIT.....		
		45
3.1	Introduction .....	45
3.2	Materials and Methods.....	48
3.3	Results and Discussion.....	51
3.3.1	Effect of internal pressure in the absorption tank.....	51
3.3.2	Effect of inlet gas supplying pressure.....	52
3.3.3	Effect of gas-to-liquid ratio .....	54
3.3.4	Effect of CO <sub>2</sub> partial pressure and initial CO <sub>2</sub> concentration .....	55
3.3.5	Effect of temperature .....	57
3.4	Conclusions .....	59
3.5	References .....	60
CHAPTER 4 RESPONSE SURFACE METHOD FOR MODELING THE REMOVAL OF CARBON DIOXIDE FROM A SIMULATED GAS USING WATER ABSORPTION ENHANCED WITH A WATER-FILM-FORMING-UNIT.....		
		63
4.1	Introduction .....	63
4.2	Materials, experimental apparatus and methods .....	65
4.2.1	Materials and experimental apparatus .....	65

4.2.2	Plackett–Burman design .....	66
4.2.3	Response surface method (RSM) .....	68
4.3	Results and discussion.....	69
4.3.1	Screening key factors affecting the removal of CO <sub>2</sub> using tap water as the absorbent.....	69
4.3.2	Effect of operating factors on the removal of CO <sub>2</sub> using tap water as the absorbent.....	73
4.3.3	Evaluation of the models and experiment .....	79
4.4	Conclusions .....	85
4.5	References .....	86
CHAPTER 5 INFLUENCE OF WATER-FILM-FORMING-UNIT ON THE ENHANCED REMOVAL OF CARBON DIOXIDE FROM MIXED GAS USING WATER ABSORPTION APPARATUS .....		89
5.1	Introduction .....	89
5.2	Materials and Methods .....	91
5.2.1	Experimental setup and methods .....	91
5.2.2	Taguchi analysis method .....	93
5.3	Results and Discussion.....	96
5.3.1	Effect of water-film-forming-unit (WFFU).....	96
5.3.2	Effect of inlet gas supplying pressure.....	98
5.3.3	Effect of CO <sub>2</sub> initial concentration .....	99
5.3.4	Effect of gas-to-liquid ratio .....	101
5.3.5	Effect of temperature .....	102
5.3.6	Taguchi method results.....	103
5.4	Conclusions .....	108
5.5	References .....	108
CHAPTER 6 CONCLUSIONS AND FUTURE WORKS .....		111
6.1	Conclusions .....	111
6.1.1	Performance of CO <sub>2</sub> removal process using a water scrubber enhanced with a WFFU .....	111

6.1.2	Response surface method (RSM) with central composite design (CCD) for modeling the removal of carbon dioxide using water absorption enhanced with a WFFU .....	112
6.1.3	Influence of WFFU on the enhanced removal of carbon dioxide from mixed gas using water absorption apparatus .....	113
6.2	Future works.....	114
	LIST OF PUBLICATIONS AND PRESENTATIONS .....	115

## LIST OF FIGURES

<b>Figure 2.1</b>	Radiative forcing estimates in 2011 relative to 1750 and aggregated uncertainties for the main drivers of climate change.....	10
<b>Figure 2.2</b>	Global greenhouse gas emissions, per country and region.....	11
<b>Figure 2.3</b>	Total anthropogenic GHG emissions (GtCO <sub>2</sub> eq/yr) by economic sectors and country income groups .....	13
<b>Figure 2.4</b>	Contribution to 2016 greenhouse gas emissions per emission category .....	14
<b>Figure 2.5</b>	Various carbon capture, storage and utilization selections .....	15
<b>Figure 2.6</b>	Carbon capture options .....	17
<b>Figure 2.7</b>	Technology options for CO <sub>2</sub> separation .....	18
<b>Figure 2.8</b>	Options for storing CO <sub>2</sub> in deep underground geological formation.....	26
<b>Figure 2.9</b>	A flow-chart of microalgae system for combined biofuels production, CO <sub>2</sub> bio-mitigation, and N/P removal from wastewater .....	29
<b>Figure 2.10</b>	Schematic structure of microbubble .....	30
<b>Figure 2.11</b>	The behaviors of macro, micro and nanobubbles in water.....	31
<b>Figure 2.12</b>	The major properties of bubbles according to bubble sizes .....	32
<b>Figure 2.13</b>	Schematic diagram of (a) conventional bubbles and (b) liquid-films.....	33
<b>Figure 3.1</b>	Experimental apparatus used for CO <sub>2</sub> absorption.....	48
<b>Figure 3.2</b>	(a) Structure of WFFU, (b) a fine-bubble generator (Part A) and (c) theory of making fine-bubbles. ....	50
<b>Figure 3.3</b>	CO <sub>2</sub> removal efficiency and absorption rate at different CO <sub>2</sub> concentrations of inlet gas (G <sub>1</sub> , G <sub>2</sub> , and G <sub>3</sub> ) under internal pressure conditions of 0.06 and 0.10 MPa. Water flow rate: 14 L min <sup>-1</sup> ; total gas flow rate: 20 L min <sup>-1</sup> ; total inlet gas supplying pressure: 0.50 MPa; and temperature: 20 °C.....	52
<b>Figure 3.4</b>	Removal efficiency and absorption rate of CO <sub>2</sub> at different compositions of inlet gas under various total inlet gas supplying pressures. Water flow rate: 14 L min <sup>-1</sup> ; internal pressure: 0.06 MPa; and temperature: 20 °C. (a) Total gas flow rate: 10 L min <sup>-1</sup> ; (b) Total gas flow rate: 20 L min <sup>-1</sup> .....	53

<b>Figure 3.5</b>	(a) Removal efficiency of CO <sub>2</sub> at different compositions of inlet gas with a changing G/L ratio. (b) Absorption rate of CO <sub>2</sub> and pH of outlet water at different compositions of inlet gas with a changing G/L ratio. Water flow rate: 14 L min <sup>-1</sup> ; internal device pressure: 0.06 MPa; total inlet gas supplying pressure: 0.50 MPa; and temperature: 20 °C.....	55
<b>Figure 3.6</b>	Removal efficiency of CO <sub>2</sub> , (b) absorption rate of CO <sub>2</sub> , and (c) pH of the absorbed water at different initial CO <sub>2</sub> partial pressures with a total gas flow rate of 15 L min <sup>-1</sup> and 20 L min <sup>-1</sup> ; Water flow rate: 14 L min <sup>-1</sup> ; internal device pressure: 0.06 MPa; total inlet gas supplying pressure: 0.50 MPa; and temperature: 20 °C.....	57
<b>Figure 3.7</b>	Removal efficiency and absorption rate of CO <sub>2</sub> in water at different gas compositions: (a) 15% CO <sub>2</sub> –85% N <sub>2</sub> , (b) 25% CO <sub>2</sub> –75% N <sub>2</sub> , and (c) 35% CO <sub>2</sub> –65% N <sub>2</sub> . Total gas flow rate: 20 L min <sup>-1</sup> ; water flow rate: 14 L min <sup>-1</sup> ; internal device pressure: 0.06 MPa; total inlet gas supplying pressure: 0.50 MPa.....	58
<b>Figure 4.1</b>	Experimental apparatus used for CO <sub>2</sub> absorption: (1) CO <sub>2</sub> and N <sub>2</sub> cylinders; (2) mass flow controllers; (3) water tank; (4) pump; (5) reactor; (6) liquid-film-forming device; (7) exhaust gas valve; and (8) blowdown valve.....	66
<b>Figure 4.2</b>	Correlation between observed and predicted values for (a) removal efficiency and (b) absorption rate.....	75
<b>Figure 4.3</b>	Three-dimensional response surface plots and contour plots of removal efficiency interactions between: (a) gas supplying pressure and G/L ratio; (b) CO <sub>2</sub> initial concentration and G/L ratio; (c) gas supplying pressure and temperature. ....	77
<b>Figure 4.4</b>	Three-dimensional response surface plots and contour plots of absorption rate interaction between: (a) gas supplying pressure and G/L ratio; (b) CO <sub>2</sub> initial concentration and G/L ratio; (c) gas supplying pressure and temperature...	78
<b>Figure 4.5</b>	CO <sub>2</sub> Concentration dissolving into 60 L of water and the change of pH during 60 minutes in two cases of with and without using liquid-film-forming-device	

	(WFFU). Inlet gas supplying pressure: 0.50 MPa; inlet gas composition: 15% CO <sub>2</sub> –85% N <sub>2</sub> ; G/L ratio: 1.43; and temperature: 20 °C. ....	85
<b>Figure 5.1</b>	Schematic diagram of the apparatus used for the removal of carbon dioxide in this study.....	92
<b>Figure 5.2</b>	Snapshots of the production of water-films and fine bubbles in the absorption tank. ....	92
<b>Figure 5.3</b>	Effect of the water-film-forming-unit (WFFU) on (a) CO <sub>2</sub> removal efficiency and (b) absorption rate. Operating conditions: gas supplying pressure = 0.30 MPa; G/L ratio = 1.07; total gas flow rate = 15 L min <sup>-1</sup> ; water flow rate = 14 L min <sup>-1</sup> ; and temperature = 15°C.....	97
<b>Figure 5.4</b>	Effect of gas supplying pressure on (a) CO <sub>2</sub> removal efficiency and (b) absorption rate. Operating conditions: G/L ratio = 1.07; total gas flow rate = 15 L min <sup>-1</sup> ; water flow rate = 14 L min <sup>-1</sup> ; feed gas composition = 25% CO <sub>2</sub> and 75% N <sub>2</sub> ; and temperature = 15 °C. ....	99
<b>Figure 5.5</b>	Effect of CO <sub>2</sub> initial concentration on (a) CO <sub>2</sub> removal efficiency and (b) absorption rate. Operating conditions: gas supplying pressure = 0.50 MPa; G/L ratio = 1.07; total gas flow rate = 15 L min <sup>-1</sup> ; water flow rate = 14 L min <sup>-1</sup> ; and temperature = 15 °C. ....	100
<b>Figure 5.6</b>	Effect of G/L ratio on CO <sub>2</sub> removal efficiency and absorption rate with a feed gas composition of (a) 15% CO <sub>2</sub> and 85% N <sub>2</sub> and (b) 35% CO <sub>2</sub> and 65% N <sub>2</sub> . Operating conditions: gas supplying pressure = 0.50 MPa; water flow rate = 14 L min <sup>-1</sup> ; and temperature = 15 °C.....	102
<b>Figure 5.7</b>	Effect of liquid temperature on CO <sub>2</sub> removal efficiency and absorption rate. Operating conditions: gas supplying pressure = 0.30 MPa; G/L ratio = 1.07; total gas flow rate = 15 L min <sup>-1</sup> ; water flow rate = 14 L min <sup>-1</sup> ; and feed gas composition = 15% CO <sub>2</sub> and 85% N <sub>2</sub> .....	103
<b>Figure 5.8</b>	S/N ratios and delta values for each factor influencing the (a) removal efficiency and (b) absorption rate. ....	105
<b>Figure 5.9</b>	Contribution percentages and ranking of five controlling factors on the (a) removal efficiency and (b) absorption rate of CO <sub>2</sub> . ....	106



## LIST OF TABLES

<b>Table 1.1</b>	Comparison of different carbon dioxide removal technologies .....	1
<b>Table 3.1</b>	Typical CO <sub>2</sub> content in exhausted gas .....	46
<b>Table 4.1</b>	Levels of the experimental variables, estimated effects, and P-value studied in the Plackett-Burman design .....	67
<b>Table 4.2</b>	Plackett-Burman design matrix for evaluating influent factors with removal efficiency and absorption rate as responses .....	70
<b>Table 4.3</b>	Central composite design matrix for the experimental design and predicted responses for removal efficiency $E$ (%) and absorption rate $R$ (mol s <sup>-1</sup> L <sup>-1</sup> )... ..	71
<b>Table 4.4</b>	Significance of regression coefficients for removal efficiency $E$ (%) and absorption rate $R$ (mol s <sup>-1</sup> L <sup>-1</sup> ) .....	73
<b>Table 4.5</b>	Analysis of variance (ANOVA) for the parameters of central composite design (CCD) for removal efficiency $E$ (%) and absorption rate $R$ (mol s <sup>-1</sup> L <sup>-1</sup> ).....	74
<b>Table 4.6</b>	Experimental confirmation for removal efficiency $E$ (%) and absorption rate $R$ (mol s <sup>-1</sup> L <sup>-1</sup> ) .....	82
<b>Table 4.7</b>	Comparison of different CO <sub>2</sub> removal technologies .....	83
<b>Table 5.1</b>	Controlling factors and their levels.....	94
<b>Table 5.2</b>	Taguchi's L <sub>18</sub> orthogonal design and CO <sub>2</sub> removal efficiency, absorption rate and S/N ratio results.....	95
<b>Table 5.3</b>	S/N response table for CO <sub>2</sub> removal efficiency and absorption rate .....	104
<b>Table 5.4</b>	Experimental verification under the optimum conditions .....	107

## LIST OF ABBREVIATIONS

- ANOVA: Analysis of variance
- Adj-  $R^2$ : Adjusted determination coefficient
- AFOLU: Agriculture, forestry and other land use
- CCD: Central composite design
- CCS: Carbon capture and storage
- CO<sub>2</sub>: Carbon dioxide
- Conc.: Concentration
- E: Removal efficiency
- Eq: Equivalent
- EOR: Enhanced oil recovery
- GC: Gas chromatography
- G/L: Gas-to-liquid ratio
- G<sub>1</sub>: Mixture gas of 15% CO<sub>2</sub> and 85% N<sub>2</sub>
- G<sub>2</sub>: Mixture gas of 25% CO<sub>2</sub> and 75% N<sub>2</sub>
- G<sub>3</sub>: Mixture gas of 35% CO<sub>2</sub> and 65% N<sub>2</sub>
- GHG: Greenhouse gas
- GSP: Gas supplying pressure
- Gt: Gigatonne
- L min<sup>-1</sup>: Liter per minute
- N<sub>2</sub>: Nitrogen
- P*-value: Probability unit
- R: Absorption rate

RF: Radiative forcing

R<sup>2</sup>: Determination coefficient

RSM: Response surface method

Temp.: Temperature

WFFU: Water-film-forming-unit

X<sub>1</sub>: Symbol for the factor of gas supplying pressure

X<sub>2</sub>: Symbol for the factor of CO<sub>2</sub> initial concentration

X<sub>3</sub>: Symbol for the factor of G/L ratio

X<sub>4</sub>: Symbol for the factor of temperature

# CHAPTER 1

## INTRODUCTION

### 1.1 Background and problem statement

Global warming and climate change have recently resulted in several negative influences on the environment, living creatures and human health. Therefore, finding out the solutions so as to mitigate the greenhouse effects, which are related to the high amount of greenhouse gases in the atmosphere, is currently global concerns (Nguyen *et al.*, 2018). In the comparison among numerous greenhouse gases including CO<sub>2</sub>, CH<sub>4</sub>, N<sub>2</sub>O, CFCs and F-gases, CO<sub>2</sub> alone contributes a major percentage of more than 80% to the total greenhouse gas emissions (Lee *et al.*, 2012). As a result, only does CO<sub>2</sub> occupy over 60% of the total greenhouse effect (Mondal *et al.*, 2012, Yu *et al.*, 2012, Ma'mun *et al.*, 2007). As a consequence, the development of a method which can capture CO<sub>2</sub> from flue gas effectively and available is essential and urgent. **Table 1.1** presents various popular technologies using to reduce the emission of CO<sub>2</sub> from gas streams.

**Table 1.1** Comparison of different carbon dioxide removal technologies

Technology	Type	Advantage	Disadvantage
Chemical absorption	Amine absorption (MEA, DEA, MDEA, AMP)	<ul style="list-style-type: none"> <li>– High absorption efficiency (&gt;90%) and applicable for CO<sub>2</sub> capture at low concentrations (Kenarsari <i>et al.</i>, 2013, Leung <i>et al.</i>, 2014)</li> <li>– Reversible solvent</li> <li>– Most mature and developed process for CO<sub>2</sub> separation and already implemented in industry on a large scale (Kenarsari <i>et al.</i>, 2013, Leung <i>et al.</i>, 2014)</li> </ul>	<ul style="list-style-type: none"> <li>– High equipment corrosion rate (Kenarsari <i>et al.</i>, 2013, Olajire, 2010)</li> <li>– High energy consumption due to the supply of heat for absorbent regeneration (Kenarsari <i>et al.</i>, 2013)</li> <li>– Environmental impacts are related to solvent loss or degradation → not environmentally friendly</li> <li>– Waste chemical and drainage wastewater require treatment (Andriani <i>et al.</i>, 2014)</li> </ul>
Physical absorption	Selexol process Rectisol process	<ul style="list-style-type: none"> <li>– Low toxicity (Kenarsari <i>et al.</i>, 2013)</li> </ul>	<ul style="list-style-type: none"> <li>– Dependent on temperature and pressure, so difficult to apply on a large-scale in</li> </ul>

	Purisol process Water absorption	<ul style="list-style-type: none"> <li>– Low corrosion (Kenarsari <i>et al.</i>, 2013)</li> <li>– Low energy consumption and low energy required for sorbent regeneration (Kenarsari <i>et al.</i>, 2013, Songolzadeh <i>et al.</i>, 2014)</li> <li>– No special chemicals required if water is used as solvent (Andriani <i>et al.</i>, 2014)</li> </ul>	<ul style="list-style-type: none"> <li>industrial plants (Songolzadeh <i>et al.</i>, 2014)</li> <li>– High pressure is required and low efficiency for CO<sub>2</sub> removal (Kenarsari <i>et al.</i>, 2013, Olajire, 2010)</li> </ul>
Adsorption	Pressure swing adsorption (PSA)	<ul style="list-style-type: none"> <li>– Process is reversible and the adsorbent can be recycled (Leung <i>et al.</i>, 2014)</li> <li>– High adsorption efficiency achievable (&gt;85%) (Leung <i>et al.</i>, 2014)</li> <li>– No by-products such as wastewater because of using solids to adsorb CO<sub>2</sub> (Mondal <i>et al.</i>, 2012)</li> </ul>	<ul style="list-style-type: none"> <li>– Requires high temperature adsorbent, high energy for CO<sub>2</sub> desorption, and has high operation costs (Leung <i>et al.</i>, 2014)</li> <li>– Low selectivity and capacity of available adsorbent CO<sub>2</sub>. Rarely applied to large-scale separation of CO<sub>2</sub> (Kenarsari <i>et al.</i>, 2013, Mondal <i>et al.</i>, 2012)</li> </ul>
Membrane separation	Gas/Gas Gas/Liquid	<ul style="list-style-type: none"> <li>– Process has been applied to separation of other gases (Leung <i>et al.</i>, 2014)</li> <li>– More than 80% separation efficiency (Leung <i>et al.</i>, 2014)</li> <li>– No waste stream and no regeneration process (Kenarsari <i>et al.</i>, 2013)</li> </ul>	<ul style="list-style-type: none"> <li>– Operational problems include low fluxes and fouling (Leung <i>et al.</i>, 2014)</li> <li>– High cost of membrane. The membrane is easily contaminated and plugged by impurities in the feed gas (Kenarsari <i>et al.</i>, 2013)</li> <li>– Membrane often suffers thermal shock and chemical corrosion (Xiao <i>et al.</i>, 2014)</li> <li>– No large-scale operation experience (Leung <i>et al.</i>, 2014)</li> </ul>

Taken together, each of technologies mentioned above has their benefits and drawbacks with reference to evaluating factors consisting of removal capacity, operation, cost, energy, equipment, and environmental influence. Upon these methods, due to the fact that absorption is the most mature method that has been in practical application for 60 years, it is the most popular and commercial method for separating CO<sub>2</sub> from the exhausted gases (Babu, 2014,

Rao & Rubin, 2002). The basic fundamental of this technique is to absorb one or more substances from a mixture of gas into a liquid phase through the boundary of vapor–liquid phase (Nguyen *et al.*, 2018). Physical absorption and chemical absorption are generally concerned as two major kinds of absorption method. The difference between these two methods is whether a chemical reaction happens after the substances dissolving into an aqueous phase or not (Aresta, 2013). Due to the high removal performance, chemical absorption – especially, amine absorption – is broadly applied for the capture of CO<sub>2</sub> from industrial emitted gases. Nevertheless, this method remains several restrictions. Firstly, because of the use of organic amine absorbent, this method demands high energy consumption for the amine regeneration process. Next, this process leads to a high rate of oxidization and produces toxic volatile degradation substances (Nguyen *et al.*, 2018). Additionally, the emitted amine is possible to degrade to nitrosamines and nitramines which jeopardize human health and the environment (Leung *et al.*, 2014). As a consequence, this method is not environmentally friendly. These negative issues can be solved by using the method of physical absorption – water absorption (Nguyen *et al.*, 2018).

Water absorption is the technique that is the most cost-effective and friendly to the environment since comparing to other methods such as chemical absorption, cryogenics or membrane. Herein, water is used as a solvent so the drainage effluent which is CO<sub>2</sub>-rich water can directly or indirectly use for other industrial- or lab-scale application and for storing CO<sub>2</sub>. For instance, the CO<sub>2</sub>-rich water after absorption can use for cultivating microalga to produce biofuels and biomass and mineral carbonating. The interaction between CO<sub>2</sub> and water also is weak so CO<sub>2</sub> can be recovered in the manner of saving cost and energy.

However, the most important drawback of water scrubbing is that in order to achieve high absorption performance, the high working pressure is required over 1.0 MPa (Ryckebosch *et al.*, 2011) which means that high energy and cost requirement. Water scrubbing was used to remove CO<sub>2</sub> and upgrade a landfill gas consisting of 53.2% CH<sub>4</sub>, 40.8% CO<sub>2</sub>, 0.4% O<sub>2</sub> and 4.9% N<sub>2</sub> in the pilot-scale packed column (Rasi *et al.*, 2008). The results depicted that CO<sub>2</sub> removal ability was about 90.0% as the operational conditions are that the pressure is 3.0 MPa, water flow rate is 10 Lmin<sup>-1</sup> and gas flow rate is 50 L min<sup>-1</sup> (Rasi *et al.*, 2008). Another research found that with the landfill gas comprising 50.8 – 57.9% CH<sub>4</sub>, and 37.8 – 43.6% CO<sub>2</sub>, the CO<sub>2</sub>

removal rates at water flow rate of 11 L min<sup>-1</sup>, gas flow rate of 7.41 Nm<sup>3</sup>h<sup>-1</sup> and water temperature of 10 – 15 °C were 85.8% at pressure of 2.0 MPa, 87.0% at pressure of 2.3 MPa and 88.9% at pressure of 2.5 MPa (Läntelä *et al.*, 2012). Xiao and his group also conducted research of CO<sub>2</sub> removal using water scrubbing (Xiao *et al.*, 2014). The obtained data presented that the removal of CO<sub>2</sub> can fluctuate between 24.4 – 94.2% at the range of pressure (0.8 – 1.2 MPa), inlet CO<sub>2</sub> content (25 – 45 %), water flow rate/gas flow rate ratio (0.15 – 0.5) and temperature (10 – 40 °C) (Xiao *et al.*, 2014).

The restrict requirement for pressure when using water absorption is not limited for absorption pressure, it also requires high gas partial pressure. Water scrubbing method has just applied for the feed gas containing high CO<sub>2</sub> partial pressure. Hence, water scrubbing is limited to use in pre-combustion or oxy-fuel combustion system and in upgrading fuel gas such as biogas, natural gas or landfill gas. The utilization of microbubble- and liquid-film-forming apparatus can remedy this issue. Both types of gas bubbles prove that they are innovated technologies to not only produce numerous boundary and interfacial contact area but also stimulate mass transfer between two phases of gas and water (Bredwell & Worden, 1998, Imai & Zhu, 2011, Jamnongwong *et al.*, 2016, Zhu *et al.*, 2007a, Sadatomi *et al.*, 2012). With these properties, the produce of a large number of microbubbles and liquid-films in the liquid bulk can improve a gas dissolution rate which results in the circumstance that gas saturation concentration can reach in short time with the saving of energy consumption and the low pressure for compressing gas phase (Sadatomi *et al.*, 2012, Jamnongwong *et al.*, 2016, Temesgen *et al.*, 2017, Zhu *et al.*, 2007b, Zhu *et al.*, 2007a). Generally, it is expected that with the utility of microbubbles and liquid-film generator, the advanced water scrubbing can capture CO<sub>2</sub> effectually for every type of feed gas even though feed gas containing low CO<sub>2</sub> partial pressure since low mode pressure is applied

## **1.2 Dissertation objectives**

The goal of this study is to explore an innovated water scrubbing which can improve the effectivity through the support of water-film-forming-unit (WFFU) for capturing CO<sub>2</sub> from the mixed gas with N<sub>2</sub>. So as to accomplish the study target, the research was carried out to achieve four objectives:

- To investigate the effect of key factors such as internal pressure, gas supplying pressure, gas-to-liquid flow rate ratio, initial CO<sub>2</sub> content and liquid temperature on the CO<sub>2</sub> removal efficiency and absorption rate when using the water absorption advanced with WFFU.
- To evaluate the effects and benefits of WFFU in improving the performance of water absorption process through comparing the obtained results of the CO<sub>2</sub> removal efficiency and absorption rate in three cases of experiments consisting of using non-WFFU, 1-WFFU and 2-WFFUs.
- To assess intensively the effect of gas supplying pressure on the absorption process which is the primary advantage of the conventional water scrubber. Therefore, it can be concluded that the presence of WFFU can improve the absorption capacity at low pressure as well as reduce the effect of pressure when applying water absorption for CO<sub>2</sub> capture.
- To apply statistic tools such as Taguchi method, Plackett-Burman and Response Surface Method for evaluating thoroughly the effect of key factors on responses and the interaction among factors, determining the contribution percentage of each factor on responses and exploring the optimal conditions.

### **1.3 Structure of the dissertation**

**Chapter 1** Introduction

**Chapter 2** Literature review

**Chapter 3** Performance of a carbon dioxide removal process using a water scrubber with the aid of a water-film-forming-unit

**Chapter 4** Response surface method for modeling the removal of carbon dioxide from a simulated gas using water absorption enhanced with a water-film-forming-unit

**Chapter 5** Influence of water-film-forming-unit on the enhanced removal of carbon dioxide from mixed gas using water absorption apparatus

**Chapter 6** Conclusions and future works



## 1.4 References

- Andriani, D., Wresta, A., Atmaja, T. D. & Saepudin, A. 2014. A review on optimization production and upgrading biogas through CO<sub>2</sub> removal using various techniques. *Applied biochemistry and biotechnology*, **172** (4), 1909-1928.
- Aresta, M. 2013. Carbon dioxide recovery and utilization, Springer Science & Business Media. Germany.
- Babu, P. V. 2014. Hydrate based gas separation (HBGS) technology for precombustion capture of carbon dioxide. PhD thesis. National University of Singapore, Singapore.
- Bredwell, M. D. & Worden, R. M. 1998. Mass-transfer properties of microbubbles. 1. Experimental studies. *Biotechnology Progress*, **14** (1), 31-38.
- Imai, T. & Zhu, H., 2011. Improvement of oxygen transfer efficiency in diffused aeration systems using liquid-film-forming apparatus, *Mass Transfer-Advanced Aspects*. InTech.
- Jamnongwong, M., Charoenpittaya, T., Hongprasith, N., Imai, T. & Painmanakul, P. 2016. Study of Liquid Film Forming Apparatus (LFFA) mechanisms in terms of oxygen transfer and bubble hydrodynamic parameters. *Engineering Journal (Eng. J.)*, **20** (3), 77-90.
- Kenarsari, S. D., Yang, D., Jiang, G., Zhang, S., Wang, J., Russell, A. G., Wei, Q. & Fan, M. 2013. Review of recent advances in carbon dioxide separation and capture. *Rsc Advances*, **3** (45), 22739-22773.
- Läntelä, J., Rasi, S., Lehtinen, J. & Rintala, J. 2012. Landfill gas upgrading with pilot-scale water scrubber: performance assessment with absorption water recycling. *Applied energy*, **92**, 307-314.
- Lee, Z. H., Lee, K. T., Bhatia, S. & Mohamed, A. R. 2012. Post-combustion carbon dioxide capture: Evolution towards utilization of nanomaterials. *Renewable and Sustainable Energy Reviews*, **16** (5), 2599-2609.
- Leung, D. Y., Caramanna, G. & Maroto-Valer, M. M. 2014. An overview of current status of carbon dioxide capture and storage technologies. *Renewable and Sustainable Energy Reviews*, **39**, 426-443.
- Ma'mun, S., Svendsen, H. F., Hoff, K. A. & Juliussen, O. 2007. Selection of new absorbents for carbon dioxide capture. *Energy Conversion and Management*, **48** (1), 251-258.
- Mondal, M. K., Balsora, H. K. & Varshney, P. 2012. Progress and trends in CO<sub>2</sub> capture/separation technologies: A review. *Energy*, **46** (1), 431-441.

- Nguyen, D.-M. K., Imai, T., Dang, T.-L. T., Kanno, A., Higuchi, T., Yamamoto, K. & Sekine, M. 2018. Response surface method for modeling the removal of carbon dioxide from a simulated gas using water absorption enhanced with a liquid-film-forming device. *Journal of Environmental Sciences*, **65**, 116-126.
- Olajire, A. A. 2010. CO<sub>2</sub> capture and separation technologies for end-of-pipe applications – A review. *Energy*, **35** (6), 2610-2628.
- Rao, A. B. & Rubin, E. S. 2002. A technical, economic, and environmental assessment of amine-based CO<sub>2</sub> capture technology for power plant greenhouse gas control. *Environmental science & technology*, **36** (20), 4467-4475.
- Rasi, S., Läntelä, J., Veijanen, A. & Rintala, J. 2008. Landfill gas upgrading with countercurrent water wash. *Waste Management*, **28** (9), 1528-1534.
- Ryckebosch, E., Drouillon, M. & Vervaeren, H. 2011. Techniques for transformation of biogas to biomethane. *Biomass and bioenergy*, **35** (5), 1633-1645.
- Sadatomi, M., Kawahara, A., Matsuura, H. & Shikatani, S. 2012. Micro-bubble generation rate and bubble dissolution rate into water by a simple multi-fluid mixer with orifice and porous tube. *Experimental Thermal and Fluid Science*, **41**, 23-30.
- Songolzadeh, M., Soleimani, M., Takht Ravanchi, M. & Songolzadeh, R. 2014. Carbon dioxide separation from flue gases: a technological review emphasizing reduction in greenhouse gas emissions. *The Scientific World Journal*, **2014**, 1-34.
- Temesgen, T., Bui, T. T., Han, M., Kim, T.-i. & Park, H. 2017. Micro and nanobubble technologies as a new horizon for water-treatment techniques: A review. *Advances in colloid and interface science*, **246**, 40-51.
- Xiao, Y., Yuan, H., Pang, Y., Chen, S., Zhu, B., Zou, D., Ma, J., Yu, L. & Li, X. 2014. CO<sub>2</sub> removal from biogas by water washing system. *Chinese Journal of Chemical Engineering*, **22** (8), 950-953.
- Yu, C.-H., Huang, C.-H. & Tan, C.-S. 2012. A review of CO<sub>2</sub> capture by absorption and adsorption. *Aerosol and Air Quality Research*, **12** (5), 745-769.
- Zhu, H., Imai, T., Tani, K., Ukita, M., Sekine, M., Higuchi, T. & Zhang, Z. 2007a. Enhancement of oxygen transfer efficiency in diffused aeration systems using liquid-film-forming apparatus. *Environmental technology*, **28** (5), 511-519.

Zhu, H., Imai, T., Tani, K., Ukita, M., Sekine, M., Higuchi, T. & Zhang, Z. 2007b. Development of high efficient oxygen supply method by using contacting water-liquid film with air. *Journal of Water and Environment Technology*, **5** (2), 57-69.

## CHAPTER 2

### LITERATURE REVIEW

#### 2.1 Environmental issues of greenhouse gases and carbon dioxide

##### 2.1.1 Global emissions of greenhouse gases and carbon dioxide

Climate change or global warming recently becomes the most global concern due to several world spread drawbacks. It refers to the rise in average surface temperature on the Earth with various pieces of physical evidence related to (1) the alterations in temperature, (2) the alterations in energy budget and heat content, (3) the alterations in circulation and modes of variability, (4) the alterations in the water cycle and cryosphere, (5) the alterations in sea level, (6) the alterations in extremes, and finally, (7) the alterations in carbon and other biogeochemical cycles (Stocker *et al.*, 2013). According to the calculation by a linear trend, the worldwide averaged temperature which is combined between land temperature and oceanic temperature reveal an increasing temperature of 0.85 °C in the period of 1880 – 2012. Excepting for glaciers on the periphery of the ice sheets, the global average rate of ice loss from glaciers from 1971 to 2009 was 226 Gt yr<sup>-1</sup> compared to 275 Gt yr<sup>-1</sup> over the period 1993 to 2009 (Stocker *et al.*, 2013). Due to the ice loss, the mean rate of global averaged sea level rise was 2.0 mm yr<sup>-1</sup> in the time of 1971 – 2010 and 3.2 mm yr<sup>-1</sup> in the time of 1993 – 2010 (Stocker *et al.*, 2013). Climate change also influences carbon cycle processes in the manner that increases CO<sub>2</sub> in the atmosphere which is able to increase ocean acidification. The reality is that 0.1 unit of the oceanic surface pH has reduced since the start of the industrialized era (Stocker *et al.*, 2013).

It cannot be denied that over a half of detected growth in global average surface temperature from 1951 to 2010 was resulted by the upward trend in anthropogenic greenhouse gases (GHGs) emission and another anthropogenic forcing together (Stocker *et al.*, 2013). Only did GHGs contribute to the global mean surface warming in the range of 0.5 °C to 1.3 °C (Stocker *et al.*, 2013). Alternatively, the total radiative forcing (RF) is vital and essential to evaluate the drivers of climate change due to the fact that positive RF is the cause for the surface warming while negative RF is the cause for the surface cooling. Based on the statistics, since 1750, the

highest involvement to total RF originated from the increases of CO<sub>2</sub> concentration in the atmosphere. Owing to a conjunction of the positive RF resulted by the majority of greenhouse gas concentrations and the negative RF resulted by NO<sub>x</sub>, aerosols and precursors, the total anthropogenic RF for 2011 relative to 1750 is 2.29 W m<sup>-2</sup> (**Figure 2.1**) (Stocker *et al.*, 2013).

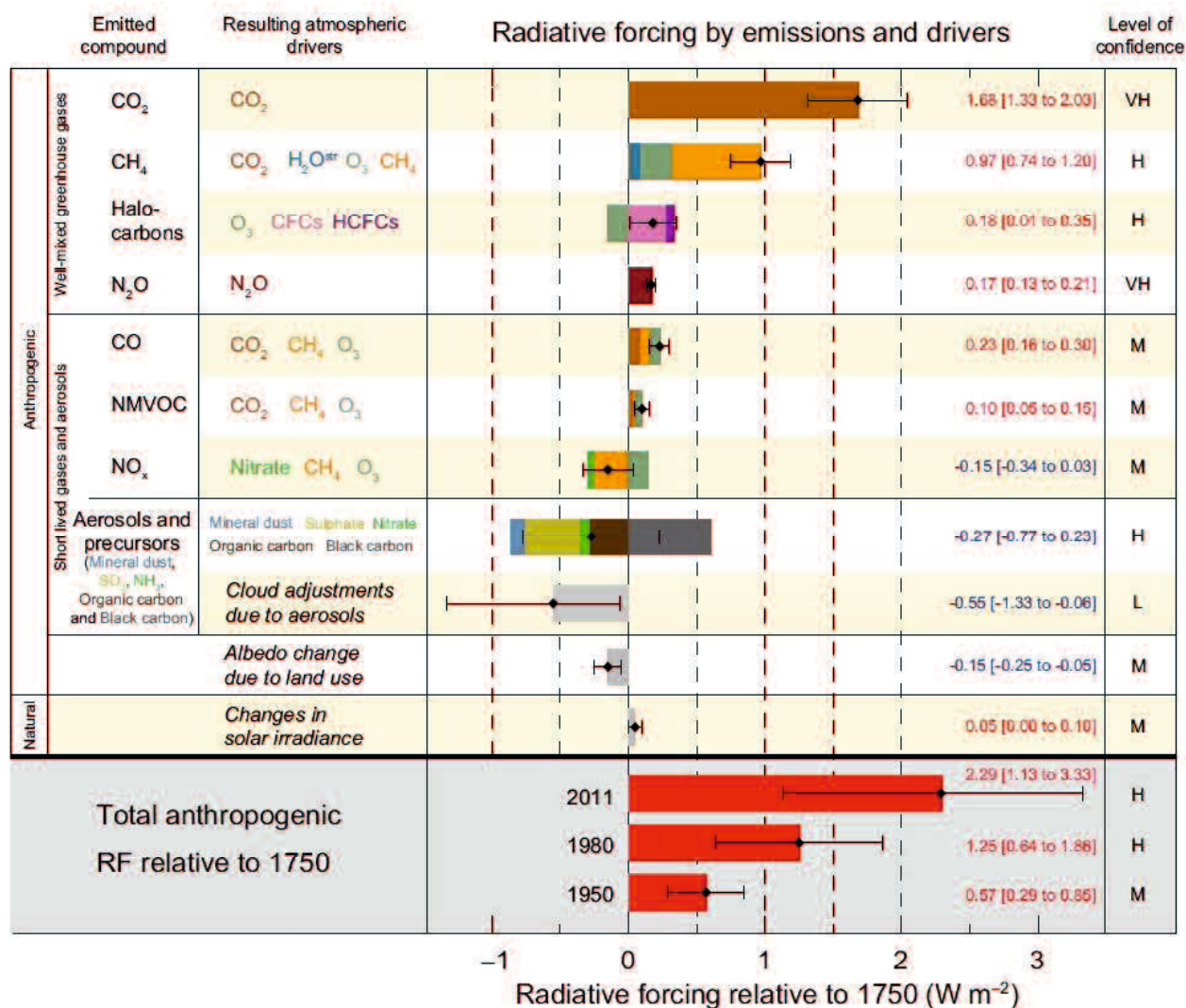


**Figure 2.1** Radiative forcing estimates in 2011 relative to 1750 and aggregated uncertainties for the main drivers of climate change (Stocker *et al.*, 2013).

Specifically, the RF from emissions of well-mixed greenhouse gases (the first group in **Figure 2.1** which consisting of CO<sub>2</sub>, CH<sub>4</sub>, N<sub>2</sub>O, and Halocarbons) for 2011 relative to 1750 is 3.00 W m<sup>-2</sup>. The RF value for CO<sub>2</sub> emission alone of 1.68 W m<sup>-2</sup>, for CH<sub>4</sub> emission alone of 0.97 W m<sup>-2</sup>, for stratospheric ozone-depleting halocarbons of 0.18 W m<sup>-2</sup> and for N<sub>2</sub>O emission alone of 0.17 W m<sup>-2</sup> (Stocker *et al.*, 2013).

The most abundant and noticeable greenhouse gases are carbon dioxide (CO<sub>2</sub>), methane (CH<sub>4</sub>), nitrous oxide (N<sub>2</sub>O), chlorofluorocarbons (CFCs) and fluorinated gases (F-gases). Based on the report in 2016, total greenhouse gas emissions remains a slight upward trend by about 0.5% (±0.1%), to about 49.3 Gt in CO<sub>2</sub> equivalent (Gt CO<sub>2</sub> eq) (Olivier *et al.*, 2017). As presented in **Figure 2.2**, within 49.3 Gt in CO<sub>2</sub> equivalent (equivalent to 100% share of total global GHG emissions), five largest country – China, United States, India, Russian Federation and Japan – and European Union occupied 68% of total global CO<sub>2</sub> emission and about 63% of total global GHG emissions (Olivier *et al.*, 2017).

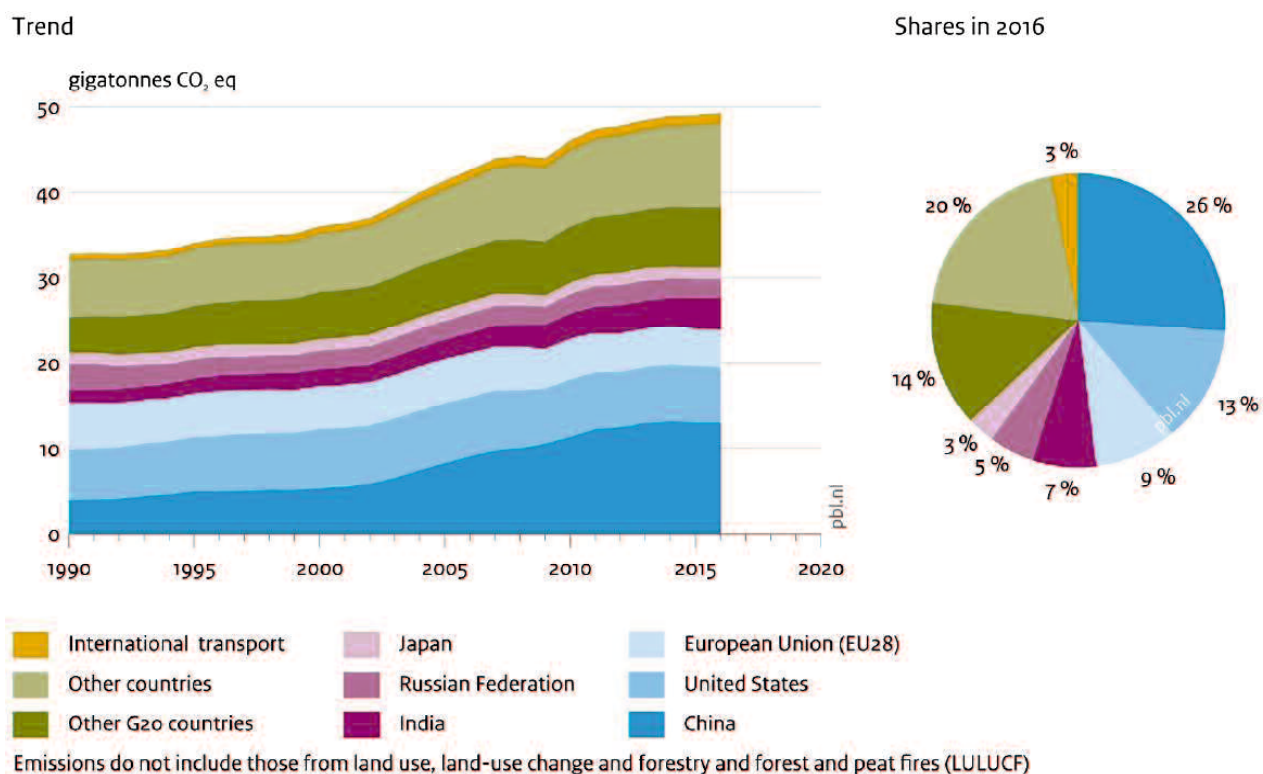


**Figure 2.2** Global greenhouse gas emissions, per country and region (Olivier *et al.*, 2017).

Total anthropogenic GHG emissions follow a significant increasing trend year by year and reveal different values depending on economic sectors and country income groups (see **Figure 2.3**). In **Figure 2.3(a)**, the pie chart shows direct GHG emission shares (in % of total anthropogenic GHG emissions) of five major economic sectors in 2010 (Edenhofer *et al.*, 2014). Herein, the five major economic sectors and their percentages are electricity and heat production (25%), agriculture, forestry and other land use (AFOLU) (24%), industry (21%), transport (14%), buildings (6.4%) and other energy (9.6%) (Edenhofer *et al.*, 2014).

The bar chart in **Figure 2.3(b)** illustrates the total anthropogenic GHG emissions by five main economic sectors and country income groups in three typical years of 1970, 1990 and 2010 (Edenhofer *et al.*, 2014). There are five types of country income groups consisting of bunkers, low income, lower mid income, upper mid income, and high income (Edenhofer *et al.*, 2014). It is clear to notice that the huge number of GHG emissions derive from high income and developed countries. In these countries, most emissions originate from the supply of energy and electricity. In contrast, the total emissions of low-income countries are dominated by AFOLU (Edenhofer *et al.*, 2014, Ausubel *et al.*, 2013).

Globally, CO<sub>2</sub>, CH<sub>4</sub>, N<sub>2</sub>O and F-gases are the crucial anthropogenic greenhouse gases. The emitted majority source for CO<sub>2</sub> is the combustion of fossil fuel. CO<sub>2</sub> can also be released from direct anthropogenic impacts on forestry and other land use, for example, deforestation, land clearing for agriculture, and soil degradation (EPA, 2018). Similarly, the reforestation, improvement of soils, and other activities can extract CO<sub>2</sub> from the land to the environment (EPA, 2018). Meanwhile, the emission of CH<sub>4</sub> can be completed under the agricultural activities, waste management, energy use, and biomass burning (EPA, 2018). For the emission of N<sub>2</sub>O, it has been concerned by agricultural activities, the use of fertilizer and fossil fuel combustion. Finally, fluorinated gases (F-gases) containing hydrofluorocarbons (HFCs), perfluorocarbons (PFCs), and sulfur hexafluoride (SF<sub>6</sub>) originated from manufacturing processes, refrigeration, and the use of various electrical products (EPA, 2018).

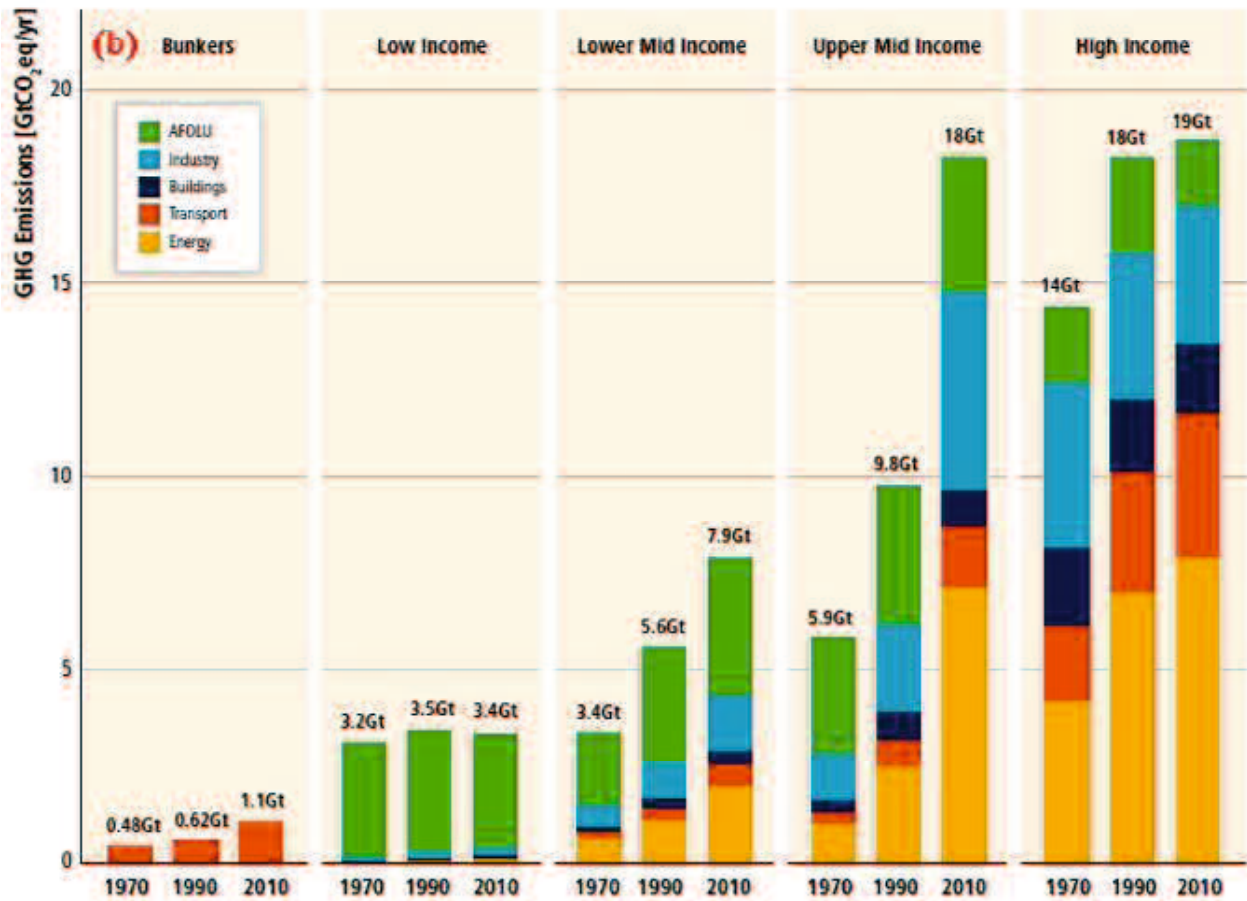
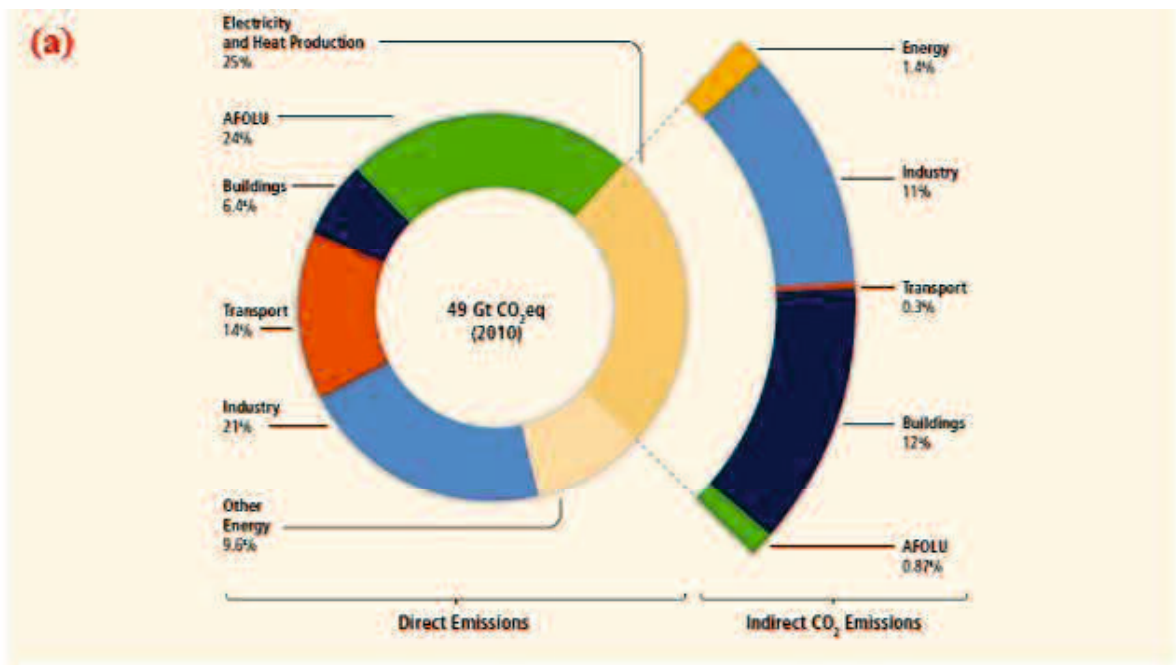


**Figure 2.3** Total anthropogenic GHG emissions (GtCO<sub>2</sub> eq/yr) by economic sectors and country income groups (Edenhofer *et al.*, 2014).



Based on the report of PBL Netherlands Environmental Assessment Agency 2017, in 2016, among greenhouse gases, CO<sub>2</sub> is a major and primary component with the contribution percentage of 72%. Next percentage is attributed from CH<sub>4</sub> (19%), N<sub>2</sub>O (6%) and F-gases (3%). These numbers have been changed for each country but with the highest contribution percentage, CO<sub>2</sub> is always the key factor in the total GHG emissions (Olivier *et al.*, 2017). The detailed data have been introduced in **Figure 2.4**.

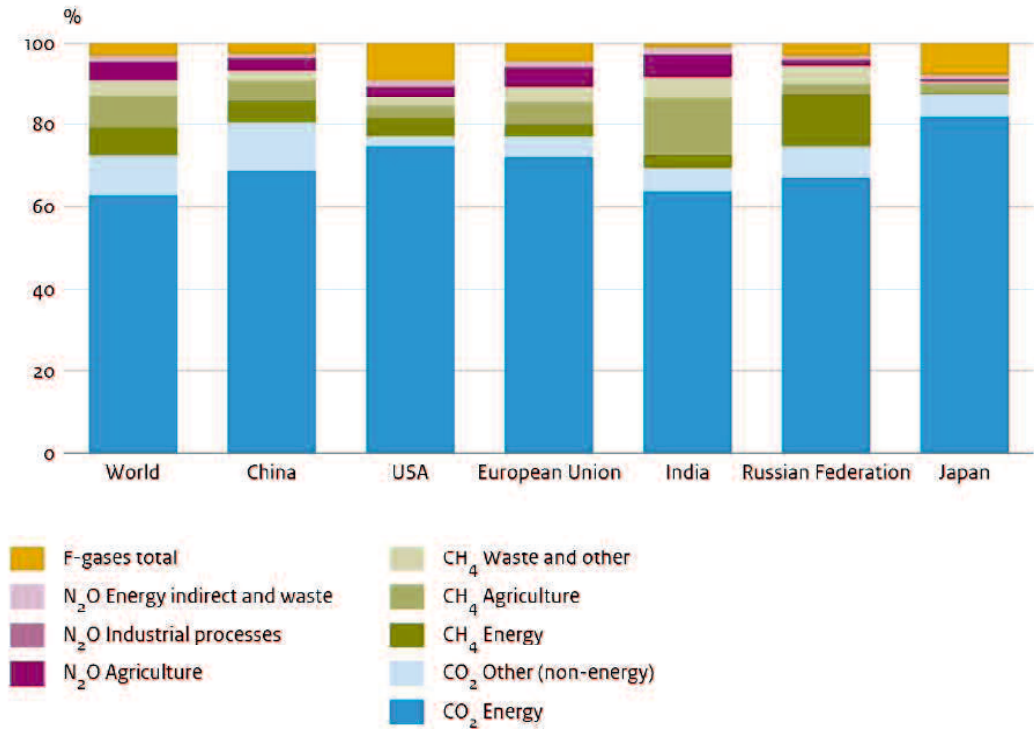


**Figure 2.4** Contribution to 2016 greenhouse gas emissions per emission category (Olivier *et al.*, 2017).

## 2.2 Carbon dioxide capture and storage (CCS)

### 2.2.1 Overview of Carbon capture and Storage

To address problems of climate change and reduce CO<sub>2</sub> emissions, solutions are completed based on three basic options: decreasing energy intensity, decreasing carbon intensity, and increasing the capture of CO<sub>2</sub> (Olajire, 2010). Specifically, various approaches have been suggested: (1) improve energy effectiveness and promote energy conservation; (2) increase the

utilization of low carbon fuels; (3) deploy renewable energy; (4) apply geoen지니어ing approaches; and (5) CO<sub>2</sub> capture and storage (Leung *et al.*, 2014).

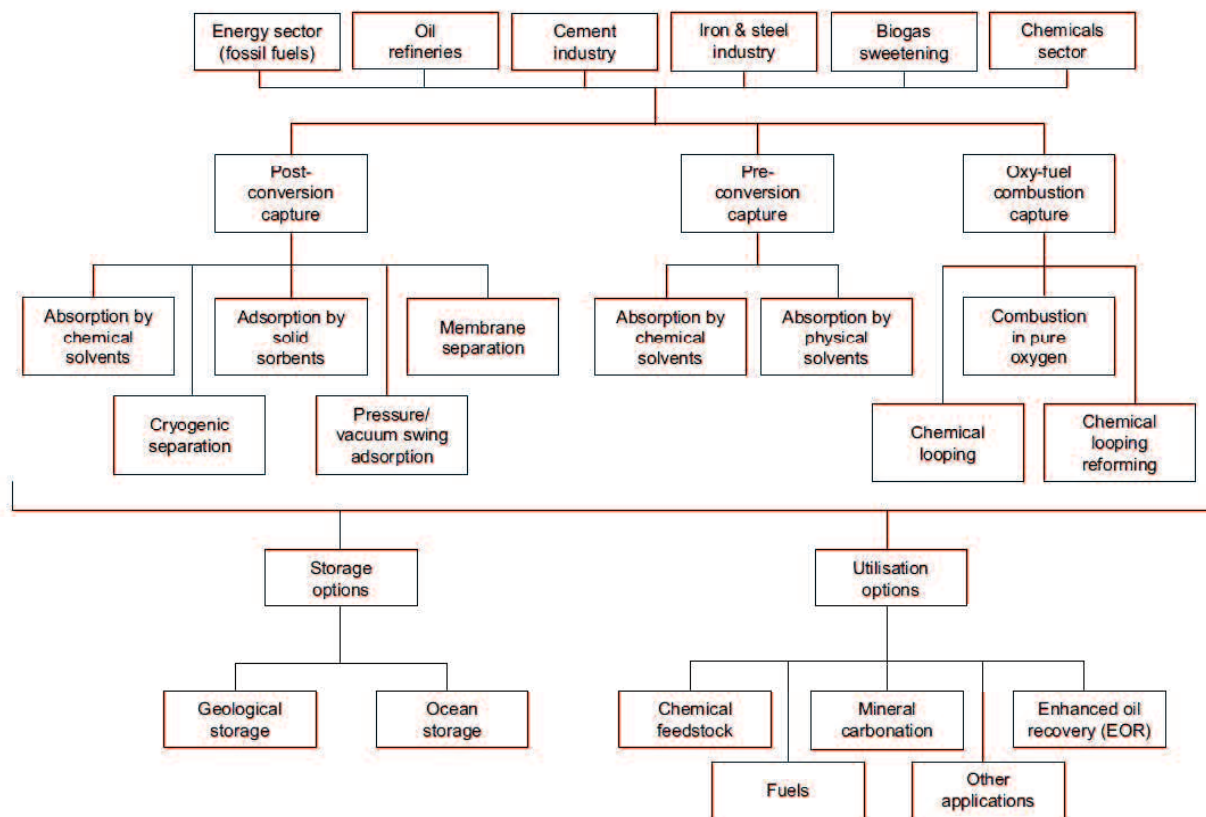


**Figure 2.5** Various carbon capture, storage and utilization selections (Cuéllar-Franca & Azapagic, 2015).

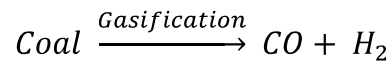
It can be seen that although the use of energy alternatives such as wind, solar, and nuclear energy or clean fuels can be considered as green energy, the application of these energies remain levels of risks and cost and they also cannot satisfy our need of energy. Therefore, carbon dioxide capture and storage has recently considered as the promising remedy, at least as the effective short-term solution, to deal with climate change. CCS includes a group of technologies consisting of CO<sub>2</sub> capture, separation, transport, storage, and monitoring (**Figure 2.5**). In term of CCS, there are two ways to reach the purpose of reducing CO<sub>2</sub> emissions. The first one is accomplished upon the procedure of capturing of CO<sub>2</sub> from the industrial sources, transforming to CO<sub>2</sub> pure form and finally pumping to the deep ocean for the long-term storage. The second approach is to capture CO<sub>2</sub> from the environment by improving natural biological progressions that can separate CO<sub>2</sub> in plants, soils, and oceanic sediments (Benson & Orr,

2008). According to technical and economic estimations, CCS could contribute 20% of CO<sub>2</sub> emission reduction (Benson & Orr, 2008) and CCS open an optimistic prospect for reducing CO<sub>2</sub>.

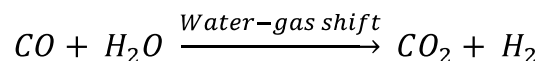
### 2.2.2 Capture technologies

The CO<sub>2</sub> capture can be sorted into three options: post – conversation capture, pre – conversation capture, and oxy – fuel combustion (shown in **Figure 2.6**). **Post – combustion capture** is the method in which CO<sub>2</sub> was captured from the waste gas stream after the fossil fuel is burnt. Post – combustion technologies is preferred as the most mature and potential scheme for retrofitting to existing power plants (Leung *et al.*, 2014, Kenarsari *et al.*, 2013, Romeo *et al.*, 2008, Thiruvengkatachari *et al.*, 2009). Since a CO<sub>2</sub> content in the combustion flue gas is low (i.e. 7 – 14% for coal-fired and 4% for gas-fired) (Leung *et al.*, 2014) and partial pressure of CO<sub>2</sub> separation, it requires a huge amount of energy and high cost for capturing, compressing, and enriching concentration of CO<sub>2</sub> (>95.5%) to transport and storage. And also, because the concentration of CO<sub>2</sub> in the flue gases emitting from the power plants is low, a large size equipment and high capital cost are required (Olajire, 2010).

**Pre – combustion capture** applied new gasification technique to produce the easily burnable gas and then sequester CO<sub>2</sub> before burning (Kenarsari *et al.*, 2013). For coal, the gasification process is carried out in a gasifier with sub-stoichiometric amounts of oxygen at the elevated pressure of 30 – 70 atm in other to create a “synthesis gas” mixture of CO and H<sub>2</sub> (Gibbins & Chalmers, 2008, Leung *et al.*, 2014):

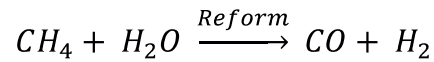


The sync gas after producing is introduced to a catalytic reactor named “shift converter”, in which CO creates with water to make CO<sub>2</sub> and H<sub>2</sub> (Olajire, 2010, Leung *et al.*, 2014):



After that, the produced hydrogen is separated from CO<sub>2</sub> and used as fuel. This procedure can be utilized for Integrated Gasification Combined Cycle (IGCC) power plants using coal (Leung *et al.*, 2014). With the high concentration of CO<sub>2</sub> (20 – 40%) and high CO<sub>2</sub> partial pressure (about 10 bar) promote the separation easier and more cost-effective (Kenarsari *et al.*, 2013, Rubin *et al.*, 2012).

For biomass and natural gas, since they contain lots of CH<sub>4</sub>, can be reformed to the sync gas as follow (Leung *et al.*, 2014):



However, the most drawbacks of pre – combustion capture are high capital costs (Olajire, 2010) and high costs for the shift reaction (Gibbins & Chalmers, 2008).

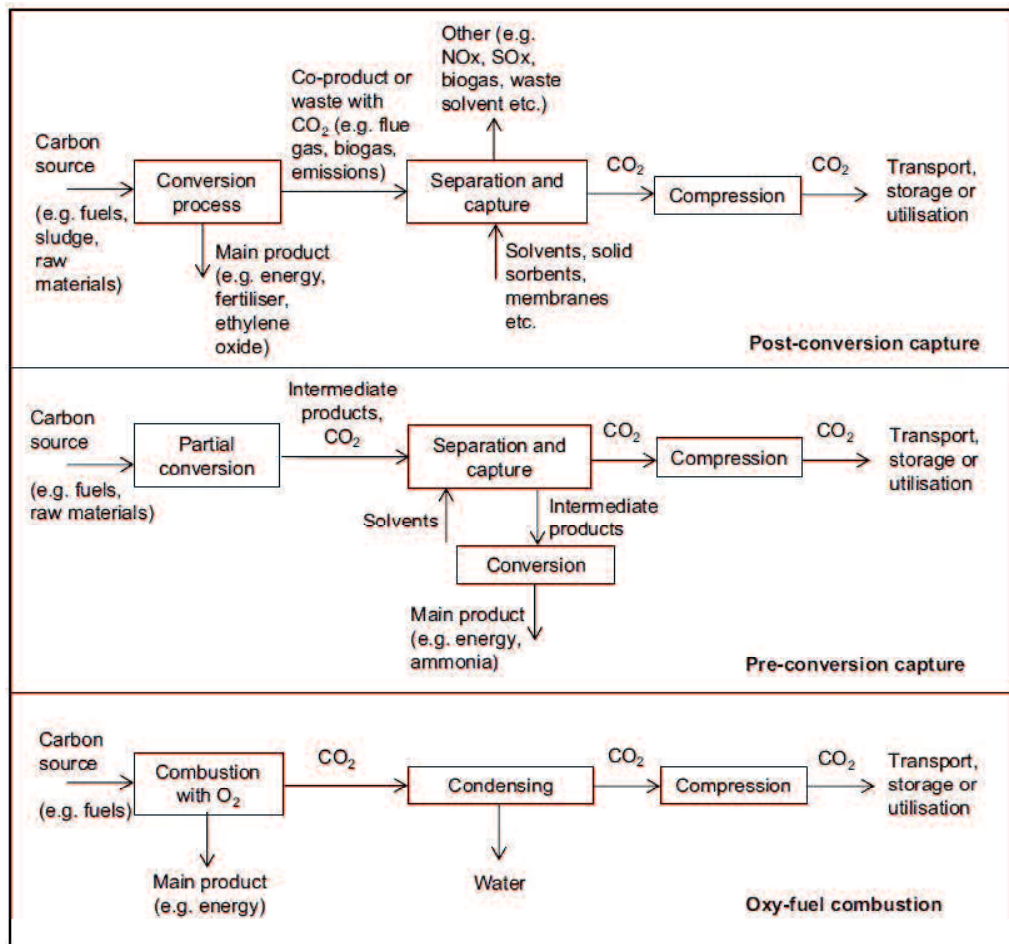


**Figure 2.6** Carbon capture options (Cuéllar-Franca & Azapagic, 2015).

**Oxygen-fuel combustion** process actually modified post – combustion method which uses pure O<sub>2</sub>, instead of air, to burn fossil fuel. The combustion with O<sub>2</sub> will produce the flue gas with high content of CO<sub>2</sub> (80 – 98% depend on used fuel) (Leung *et al.*, 2014) and free-form nitrogen, NO and NO<sub>2</sub> (Cuéllar-Franca & Azapagic, 2015). The high CO<sub>2</sub> concentration of over 80% will reduce the cost of compressing, transporting, and storing. Nevertheless, due to the

high consumption of oxygen, it is expensive or needs to improve the advanced oxygen separation to reduce the energy and cost requirements.

### 2.2.3 CO<sub>2</sub> separation techniques

Several technologies are existing for separation from the flue gas, including absorption, adsorption, cryogenics, and membrane as depicted in **Figure 2.7**. The choice of the appropriate technology relies strongly on the characteristics or properties of the exhausted gas and plant (Olajire, 2010).

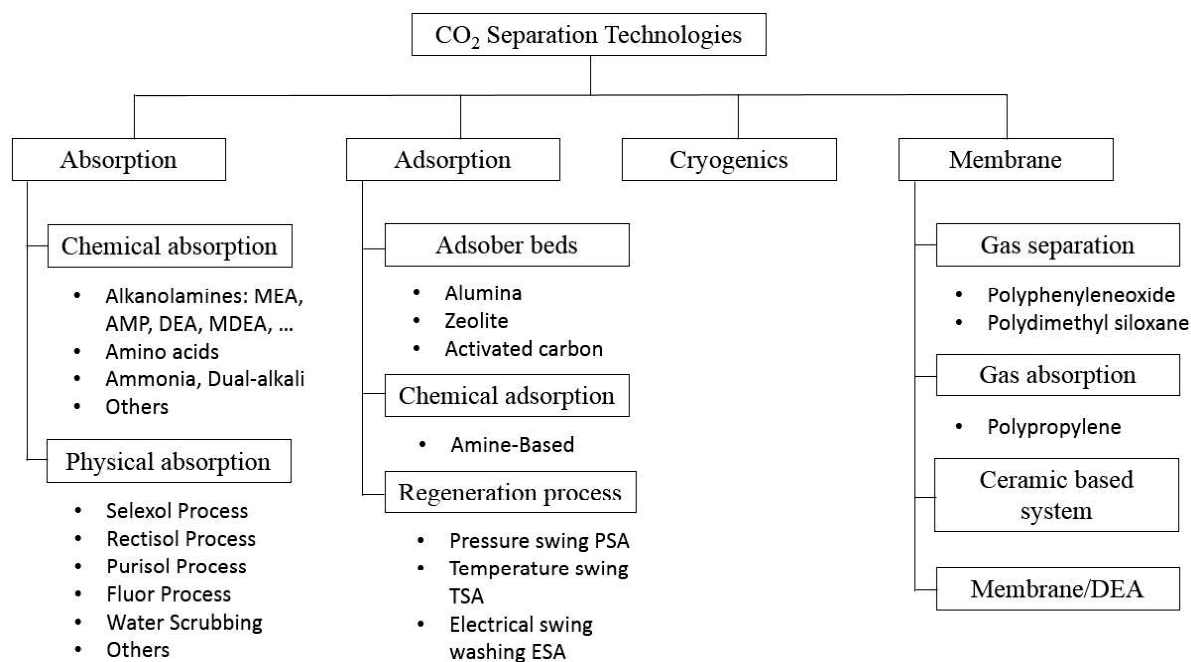


**Figure 2.7** Technology options for CO<sub>2</sub> separation (modified from (Olajire, 2010)).

#### 2.2.3.1 Absorption

Absorption has well-established process in use of CO<sub>2</sub> capture for at least 60 years. The selected solvents have to satisfy conditions: a high capacity of CO<sub>2</sub> absorption, high absorption kinetics, negligible vapor pressure, high chemical and thermal stability, and non-hazard (Ma'mun, 2005). There is two types of absorption: chemical and physical absorption.

Chemical absorption is recommended in use with the low to moderate CO<sub>2</sub> partial pressure (Olajire, 2010). This technique relies on the acid-base neutralization reactions between acidic CO<sub>2</sub> and alkaline solvents (Olajire, 2010). Normally, the flue gas containing CO<sub>2</sub> is firstly introduced from the bottom of the absorber and interactions counter-currently with CO<sub>2</sub>-lean

absorbent entering from the top of absorber (Mondal *et al.*, 2012, Leung *et al.*, 2014). Next, the CO<sub>2</sub>-rich solvent is fed to regenerator to recover solvent and CO<sub>2</sub> through a stripping or regenerative process by heating and/or depressurization (Mondal *et al.*, 2012, Leung *et al.*, 2014). The operation pressure is around 1.0 bar and the temperature in the absorber of 40 – 60 °C and in the stripper of 120 – 140 °C (Yu *et al.*, 2012). Some of typical chemical absorbents are monoethanol amine (MEA), diethanol amine (DEA), N-methyldiethanolamine (MDEA), 2-amino 2-methyl 1-propanol (AMP), piperazine (PZ), NaOH, NH<sub>3</sub>, K<sub>2</sub>CO<sub>3</sub>, KOH, Na<sub>2</sub>CO<sub>3</sub>. Among these solvents, alkanolamines are extensively applied for CO<sub>2</sub> capture. The advantages include high removal efficiency (more than 90%), quick reaction, and possibly commercialized application. In contrast, many negatives – low CO<sub>2</sub> loading capacity, high corrosion rate for the equipment, the degradation of amine by the presence of SO<sub>2</sub>, NO<sub>2</sub>, HCl/HF, and O<sub>2</sub> in the flue gas, creation of volatile compounds, and high energy consumption for regenerating – exist when using amine solvent (Leung *et al.*, 2014, Mondal *et al.*, 2012, Olajire, 2010, Nik *et al.*, 2011). The alternative solvent for amine is ammonia. The aqueous ammonia scrubbing technology can prevent the capacity, degradation, and corrosion problem. The energy requirement for regeneration in this method is also lower than amine absorption. Furthermore, the by-products of this technique are ammonium bicarbonate, ammonium nitrate, ammonium sulfate which are used as fertilizer (Olajire, 2010).

For physical absorption, CO<sub>2</sub> is absorbed in an absorbent under a high pressure and a low temperature according to Henry's Law. The desorption is accomplished by reducing pressure and enhancing temperature (Yu *et al.*, 2012). Solvents in physical absorption are organic solvents which can physically absorb CO<sub>2</sub> without chemical reactions. In physical absorption process, CO<sub>2</sub> is removed from the inlet gas by the difference between the solubility of CO<sub>2</sub> and that of other gases. Based on Henry's Law, the solubility of a certain gas depends on this gas's partial pressure and the temperature. Therefore, higher CO<sub>2</sub> partial pressure and lower temperature are, higher amount of CO<sub>2</sub> molecules absorb in the solvents. Noticeably, because in physical absorption, it does not happen chemical reaction and the absorption is only physical interaction between gas and liquid, the interaction between CO<sub>2</sub> and the absorbent is weak which provide circumstances to decrease the energy requirement for regeneration (Olajire, 2010). Selexol process is one of physical absorption technique. The Selexol process uses dimethylether of polyethylene glycol as absorption solvent at 0 – 5 °C for selective or

simultaneous removal of CO<sub>2</sub> and H<sub>2</sub>S (Olajire, 2010). Methanol is a solvent of Rectisol process. This process is normally carry out at – 30 to – 100°F and deal with the flue gas containing sulfur and low quantities of ethane and heavier component (Yu *et al.*, 2012, Weiss, 1988). Fluor process which uses propylen carbonate is favored for the feed gas with CO<sub>2</sub> partial pressure of over 60 psi (Yu *et al.*, 2012). Based on physical absorption, CO<sub>2</sub> can be captured in the system with low energy requirement for regeneration (20% lower than chemical absorption), low vapor pressure, low toxicity, and low corrosive rate (Songolzadeh *et al.*, 2014).

### **2.2.3.2 Water scrubbing**

Water scrubbing is classified into physical absorption group where water is used as an absorbent for dissolving CO<sub>2</sub>. This method generally applies in upgrading biogas, landfill, and natural gas. Biogas, landfill gas and natural gas typically contains CH<sub>4</sub>, CO<sub>2</sub>, and the trace amount of H<sub>2</sub>S, N<sub>2</sub>, H<sub>2</sub>O, NH<sub>3</sub> and O<sub>2</sub> (Andriani *et al.*, 2014, Petersson & Wellinger, 2009). Upgrading is the process to improve the fuel standard which is in direct proportion to methane content in such gases when removing unwanted components, especially CO<sub>2</sub> and H<sub>2</sub>S. Because H<sub>2</sub>S is poisonous and causes corrosion, it needs to pre-separate (Sun *et al.*, 2015). The principle of water scrubbing process is based on the approximately 25 times lower solubility of methane in the comparison of CO<sub>2</sub> (Bauer *et al.*, 2013).

The biogas containing mostly CH<sub>4</sub> and CO<sub>2</sub> are compressed and fed into the bottom of a water scrubber column at high pressure of 1.0 – 2.0 MPa while high pressure water is added from the top of the scrubber to attain a gas – liquid counter flow (Ryckebosch *et al.*, 2011). Due to much higher solubility, CO<sub>2</sub> dissolves into water while CH<sub>4</sub> still remain in gas phase. However, since CO<sub>2</sub> has a low solubility in water, the high pressure of 1.0 – 2.0 MPa has to remain in the water scrubbing process to enhance CO<sub>2</sub> dissolving rate. Besides, the scrubber column needs to be equipped with random packing to enlarge the specific surface for gas-liquid contact (Ryckebosch *et al.*, 2011). Furthermore, the small value of CO<sub>2</sub> diffusivity in water (0.138 cm<sup>2</sup>/s) reveals the CO<sub>2</sub> mass transfer from the gas phase into the water is very slow, followed by a slow CO<sub>2</sub> absorption rate in water and long retention time of liquid phase (Andriani *et al.*, 2014). To deal with this issue, a large column/absorption tower volume is required (Andriani *et al.*, 2014).

Water scrubbing can be considered as the simplest process and the best option in term of operation costs (Cozma *et al.*, 2013, Andriani *et al.*, 2014, Ofori-Boateng & Kwofie, 2009). When water is used as solvent, based on the cost of water, the availability/possibility of other alternative water source (i.e. water from a sewage treatment plant or seawater), it is available to choose tween two options: (1) to regenerate by de-pressuring or stripping with air and recycle water or (2) to use water only for once in a single pass system. Herein, with no chemical utilization and no toxic by-products, water scrubbing is assessed to be a better option for the environment when compared with other methods such as chemical scrubbing, cryogenic separation, pressure swing adsorption, and membrane separation (Cozma *et al.*, 2013).

### **2.2.3.3 Adsorption**

Adsorption is the removal process by attaching one or few components on certain solid phase. This process happens with the aid of intermolecular force between gases and solid surface (Mondal *et al.*, 2012). Adsorption capture technology requires to select and develop an adsorbent owning characteristics including low cost raw materials, low heat capacity, high CO<sub>2</sub> adsorption capacity, high CO<sub>2</sub> selectivity, quick adsorption/desorption kinetics, and good thermal chemical and mechanical stabilities under extensive cycling (Choi *et al.*, 2009, Sayari & Belmabkhout, 2010, Yu *et al.*, 2012). Similar to absorption separation, the CO<sub>2</sub> adsorbents place into two main groups: physical and chemical adsorbents.

The popular physical adsorbents are carbonaceous adsorbents (such as activated carbon), zeolites, and metal-organic frameworks (MOFs). Due to several advantages – low cost, huge amount availability, high thermal stability, and low moisture sensitivity – activated carbon have full-growth in micro- and mesoporosities that are suitable for industrial and technological-scale (Olajire, 2010, Yu *et al.*, 2012). In order to enhance the CO<sub>2</sub> adsorption ability and selectivity, it needs to increase surface area and pore structure of the carbonaceous material or to enhance the alkalinity via the chemical modification on surface of materials (Yu *et al.*, 2012). Yet, the selectivity CO<sub>2</sub>/N<sub>2</sub> of activated carbon is relatively low. Meanwhile, that value of zeolite is 5 – 10 times more than carbonaceous materials (Songolzadeh *et al.*, 2014). The adsorption capacity of zeolites strongly depends on their size, charge density, and chemical composition of cations in their porous structures (Wang *et al.*, 2011). A new adsorbent which attracts numerous interests is metal-organic frameworks (MOFs) which are crystalline with



two- or three-dimensional porous structures (Songolzadeh *et al.*, 2014). This material possesses high surface area, controllable pore structures, and tunable pore surface properties which is enabled to tune by adjusting the metallic clusters or the organic ligands (Yu *et al.*, 2012). However, the application of MOFs needs more practical.

Chemical adsorption is motivated by a chemical reaction happening at the exposed surface (Songolzadeh *et al.*, 2014). The interaction or reaction between acidic CO<sub>2</sub> molecules and modified principally active sites on the surface enables CO<sub>2</sub> adsorption via the production of covalent bonding (Yu *et al.*, 2012). The chemical adsorbents categories into many groups: metal oxide (CaO, MgO), metal salts from alkali metal (Li<sub>2</sub>ZrO<sub>3</sub>, Li<sub>4</sub>SiO<sub>4</sub>), hydrotalcites and double salts, and organics (amine-based adsorbents) (Martunus *et al.*, 2012, Yu *et al.*, 2012). For the type of metal oxide, CaO is used widely due to its high CO<sub>2</sub> adsorption capacity, high raw material availability, and low cost. The adsorption process by metal oxide contains many cycles consisting of transforming metal oxide to metal carbonates at 923 K, regenerating sorbent in carbonation reactor at 1123 K, and concentrating CO<sub>2</sub> to storage (Dou *et al.*, 2010, Kotyczka-Moranska *et al.*, 2012). The adsorption reaction of CO<sub>2</sub> by lithium zirconate (Li<sub>2</sub>ZrO<sub>3</sub>) is reversible at 723 – 863 K with the capacity of 4.85 mol CO<sub>2</sub>/kg sorbent (Olajire, 2010, Songolzadeh *et al.*, 2014, Yang *et al.*, 2008). Comparing to lithium zirconate, lithium silicate (Li<sub>4</sub>SiO<sub>4</sub>) can adsorb CO<sub>2</sub> with a larger capacity of 8.2 mol CO<sub>2</sub>/kg sorbent at 993 K (Yang *et al.*, 2008).

The main benefits of the adsorption method are no by-product such as wastewater and low energy. The drawbacks of this method are low CO<sub>2</sub> selectivity and capacity of materials, lower removal capacity when comparing to absorption and cryogenics method, and requirements for generation and reusability of sorbents (Mondal *et al.*, 2012).

The adsorbent generation process is essential and compulsive in the adsorption systems. Four main generation strategies are pressure swing adsorption (PSA), temperature swing adsorption (TSA), vacuum swing adsorption (VSA), and electric swing adsorption (ESA). In PSA, the feed gas enters the packed bed at elevated pressure and low temperature until the adsorption of CO<sub>2</sub> achieves equilibrium conditions at the exit (Mondal *et al.*, 2012). Stopping the flow of feed gas, depressurizing and elutriating the adsorbed components with a gas owning low absorptivity can regenerate the beds (Mondal *et al.*, 2012). In TSA, the regeneration is

operated by rising system temperature with hot air and steam (120 – 135 °C). The regeneration time of TSA is longer than PSA but the CO<sub>2</sub> recovery of TSA is more than 95% while that of PSA is more than 80% (Leung *et al.*, 2014). VSA is preferred as special PSA with the regeneration takes place at lower atmospheric pressure. The ESA uses a low voltage electric current to regenerate sorbents. In ESA, heat is regenerated by the Joule effect. ESA can be concerned more cost-effective than PSA and TAS because of several benefits including less heat demanded, fast heating rate, higher desorption kinetics and dynamics, and independent control of gas and heat flowrates (An *et al.*, 2011, Yu *et al.*, 2012).

#### **2.2.3.4 Cryogenic distillation**

CO<sub>2</sub> can be separated, condensed, and purified from the mixed gas through cryogenic distillation method which uses fractional condensation and distillation technique at low pressure (-100 to -135 °C) and high pressure (100 – 200 atm) (Leung *et al.*, 2014, Olajire, 2010). Herein, CO<sub>2</sub> recovered rate can get more than 90%. The innovated cryogenic CO<sub>2</sub> capture using Stirling coolers which consisting of four processes – isothermal expansion, cooling under a constant condition, isothermal compression, and heating under a constant condition – can separate 96% CO<sub>2</sub> from the flue gas with 1.5 MJ/kg CO<sub>2</sub> energy consumption (Song *et al.*, 2012, Songolzadeh *et al.*, 2014). With 1.8 MJ/kg CO<sub>2</sub> energy consumption Another innovated cryogenic process for capturing CO<sub>2</sub> using dynamically operated packed beds can recover 99% of CO<sub>2</sub> from an inlet gas owning 10 vol.% CO<sub>2</sub> and 1 vol.% H<sub>2</sub>O (Song *et al.*, 2012, Tuinier *et al.*, 2011, Songolzadeh *et al.*, 2014).

One advantage of cryogenic distillation is to recover CO<sub>2</sub> as liquid CO<sub>2</sub> which can be easily piped or pumped to the injection site for enhanced oil and coal-bed methane recovery (Olajire, 2010). Because of no solvents and other components, this method is eco-friendly. The cryogenic separation can be utilized for the industrial-scale application (Songolzadeh *et al.*, 2014). However, because the presence of SO<sub>x</sub>, NO<sub>x</sub>, and H<sub>2</sub>O in feed gas can lead to the plugging by ice, dropping of pressure, corrosion, and fouling, it requires to firstly remove all trace of water which means that increasing operation cost (Mondal *et al.*, 2012). Another limitation is high energy consumption to remain the refrigeration condition and high pressure which also result in several operational issues (Songolzadeh *et al.*, 2014, Shimekit & Mukhtar, 2012, Ravanchi *et al.*, 2011, Lively *et al.*, 2012).

### **2.2.3.5 Membrane**

Membrane capture is a novel method which applies selective membranes to separate particular components from a feed gas (Olajire, 2010). Membranes are semi-permeable barriers which can capture substances by various techniques (solution/diffusion, adsorption/diffusion, molecular sieve, and ionic transport) (Olajire, 2010). Membranes can be made of various materials such as organic (polymetric) and inorganic (carbon, zeolite, ceramic, or metallic) and can be porous or non-porous (Mondal *et al.*, 2012). The principle of membranes process is divided into two major groups: gas separation and gas absorption. Gas separation is completed under the mechanism of selective permeation of mixture components through the pores of the membrane leading to one substance diffuses over the membrane quicker than others (Mondal *et al.*, 2012). Gas absorption membranes are hybrid systems consisting of microporous solid membrane that supports for the contacting of gas and liquid (Babu, 2014). The CO<sub>2</sub> can diffuse through the membrane and it is separated by the absorption into a liquid such as a amine. With high efficient membrane, the CO<sub>2</sub> removal efficiency can reach 82% - 88% (Audus, 2000, Gielen, 2003).

Membrane capture technology is a continuous, steady-state, clean, simple, and easy to scale up process and ideal as an energy-saving method for CO<sub>2</sub> separation (Songolzadeh *et al.*, 2014). Other gains of this method are no generation energy required and no waste stream. On the other hand, due to the fact that membrane capture cannot continuously achieve a high percentage of separation, multiple stages, and recycling are obligatory (Olajire, 2010). Membrane process is not suitable for high flow rate applications (Songolzadeh *et al.*, 2014). The stability of membrane under high pressure or temperature and the sensitivity of SO<sub>x</sub> and NO<sub>x</sub> are also essential concerns when applying membrane capture. Operational issues including membrane wetting, fouling, and plugging can occur (González-Salazar, 2015).

### **2.2.4 CO<sub>2</sub> transport**

Commercially, CCS requires an infrastructure for the transportation of trapped CO<sub>2</sub> from the emitted point to storage sites or to CO<sub>2</sub> industrial utilization facilities. Pipelines are seen as the most practical method for onshore transport of high quantities of CO<sub>2</sub> via long distances (Leung *et al.*, 2014, Svensson *et al.*, 2004). In order to reach lower friction drop along a pipeline per unit mass of CO<sub>2</sub>, CO<sub>2</sub> is transported efficiently and economically in the dense phases such

as liquid and supercritical regime (Johnsen *et al.*, 2011, Witkowski *et al.*, 2015). Supercritical form at which CO<sub>2</sub> exists as a fluid state is a favored condition for pipelining CO<sub>2</sub>. The supercritical state is held at or above CO<sub>2</sub> critical temperature (31.1 °C) and critical pressure (72.9 atm) (Al-Marzouqi *et al.*, 2007). Hence, the representative range of temperature and pressure for a CO<sub>2</sub> pipeline are 85 – 150 bar and 13 – 44 °C, respectively to guarantee a stable single-phase flow in the pipeline (Leung *et al.*, 2014, Forbes *et al.*, 2008). However, if CO<sub>2</sub> stream contains impurities, the boundaries of pressure and temperature can be changed. The presence of water concentration above 50 ppm can be the reason leading to the corrosion problems due to the generation of carbonic acid inside the pipelines (Leung *et al.*, 2014).

In case of employing pipeline for CO<sub>2</sub> transportation, it needs to concern about the effects of corrosion and potential brittle fractures propagation – which can happen by the harsh cooling due to the leakage of supercritical CO<sub>2</sub> – on the pipelines' integrity of long-term exposure to CO<sub>2</sub> fluxes (Leung *et al.*, 2014).

### 2.2.5 CO<sub>2</sub> storage

After capturing, CO<sub>2</sub> can be compressed, shipped/pipelined, pumped down, and stored in the ground, ocean or as mineral carbonate (Metz *et al.*, 2005, Li *et al.*, 2013). Among these options, CO<sub>2</sub> storage in geological formations including depleted oil and gas reservoirs, deep saline aquifers, and coal bed formations (unmineable coal beds) has recently been a potential and promising choice for storing the large quantities of CO<sub>2</sub> (Van der Zwaan & Smekens, 2009, Yang *et al.*, 2010, Celia & Nordbotten, 2009) (**Figure 2.8**). Geological storage is operated by the injection at the depths of over 1 km (Aydin *et al.*, 2010). Temperature will be higher than 31 °C and pressures are more than 100 atm to give densities of the order of 500 kg/m<sup>3</sup> (Gibbins & Chalmers, 2008, Aydin *et al.*, 2010). A typical geological storage site can store numerous tens of million tonnes of trapped CO<sub>2</sub> by diverse physical and chemical methods (Doughty, 2006, Leung *et al.*, 2014).

The geological formations happen in the basins occupied by sedimentary rocks which contain the alternating layer of sand, silt, clay, carbonate, and evaporates. Herein, the sand layers supply storage space while silt, clay, and evaporate layers equip the covers above the storage reservoir which can trap the oil, natural gas, and CO<sub>2</sub> for millions of years (Benson & Orr, 2008). The critical factors and requirements for choosing CO<sub>2</sub> geological storage site are

suitable porosity, thickness, and permeability of reservoir rock, a cap rock with good sealing ability, a stable geological environment, distance from the CO<sub>2</sub> source, potential leakage and economic matters (Leung *et al.*, 2014, Solomon *et al.*, 2008, Bachu, 2000).

The primary apprehension of CO<sub>2</sub> storage is the potential of leakage and the related damages which happen if a concentrated CO<sub>2</sub> stream escapes to the environment (Cuéllar-Franca & Azapagic, 2015). Based on the statistics, annual leakage rates fluctuate from 0.00001% to 1% up to the structure of geological formations and others (Metz *et al.*, 2005, Singh *et al.*, 2011, Pehnt & Henkel, 2009).

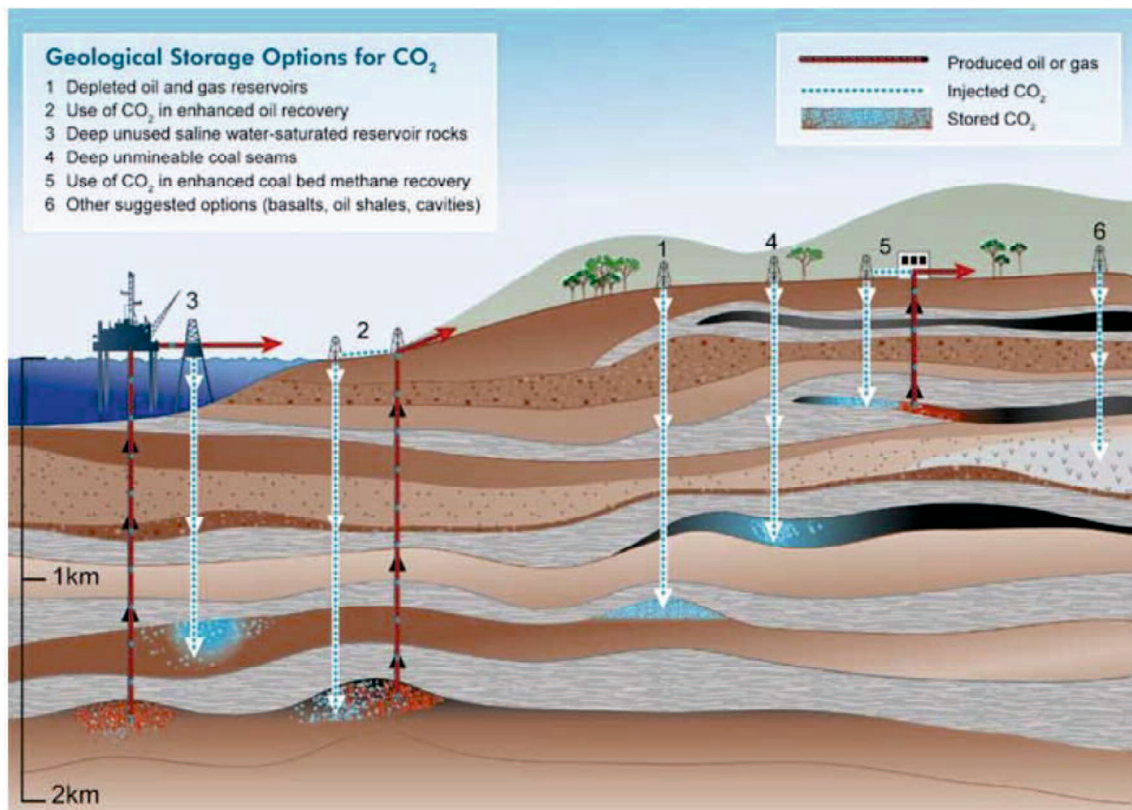


**Figure 2.8** Options for storing CO<sub>2</sub> in deep underground geological formation (Metz *et al.*, 2005, Cook, 1999).

### 2.2.6 CO<sub>2</sub> utilization

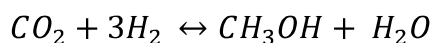
Beside CO<sub>2</sub> storage, CO<sub>2</sub> utilization can be seen as the potential and commercial solution which can support to accomplish CCS in the large scale. CO<sub>2</sub> can be applied widely in food industry, enhanced oil recovery (EOR), chemicals, and fuels conversion, mineral carbonation, biofuels, and biomass production and etc.

### 2.2.6.1 Direct utilization of CO<sub>2</sub>

In the food and beverage industry, CO<sub>2</sub> is normally used as a carbonating agent, preservative, packing gas, solvent for the extraction of flavors and in the decaffeination process (Cuéllar-Franca & Azapagic, 2015). CO<sub>2</sub> is an essential agent for synthesizing respiration stimulant and is an intermediate in the synthesis of drugs in pharmaceutical industry (Yu *et al.*, 2008). Other applications can be seen in the production of refrigerants, fire extinguishing, dry ice, fertilizer, ammonia and urea.

### 2.2.6.2 Conversion of CO<sub>2</sub> into chemicals and fuels

The conversion of CO<sub>2</sub> into chemicals and fuels is one of the interesting options for CO<sub>2</sub> utilization. CO<sub>2</sub> molecules can be utilized as a precursor for organic compounds, for example, acrylates, carbonates, or polymers in carboxylation reactions. By the reduction reactions to break C=O bonds, methane, methanol, sync gas, urea, and formic acids can be created from CO<sub>2</sub> (Yu *et al.*, 2008, Styring *et al.*, 2011). For example, methanol production can be achieved by the catalytic hydrogenative conversion of CO<sub>2</sub> with hydrogen (Rahman *et al.*, 2017). The common catalysts are metals and their oxides especially the combination of copper and zinc oxide (Nitta *et al.*, 1994, Rahman *et al.*, 2017). The reaction is:



### 2.2.6.3 Mineral carbonation

Mineral carbonation is the process that CO<sub>2</sub> undergoes a chemical reaction with a metal oxide (commonly magnesium oxide or calcium oxide) to create carbonates (Metz *et al.*, 2005, Li *et al.*, 2013). Mineral carbonation includes several reactions which can occur in a single (direct carbonation) or a multi-step (indirect carbonation) process (Cuéllar-Franca & Azapagic, 2015, Metz *et al.*, 2005). With the single step process, the extraction of metal from the mineral compounds and the carbonate precipitation happens concurrently in the same reactor (Cuéllar-Franca & Azapagic, 2015). Meanwhile, the process in indirect carbonation composes of three reactions (Metz *et al.*, 2005, Khoo *et al.*, 2011). The first step is to separate metal from the minerals with the aid of an extracting agent such as hydrochloric acids or molten salts (Cuéllar-Franca & Azapagic, 2015). Next step is to transform metal into the hydroxide form by many hydration reactions. At the final step, the captured CO<sub>2</sub> reacts with metal in hydroxide form to

get a carbonates (Cuéllar-Franca & Azapagic, 2015). The significant achievement of mineral carbonation is the formation of stable carbonates which enable to store CO<sub>2</sub> for several years without the threat of CO<sub>2</sub> leakage (Cuéllar-Franca & Azapagic, 2015) or to use for other purposes.

#### **2.2.6.4 Enhanced oil and coal-bed methane recovery**

It cannot deny that enhanced oil recovery (EOR) and coal-bed methane recovery (ECBM) are promising applications in term of increasing CO<sub>2</sub> utilization. In EOR, because CO<sub>2</sub> is injected into depleted oil/gas reservoirs, CO<sub>2</sub> pressure can be increased and the driving force to extract crude oil and gases can be provided (Leung *et al.*, 2014). EOR can reach the extraction productivity for available crude oil in the well of 30 – 60% compared to primary and secondary extraction which recover 20 – 40% (Cuéllar-Franca & Azapagic, 2015). Similarly, in ECBM, the recovery of trapped methane in the porous structure of coal seams can be accomplished by the injection of CO<sub>2</sub> into the deep coal beds (Leung *et al.*, 2014).

#### **2.2.6.5 Microalgae**

The new approach for CO<sub>2</sub> utilization is the use of captured CO<sub>2</sub> or CO<sub>2</sub> in the flue gas to cultivate microalgae which can use to produce biofuels and biomass (Brennan & Owende, 2010, Li *et al.*, 2008, Singh & Ahluwalia, 2013). Because microalgae use CO<sub>2</sub> as a carbon source, without the supply of CO<sub>2</sub>, they cannot grow up (Klinthong *et al.*, 2015). The usage of microalgae for CO<sub>2</sub> consumption has many advantages because the CO<sub>2</sub> fixation efficiency of microalgae and cyanobacteria is 10 – 50 times better than terrestrial plants (Costa *et al.*, 2000, Usui & Ikenouchi, 1997) and their biomass can also be utilized as feedstock for various biofuels, medications, cosmetic, food for humans, and livestock (de Morais & Costa, 2007, Ho *et al.*, 2011, Singh & Ahluwalia, 2013). Generally, using microalgae to consume and fix CO<sub>2</sub> provide an extremely promising tool to not only mitigate CO<sub>2</sub> but also utilize CO<sub>2</sub> for generating numerous value product especially biofuels which are the alternative option for energy supply (**Figure 2.9**).

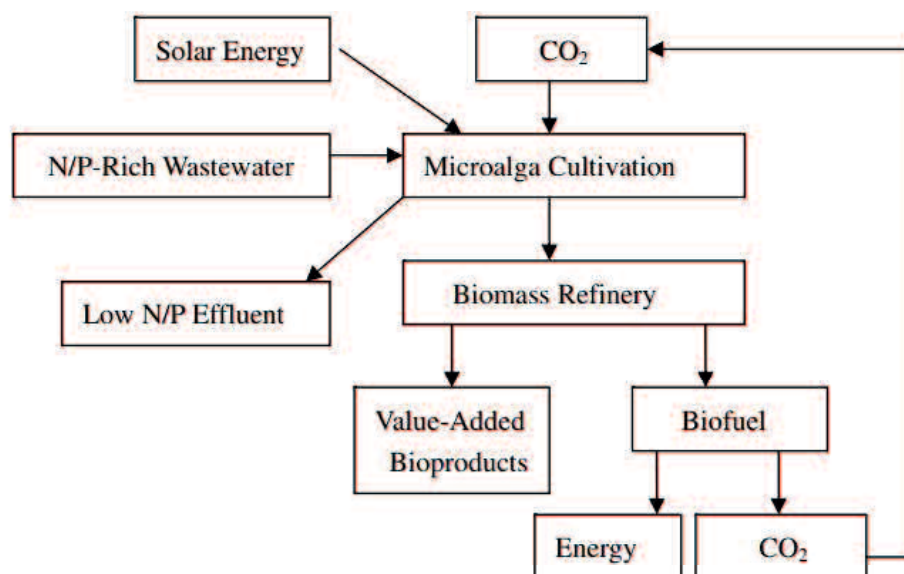


**Figure 2.9** A flow-chart of microalgae system for combined biofuels production, CO<sub>2</sub> bio-mitigation, and N/P removal from wastewater (Wang *et al.*, 2008).

## 2.3 Potential application of microbubble and liquid/water-film in the removal of carbon dioxide using water scrubbing

### 2.3.1 Characteristics of microbubble

Microbubble (MB) is defined as a fine bubble with the diameter being less than 100  $\mu\text{m}$  (Tabei *et al.*, 2007, Parmar & Majumder, 2014) and usually 10 – 50  $\mu\text{m}$  (Agarwal *et al.*, 2011, Takahashi *et al.*, 2007). Microbubbles have three main components including gas phase, shell and liquid/aqueous phase (Bredwell & Worden, 1998, Parmar & Majumder, 2013) as shown in **Figure 2.10**. The gas phase contains a single gas or combination of gases which is used to create the differences in partial pressure and gas osmotic pressure stabilizing the bubbles (Parmar & Majumder, 2013). Between the gas phase and the surrounding bulk liquid phase is a surfactant-stabilized shell of water which existed as the liquid film surrounding the gas phase (Bredwell & Worden, 1998). The surfactant molecules attach an electric double layer to reduce bubble coalescence by electrical repulsion of adjacent bubbles (Bredwell & Worden, 1998). Hence, microbubbles exhibit colloidal properties. The elasticity of shell material has a vital role in increasing the residence time of bubbles in liquid phase (Parmar & Majumder, 2013).



## Bulk Water

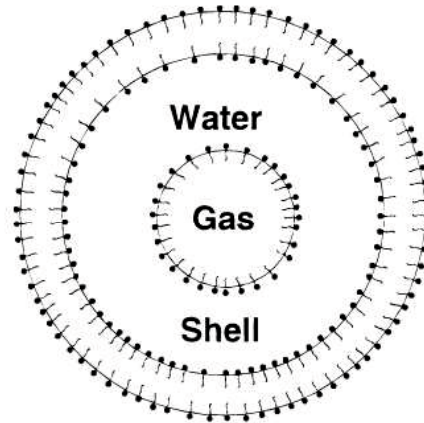


**Figure 2.10** Schematic structure of microbubble (Bredwell & Worden, 1998).

The differential behaviors of various types of bubble in a bulk-liquid medium are depicted in **Figure 2.11**. The reason for making MBs differing from the ordinary bubbles is that MBs can shrink their size is below a critical value (Xu *et al.*, 2008). The increasing of internal pressure leads to the shrinking of MBs. According to Young-Laplace equation for the difference between the external and internal pressure of a bubble  $\Delta P = 2\gamma/r$  (where  $\Delta P$  is the pressure difference,  $\gamma$  is the surface tension and  $R$  is the radius of a bubble), the internal pressure of bubble increases with a decreasing of bubble size (Xu *et al.*, 2008). The increasing of pressure is the reason for the dispersion of entrapped gases from a high-pressure region (internal bubble) to a low-pressure region (surrounding environment) (Xu *et al.*, 2008). Generally, as a consequence of decreasing bubble size and increasing internal pressure, bubbles shrink faster, burst into liquid bulk and finally disappear, followed by high mass transfer rate of gas and liquid. This process means that the entrapped gases diffuse out of the MBs and dissolve into outside liquid phase (Xu *et al.*, 2008).

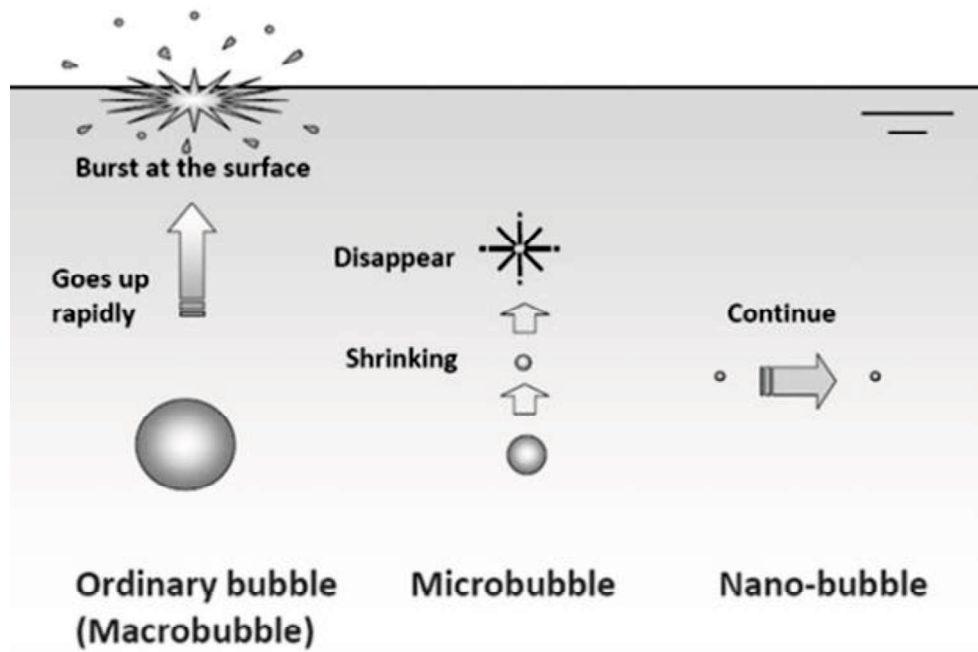


**Figure 2.11** The behaviors of macro, micro and nanobubbles in water (Agarwal *et al.*, 2011).

As shown in **Figure 2.12**, comparing to the conventional large bubbles (macro-bubbles), microbubbles present many attractive characteristics such as a much higher surface area-to-volume ratio (Xu *et al.*, 2008, Ushikubo *et al.*, 2010), or higher mass transfer rate (Parmar & Majumder, 2014) which can improve the application of MBs in many fields. In general, the important advantages of MBs are small buoyancy rate, slow rising speed, reduced frictional resistance, high inertial pressure of bubble, large gas-liquid interfacial area and long residence time (Parmar & Majumder, 2013, Xu *et al.*, 2008, Temesgen *et al.*, 2017). These properties improve the mass transfer efficiency, gas dissolution rate and gas dissolving concentration, hence, MBs is applied widely in supplying oxygen for aeration systems (aquaculture, hydroponic cultivation, aerobic fermentation, and aerobic treatment plants) (Weber & Agblevor, 2005, Hensirisak *et al.*, 2002, Park & Kurata, 2009) and in disinfection (Sumikura *et al.*, 2007, Zhang *et al.*, 2013). Furthermore, the negative zeta potential of MBs in a solution is a significant property which defines the interaction between bubbles and other materials such as oil droplets and solid particles (Parmar & Majumder, 2013). Therefore, MBs are also utilized for water treatment by flotation (Bui *et al.*, 2015, Van Le *et al.*, 2013).

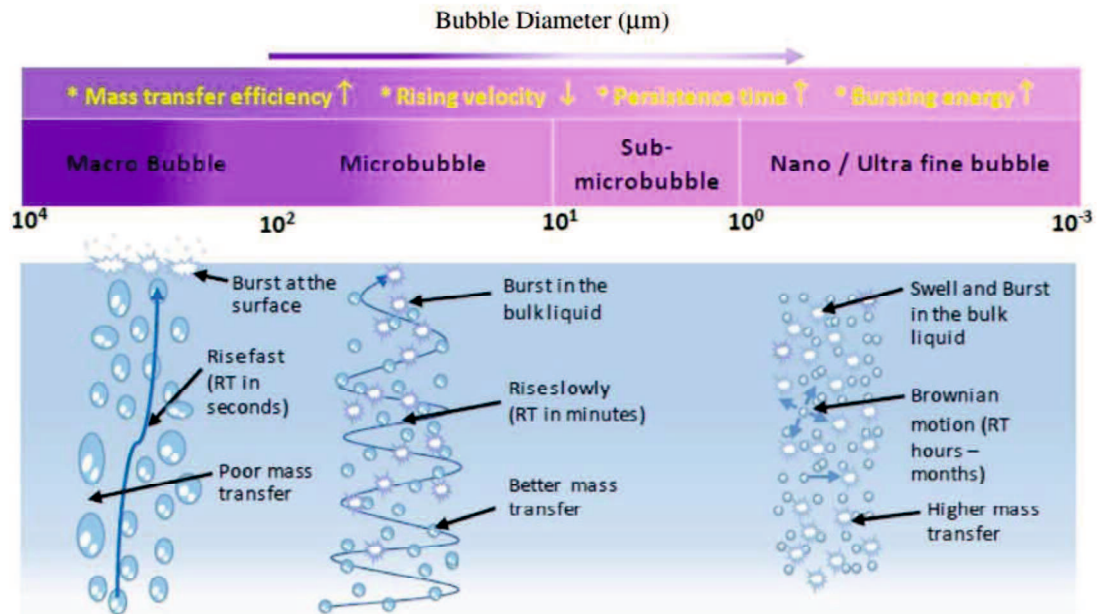


**Figure 2.12** The major properties of bubbles according to bubble sizes (Temesgen *et al.*, 2017).

### 2.3.2 Characteristics of liquid-film

Liquid-film is actually an ultrathin layer of fluid film wrapping around the bulk of one gas or a combination of gases. The presence of liquid-films in the liquid phase can enlarge noticeable the effective interfacial contact area and mass transfer between gas and liquid phase (Imai & Zhu, 2011). The total transfer of gas in liquid phase comprises of bubble transfer and surface transfer. Normally, when taking oxygen as an example, bubble transfer occupies two-thirds of total oxygen transfer while surface transfer only contribute the rest of portion (Zhu *et al.*, 2007b). To deal with this issue, liquid-film is usually used to enhance the bubble mass transfer, particularly surface transfer.

Distinguishing to conventional system with ordinary bubble, in liquid-film system, the improvement of gas transfer and gas dissolution is achieved through the dual-fold gas provisions (see **Figure 2.13**). The driving force of mass transfer across gas bubbles is the partial pressure gradients between the inside bubble and the neighboring environment outside (Zhu *et al.*, 2007b). In case of this, with liquid-film, the transfer of gas such as O<sub>2</sub>, CO<sub>2</sub> or N<sub>2</sub> can simultaneously occur through two sides of the thin liquid-film which are across the inner interface (gas bubble and liquid-film) and across the outer interface (surrounding area and liquid-film) (Zhu *et al.*, 2007b, Imai & Zhu, 2011, Zhu *et al.*, 2007a). As a result of this, the

boundary and interfacial area between gas and liquid phase enlarge for several times which finally enhance dramatically the gas transfer efficiency and gas dissolution rate.

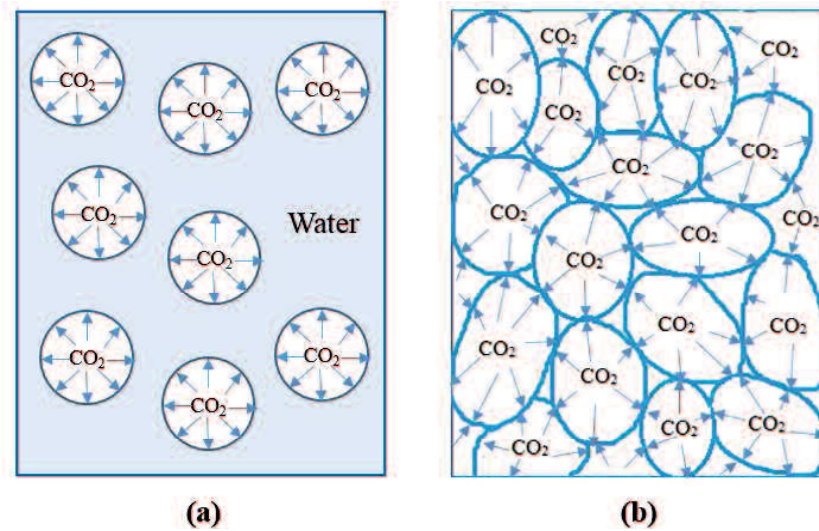


**Figure 2.13** Schematic diagram of (a) conventional bubbles and (b) liquid-films.

The application of liquid-film-forming apparatus in the diffused aeration system can improve not only the oxygen transfer for 5.3 times higher but also total volumetric mass transfer coefficient by 37% in the comparison with conventional aeration system (Zhu *et al.*, 2007a). Jamnongwong and his group concluded that the mechanism of oxygen transfer in liquid-film-forming apparatus can be divided into 4 categories: (1) Conventional mechanism ( $O_2$  transfers from the generated bubble outside the cone of liquid-film-forming apparatus), (2) Bubble collection mechanism ( $O_2$  transfers from the packed bubble inside the cone of liquid-film-forming apparatus), (3) Bubble recirculation mechanism ( $O_2$  transfers from the movement of packed bubbles into the liquid phase) and (4) Bubble-liquid foam mechanism ( $O_2$  transfers from the generated foam at the liquid surface) (Jamnongwong *et al.*, 2016). This group also reported that the volumetric mass transfer coefficient of the aeration system with liquid-film-forming apparatus are higher than that of the conventional system and the volumetric mass transfer coefficient can be increased 11 – 37% based on the generated bubble size (Jamnongwong *et al.*, 2016).

### 2.3.3 Water scrubbing advanced with the generation of microbubble and liquid-film/water-film in the removal of carbon dioxide

As discussed in **section 2.2.3.2**, it is clear to conclude that water scrubbing is the method that shows the most cost-effective and friendly to the environment since comparing to other methods such as chemical absorption, cryogenics or membrane. Furthermore, due to water used as an absorbent, it provides a simple and promising approach for utilizing CO<sub>2</sub> for other industrial- or lab-scale application and for storing CO<sub>2</sub>. Because water is absorbed solvent, the drainage effluent is CO<sub>2</sub>-rich water which can directly or indirectly use for cultivating microalga to produce biofuels and biomass and mineral carbonating. The interaction between CO<sub>2</sub> and water also is weak so CO<sub>2</sub> can be recovered in the manner of saving cost and energy.

However, some serious drawbacks about operation and effectiveness of this method make this method become lack of practicability. Ofori-Boateng and Kwofie reported that in a packed bed scrubber, 92% of the available CO<sub>2</sub> in the biogas containing 55 – 65% methane was absorbed when the raw biogas was compressed at 1.0 MPa and water were sprayed into the absorption tower at 1.3 MPa (Ofori-Boateng & Kwofie, 2009). Water scrubbing was used to remove CO<sub>2</sub> and upgrade a landfill gas consisting of 53.2% CH<sub>4</sub>, 40.8% CO<sub>2</sub>, 0.4% O<sub>2</sub> and 4.9% N<sub>2</sub> in the pilot-scale upgrading facility including absorption column (500L, 185 cm in height and 60 cm in diameter), desorption column (500L, 155 cm in height and 65 cm in diameter) and water tank (500 L) (Rasi *et al.*, 2008). The absorption tower and desorption tower were packed with pall-rings (4 × 4cm) in order to enlarge the interaction surface between two phases gas and water (Rasi *et al.*, 2008). The results showed that CO<sub>2</sub> removal efficiency was about 90.0% at the pressure of 30 bar (3.0 MPa), water flow rate 10 Lmin<sup>-1</sup> and gas flow rate of 50 Lmin<sup>-1</sup> (Rasi *et al.*, 2008). The landfill gas comprising 50.8 – 57.9% CH<sub>4</sub>, and 37.8 – 43.6% CO<sub>2</sub> was upgraded by using water absorption in the nearly same absorption system in which water was recycled back to the process after desorption (Läntelä *et al.*, 2012). The investigation of CO<sub>2</sub> at differential pressure presented that the CO<sub>2</sub> removal rates at water flow rate of 11 Lmin<sup>-1</sup>, gas flow rate of 7.41 Nm<sup>3</sup>h<sup>-1</sup> and water temperature of 10 – 15 °C was 85.8% at 20 bar (2.0 MPa), 87.0% at 23 bar (2.3 MPa) and 88.9% at 25 bar (2.5 MPa) (Läntelä *et al.*, 2012). Another research with the design – the absorption tower (50 mm in diameter and a total effective height of 0.9 m) was packed with θ-type stainless steel rings (6 mm × 6 mm) and the

desorption tower for regeneration (0.1 m in diameter and an effective height of 0.9 m) was filled with polypropylene rings – presented that the removal of CO<sub>2</sub> could fluctuate between 24.4 – 94.2% at the conditions of pressure (0.8 – 1.2 MPa), inlet CO<sub>2</sub> content (25 – 45 %), water flow rate/gas flow rate ratio (0.15 – 0.5) and temperature (10 – 40 °C) (Xiao *et al.*, 2014).

In general, the primary and important limitations of water washing is to require high pressure and huge packed tower to remain the high mass transfer and interfacial area between CO<sub>2</sub> and water. It means a high cost for capital and operational cost. The pressure in water scrubbing normally set in the range of 1.0 – 2.0 MPa (Ryckebosch *et al.*, 2011). Not only requirement for absorption pressure, but also high gas partial pressure is necessitated. Water scrubbing method has just applied for the feed gas owing high CO<sub>2</sub> partial pressure. Hence, water scrubbing is limited to use in pre-combustion or oxy-fuel combustion system and in upgrading fuel gas such as biogas, natural gas or landfill gas. The utilization of microbubble- and liquid-film-forming apparatus expresses several benefits to remedy this issue. Both types of gas bubbles prove that they are innovated technologies to not only produce numerous boundary and interfacial contact area but also stimulate mass transfer between two phases of gas and water (Bredwell & Worden, 1998, Imai & Zhu, 2011, Jamnongwong *et al.*, 2016, Zhu *et al.*, 2007a, Sadatomi *et al.*, 2012). According to these properties, the generation of microbubbles and liquid-films in the liquid bulk can improve a gas dissolution rate which leads to the fact that gas saturation concentration can reach in short time with the saving of energy consumption and the low pressure for compressing gas phase (Sadatomi *et al.*, 2012, Jamnongwong *et al.*, 2016, Temesgen *et al.*, 2017, Zhu *et al.*, 2007b, Zhu *et al.*, 2007a). Generally, it is expected that with the aid of microbubbles and liquid-film generator, the innovated water scrubbing can remove CO<sub>2</sub> effectively for every type of feed gas even though feed gas containing low CO<sub>2</sub> partial pressure since low mode pressure is applied.

## 2.4 References

- Agarwal, A., Ng, W. J. & Liu, Y. 2011. Principle and applications of microbubble and nanobubble technology for water treatment. *Chemosphere*, **84** (9), 1175-1180.

- Al-Marzouqi, A. H., Zekri, A. Y., Jobe, B. & Dowaidar, A. 2007. Supercritical fluid extraction for the determination of optimum oil recovery conditions. *Journal of Petroleum Science and Engineering*, **55** (1-2), 37-47.
- An, H., Feng, B. & Su, S. 2011. CO<sub>2</sub> capture by electrothermal swing adsorption with activated carbon fibre materials. *International Journal of Greenhouse Gas Control*, **5** (1), 16-25.
- Andriani, D., Wresta, A., Atmaja, T. D. & Saepudin, A. 2014. A review on optimization production and upgrading biogas through CO<sub>2</sub> removal using various techniques. *Applied biochemistry and biotechnology*, **172** (4), 1909-1928.
- Aresta, M. 2013. *Carbon dioxide recovery and utilization*, Springer Science & Business Media. Germany.
- Audus, H. 2000. *Proceedings of the Fifth International Conference on Greenhouse Gas Control Technologies*, Cairns, Australia, p. 16. Citeseer.
- Ausubel, J. H., Wernick, I. K. & Waggoner, P. E. 2013. Peak farmland and the prospect for land sparing. *Population and development review*, **38** (s1), 221-242.
- Aydin, G., Karakurt, I. & Aydiner, K. 2010. Evaluation of geologic storage options of CO<sub>2</sub>: Applicability, cost, storage capacity and safety. *Energy Policy*, **38** (9), 5072-5080.
- Babu, P. V. 2014. Hydrate based gas separation (HBGS) technology for precombustion capture of carbon dioxide. PhD thesis. National University of Singapore, Singapore.
- Bachu, S. 2000. Sequestration of CO<sub>2</sub> in geological media: criteria and approach for site selection in response to climate change. *Energy conversion and management*, **41** (9), 953-970.
- Bauer, F., Persson, T., Hulteberg, C. & Tamm, D. 2013. Biogas upgrading—technology overview, comparison and perspectives for the future. *Biofuels, Bioproducts and Biorefining*, **7** (5), 499-511.
- Benson, S. M. & Orr, F. M. 2008. Carbon dioxide capture and storage. *Mrs Bulletin*, **33** (4), 303-305.
- Bredwell, M. D. & Worden, R. M. 1998. Mass-transfer properties of microbubbles. 1. Experimental studies. *Biotechnology Progress*, **14** (1), 31-38.
- Brennan, L. & Owende, P. 2010. Biofuels from microalgae—A review of technologies for production, processing, and extractions of biofuels and co-products. *Renewable and Sustainable Energy Reviews*, **14** (2), 557-577.

- Bui, T. T., Nam, S.-N. & Han, M. 2015. Micro-bubble flotation of freshwater algae: a comparative study of differing shapes and sizes. *Separation Science and Technology*, **50** (7), 1066-1072.
- Celia, M. A. & Nordbotten, J. M. 2009. Practical modeling approaches for geological storage of carbon dioxide. *Groundwater*, **47** (5), 627-638.
- Choi, S., Drese, J. H. & Jones, C. W. 2009. Adsorbent materials for carbon dioxide capture from large anthropogenic point sources. *ChemSusChem*, **2** (9), 796-854.
- Cook, P. J. 1999. Sustainability and nonrenewable resources. *Environmental Geosciences*, **6** (4), 185-190.
- Costa, J. A. V., Linde, G. A., Atala, D. I. P., Mibielli, G. M. & Krüger, R. T. 2000. Modelling of growth conditions for cyanobacterium *Spirulina platensis* in microcosms. *World Journal of Microbiology and Biotechnology*, **16** (1), 15-18.
- Cozma, P., Ghinea, C., Mămăligă, I., Wukovits, W., Friedl, A. & Gavrilesco, M. 2013. Environmental impact assessment of high pressure water scrubbing biogas upgrading technology. *CLEAN–Soil, Air, Water*, **41** (9), 917-927.
- Cuéllar-Franca, R. M. & Azapagic, A. 2015. Carbon capture, storage and utilisation technologies: A critical analysis and comparison of their life cycle environmental impacts. *Journal of CO2 Utilization*, **9**, 82-102.
- de Moraes, M. G. & Costa, J. A. V. 2007. Biofixation of carbon dioxide by *Spirulina* sp. and *Scenedesmus obliquus* cultivated in a three-stage serial tubular photobioreactor. *Journal of Biotechnology*, **129** (3), 439-445.
- Dou, B., Song, Y., Liu, Y. & Feng, C. 2010. High temperature CO<sub>2</sub> capture using calcium oxide sorbent in a fixed-bed reactor. *Journal of hazardous materials*, **183** (1-3), 759-765.
- Doughty, C. 2006. Site Characterization for CO<sub>2</sub> Geologic Storage and Vice Versa-The Frio Brine Pilot as a Case Study.
- Edenhofer, O., Pichs-Madruga, R., Sokona, Y., Minx, J. C., Farahani, E., Kadner, S., Seyboth, K., Adler, A., Baum, I., Brunner, S., Eickemeier, P., Kriemann, B., Savolainen, J., Schlömer, S., Stechow, C. v. & Zwickel, T. 2014. *Climate Change 2014: Mitigation of Climate Change*, [http://www.ipcc.ch/publications\\_and\\_data/publications\\_and\\_data\\_reports.shtml](http://www.ipcc.ch/publications_and_data/publications_and_data_reports.shtml).



- EPA (United State Environmental Protection Agency) 2018. Global Greenhouse Gas Emissions Data, <https://www.epa.gov/ghgemissions/global-greenhouse-gas-emissions-data>.
- Forbes, S. M., Verma, P., Curry, T. E., Friedmann, S. J. & Wade, S. M. 2008. Guidelines for carbon dioxide capture, transport and storage. Guidelines for carbon dioxide capture, transport and storage.
- Gibbins, J. & Chalmers, H. 2008. Carbon capture and storage. *Energy policy*, **36** (12), 4317-4322.
- Gielen, D. 2003. Proceedings of the 2nd annual conference on carbon sequestration. Alexandria, VA. Citeseer.
- González-Salazar, M. A. 2015. Recent developments in carbon dioxide capture technologies for gas turbine power generation. *International Journal of Greenhouse Gas Control*, **34**, 106-116.
- Hensirisak, P., Parasukulsatid, P., Agblevor, F., Cundiff, J. & Velandar, W. 2002. Scale-up of microbubble dispersion generator for aerobic fermentation. *Applied biochemistry and biotechnology*, **101** (3), 211-227.
- Imai, T. & Zhu, H., 2011. Improvement of oxygen transfer efficiency in diffused aeration systems using liquid-film-forming apparatus, *Mass Transfer-Advanced Aspects. InTech*, pp.
- Jamnongwong, M., Charoenpittaya, T., Hongprasith, N., Imai, T. & Painmanakul, P. 2016. Study of Liquid Film Forming Apparatus (LFFA) mechanisms in terms of oxygen transfer and bubble hydrodynamic parameters. *Engineering Journal (Eng. J.)*, **20** (3), 77-90.
- Johnsen, K., Helle, K., Røneid, S. & Holt, H. 2011. DNV recommended practice: design and operation of CO<sub>2</sub> pipelines. *Energy Procedia*, **4**, 3032-3039.
- Kenarsari, S. D., Yang, D., Jiang, G., Zhang, S., Wang, J., Russell, A. G., Wei, Q. & Fan, M. 2013. Review of recent advances in carbon dioxide separation and capture. *Rsc Advances*, **3** (45), 22739-22773.
- Khoo, H. H., Bu, J., Wong, R. L., Kuan, S. Y. & Sharratt, P. N. 2011. Carbon capture and utilization: Preliminary life cycle CO<sub>2</sub>, energy, and cost results of potential mineral carbonation. *Energy Procedia*, **4**, 2494-2501.

- Klinthong, W., Yang, Y.-H., Huang, C.-H. & Tan, C.-S. 2015. A review: microalgae and their applications in CO<sub>2</sub> capture and renewable energy. *Aerosol Air Qual Res*, **15** (2), 712-742.
- Kotyczka-Moranska, M., Tomaszewicz, G. & Labojko, G. 2012. Comparison of different methods for enhancing CO<sub>2</sub> capture by CaO-based sorbents—review. *Physicochemical Problems of Mineral Processing*, **48** (1), 70-90.
- Läntelä, J., Rasi, S., Lehtinen, J. & Rintala, J. 2012. Landfill gas upgrading with pilot-scale water scrubber: performance assessment with absorption water recycling. *Applied energy*, **92**, 307-314.
- Lee, Z. H., Lee, K. T., Bhatia, S. & Mohamed, A. R. 2012. Post-combustion carbon dioxide capture: Evolution towards utilization of nanomaterials. *Renewable and Sustainable Energy Reviews*, **16** (5), 2599-2609.
- Leung, D. Y., Caramanna, G. & Maroto-Valer, M. M. 2014. An overview of current status of carbon dioxide capture and storage technologies. *Renewable and Sustainable Energy Reviews*, **39**, 426-443.
- Li, L., Zhao, N., Wei, W. & Sun, Y. 2013. A review of research progress on CO<sub>2</sub> capture, storage, and utilization in Chinese Academy of Sciences. *Fuel*, **108**, 112-130.
- Li, Y., Horsman, M., Wu, N., Lan, C. Q. & Dubois-Calero, N. 2008. Biofuels from microalgae. *Biotechnology Progress*, **24** (4), 815-820.
- Lively, R. P., Koros, W. J. & Johnson, J. 2012. Enhanced cryogenic CO<sub>2</sub> capture using dynamically operated low-cost fiber beds. *Chemical engineering science*, **71**, 97-103.
- Ma'mun, S. 2005. Selection and characterization of new absorbents for carbon dioxide capture, Ph.D thesis, the Norwegian University of Science and Technology, Norway.
- Ma'mun, S., Svendsen, H. F., Hoff, K. A. & Juliussen, O. 2007. Selection of new absorbents for carbon dioxide capture. *Energy Conversion and Management*, **48** (1), 251-258.
- Martunus, Helwani, Z., Wiheeb, A., Kim, J. & Othman, M. 2012. Improved carbon dioxide capture using metal reinforced hydrotalcite under wet conditions. *International journal of greenhouse gas control*, **7**, 127-136.
- Metz, B., Davidson, O., Coninck, H. d., Loos, M. & Meyer, L. 2005. The IPCC Special Report on Carbon Dioxide Capture and Storage, [https://www.ipcc.ch/publications\\_and\\_data/\\_reports\\_carbon\\_dioxide.htm](https://www.ipcc.ch/publications_and_data/_reports_carbon_dioxide.htm).

- Mondal, M. K., Balsora, H. K. & Varshney, P. 2012. Progress and trends in CO<sub>2</sub> capture/separation technologies: A review. *Energy*, **46** (1), 431-441.
- Nik, O. G., Chen, X. Y. & Kaliaguine, S. 2011. Amine-functionalized zeolite FAU/EMT-polyimide mixed matrix membranes for CO<sub>2</sub>/CH<sub>4</sub> separation. *Journal of Membrane Science*, **379** (1-2), 468-478.
- Nitta, Y., Suwata, O., Ikeda, Y., Okamoto, Y. & Imanaka, T. 1994. Copper-zirconia catalysts for methanol synthesis from carbon dioxide: Effect of ZnO addition to Cu-ZrO<sub>2</sub> catalysts. *Catalysis letters*, **26** (3-4), 345-354.
- Ofori-Boateng, C. & Kwofie, E. 2009. Water scrubbing: a better option for biogas purification for effective storage. *World Applied Sciences Journal*, **5**, 122-125.
- Olajire, A. A. 2010. CO<sub>2</sub> capture and separation technologies for end-of-pipe applications—a review. *Energy*, **35** (6), 2610-2628.
- Olivier, J. G. J., Schure, K. M. & Peters, J. A. H. W. 2017. Trends in Global CO<sub>2</sub> and Total Greenhouse Gas Emissions: 2017 Report, PBL Netherlands Environmental Assessment Agency, [http://www.pbl.nl/sites/default/files/cms/publicaties/pbl-2017-trends-in-global-co2-and-total-greenhouse-gas-emissions-2017-report\\_2674.pdf](http://www.pbl.nl/sites/default/files/cms/publicaties/pbl-2017-trends-in-global-co2-and-total-greenhouse-gas-emissions-2017-report_2674.pdf).
- Park, J.-S. & Kurata, K. 2009. Application of microbubbles to hydroponics solution promotes lettuce growth. *HortTechnology*, **19** (1), 212-215.
- Parmar, R. & Majumder, S. K. 2013. Microbubble generation and microbubble-aided transport process intensification—A state-of-the-art report. *Chemical Engineering and Processing: Process Intensification*, **64**, 79-97.
- Parmar, R. & Majumder, S. K. 2014. Hydrodynamics of microbubble suspension flow in pipes. *Industrial & Engineering Chemistry Research*, **53** (9), 3689-3701.
- Pehnt, M. & Henkel, J. 2009. Life cycle assessment of carbon dioxide capture and storage from lignite power plants. *International Journal of Greenhouse Gas Control*, **3** (1), 49-66.
- Petersson, A. & Wellinger, A. 2009. Biogas upgrading technologies—developments and innovations. *IEA bioenergy*, **20**, 1-19.
- Rahman, F. A., Aziz, M. M. A., Saidur, R., Bakar, W. A. W. A., Hainin, M., Putrajaya, R. & Hassan, N. A. 2017. Pollution to solution: Capture and sequestration of carbon dioxide (CO<sub>2</sub>) and its utilization as a renewable energy source for a sustainable future. *Renewable and Sustainable Energy Reviews*, **71**, 112-126.

- Rao, A. B. & Rubin, E. S. 2002. A technical, economic, and environmental assessment of amine-based CO<sub>2</sub> capture technology for power plant greenhouse gas control. *Environmental science & technology*, **36** (20), 4467-4475.
- Rasi, S., Läntelä, J., Veijanen, A. & Rintala, J. 2008. Landfill gas upgrading with countercurrent water wash. *Waste Management*, **28** (9), 1528-1534.
- Ravanchi, M. T., Sahebdehfar, S. & Zangeneh, F. T. 2011. Carbon dioxide sequestration in petrochemical industries with the aim of reduction in greenhouse gas emissions. *Frontiers of Chemical Science and Engineering*, **5** (2), 173.
- Romeo, L. M., Abanades, J. C., Escosa, J. M., Paño, J., Giménez, A., Sánchez-Biezma, A. & Ballesteros, J. C. 2008. Oxyfuel carbonation/calcination cycle for low cost CO<sub>2</sub> capture in existing power plants. *Energy Conversion and Management*, **49** (10), 2809-2814.
- Rubin, E. S., Mantripragada, H., Marks, A., Versteeg, P. & Kitchin, J. 2012. The outlook for improved carbon capture technology. *Progress in Energy and Combustion Science*, **38** (5), 630-671.
- Ryckebosch, E., Drouillon, M. & Vervaeren, H. 2011. Techniques for transformation of biogas to biomethane. *Biomass and bioenergy*, **35** (5), 1633-1645.
- Sadatom, M., Kawahara, A., Matsuura, H. & Shikatani, S. 2012. Micro-bubble generation rate and bubble dissolution rate into water by a simple multi-fluid mixer with orifice and porous tube. *Experimental Thermal and Fluid Science*, **41**, 23-30.
- Sayari, A. & Belmabkhout, Y. 2010. Stabilization of amine-containing CO<sub>2</sub> adsorbents: dramatic effect of water vapor. *Journal of the American Chemical Society*, **132** (18), 6312-6314.
- Shimekit, B. & Mukhtar, H., 2012. Natural gas purification technologies-major advances for CO<sub>2</sub> separation and future directions, *Advances in Natural Gas Technology*. InTech, pp.
- Singh, B., Strømman, A. H. & Hertwich, E. G. 2011. Comparative life cycle environmental assessment of CCS technologies. *International Journal of Greenhouse Gas Control*, **5** (4), 911-921.
- Singh, U. B. & Ahluwalia, A. 2013. Microalgae: a promising tool for carbon sequestration. *Mitigation and adaptation strategies for global change*, **18** (1), 73-95.

- Solomon, S., Carpenter, M. & Flach, T. A. 2008. Intermediate storage of carbon dioxide in geological formations: A technical perspective. *International journal of greenhouse gas control*, **2** (4), 502-510.
- Song, C.-F., Kitamura, Y., Li, S.-H. & Ogasawara, K. 2012. Design of a cryogenic CO<sub>2</sub> capture system based on Stirling coolers. *International journal of greenhouse gas control*, **7**, 107-114.
- Songolzadeh, M., Soleimani, M., Takht Ravanchi, M. & Songolzadeh, R. 2014. Carbon dioxide separation from flue gases: a technological review emphasizing reduction in greenhouse gas emissions. *The Scientific World Journal*, **2014**.
- Stocker, T. F., Qin, D., Plattner, G.-K., Tignor, M., Allen, S. K., Boschung, J., Nauels, A., Xia, Y., Bex, V. & Midgley, P. M. 2013. *Climate Change 2013: The Physical Science Basis*, [http://www.ipcc.ch/publications\\_and\\_data/publications\\_and\\_data\\_reports.shtml](http://www.ipcc.ch/publications_and_data/publications_and_data_reports.shtml).
- Styring, P., Jansen, D., Coninck, H. d., Reith, H. & Armstrong, K. 2011. Carbon Capture and Utilisation in the Green Economy, <http://co2chem.co.uk/wp-content/uploads/2012/06/CCU%20in%20the%20green%20economy%20report.pdf>.
- Sumikura, M., Hidaka, M., Murakami, H., Nobutomo, Y. & Murakami, T. 2007. Ozone micro-bubble disinfection method for wastewater reuse system. *Water Science and Technology*, **56** (5), 53-61.
- Sun, Q., Li, H., Yan, J., Liu, L., Yu, Z. & Yu, X. 2015. Selection of appropriate biogas upgrading technology-a review of biogas cleaning, upgrading and utilisation. *Renewable and Sustainable Energy Reviews*, **51**, 521-532.
- Svensson, R., Odenberger, M., Johnsson, F. & Strömberg, L. 2004. Transportation systems for CO<sub>2</sub>—application to carbon capture and storage. *Energy conversion and management*, **45** (15-16), 2343-2353.
- Tabei, K., Haruyama, S., Yamaguchi, S., Shirai, H. & Takakusagi, F. 2007. Study of micro bubble generation by a swirl jet. *Journal of Environment and Engineering*, **2** (1), 172-182.
- Takahashi, M., Chiba, K. & Li, P. 2007. Free-radical generation from collapsing microbubbles in the absence of a dynamic stimulus. *The Journal of Physical Chemistry B*, **111** (6), 1343-1347.

- Temesgen, T., Bui, T. T., Han, M., Kim, T.-i. & Park, H. 2017. Micro and nanobubble technologies as a new horizon for water-treatment techniques: A review. *Advances in colloid and interface science*, **246**, 40-51.
- Thiruvengkatachari, R., Su, S., An, H. & Yu, X. X. 2009. Post combustion CO<sub>2</sub> capture by carbon fibre monolithic adsorbents. *Progress in Energy and Combustion Science*, **35** (5), 438-455.
- Tuinier, M., van Sint Annaland, M. & Kuipers, J. 2011. A novel process for cryogenic CO<sub>2</sub> capture using dynamically operated packed beds—An experimental and numerical study. *International Journal of Greenhouse Gas Control*, **5** (4), 694-701.
- Ushikubo, F. Y., Furukawa, T., Nakagawa, R., Enari, M., Makino, Y., Kawagoe, Y., Shiina, T. & Oshita, S. 2010. Evidence of the existence and the stability of nano-bubbles in water. *Colloids and Surfaces A: Physicochemical and Engineering Aspects*, **361** (1-3), 31-37.
- Usui, N. & Ikenouchi, M. 1997. The biological CO<sub>2</sub> fixation and utilization project by RITE(1) — Highly-effective photobioreactor system —. *Energy Conversion and Management*, **38**, S487-S492.
- Van der Zwaan, B. & Smekens, K. 2009. CO<sub>2</sub> Capture and Storage with Leakage in an Energy-Climate Model. *Environmental Modeling & Assessment*, **14** (2), 135-148.
- Van Le, T., Imai, T., Higuchi, T., Yamamoto, K., Sekine, M., Doi, R., Vo, H. T. & Wei, J. 2013. Performance of tiny microbubbles enhanced with “normal cyclone bubbles” in separation of fine oil-in-water emulsions. *Chemical Engineering Science*, **94**, 1-6.
- Wang, B., Li, Y., Wu, N. & Lan, C. Q. 2008. CO<sub>2</sub> bio-mitigation using microalgae. *Applied microbiology and biotechnology*, **79** (5), 707-718.
- Wang, Q., Luo, J., Zhong, Z. & Borgna, A. 2011. CO<sub>2</sub> capture by solid adsorbents and their applications: current status and new trends. *Energy & Environmental Science*, **4** (1), 42-55.
- Weber, J. & Agblevor, F. 2005. Microbubble fermentation of *Trichoderma reesei* for cellulase production. *Process Biochemistry*, **40** (2), 669-676.
- Weiss, H. 1988. Rectisol wash for purification of partial oxidation gases. *Gas Separation & Purification*, **2** (4), 171-176.
- Witkowski, A., Rusin, A., Majkut, M., Rulik, S. & Stolecka, K. 2015. *Advances in carbon dioxide compression and pipeline transportation processes*, Springer.

- Xiao, Y., Yuan, H., Pang, Y., Chen, S., Zhu, B., Zou, D., Ma, J., Yu, L. & Li, X. 2014. CO<sub>2</sub> removal from biogas by water washing system. *Chinese Journal of Chemical Engineering*, **22** (8), 950-953.
- Xu, Q., Nakajima, M., Ichikawa, S., Nakamura, N. & Shiina, T. 2008. A comparative study of microbubble generation by mechanical agitation and sonication. *Innovative food science & emerging technologies*, **9** (4), 489-494.
- Yang, F., Bai, B., Tang, D., Shari, D.-N. & David, W. 2010. Characteristics of CO<sub>2</sub> sequestration in saline aquifers. *Petroleum Science*, **7** (1), 83-92.
- Yang, H., Xu, Z., Fan, M., Gupta, R., Slimane, R. B., Bland, A. E. & Wright, I. 2008. Progress in carbon dioxide separation and capture: A review. *Journal of environmental sciences*, **20** (1), 14-27.
- Yu, C.-H., Huang, C.-H. & Tan, C.-S. 2012. A review of CO<sub>2</sub> capture by absorption and adsorption. *Aerosol and Air Quality Research*, **12** (5), 745-769.
- Yu, K. M. K., Curcic, I., Gabriel, J. & Tsang, S. C. E. 2008. Recent advances in CO<sub>2</sub> capture and utilization. *ChemSusChem*, **1** (11), 893-899.
- Zhang, F., Xi, J., Huang, J.-J. & Hu, H.-Y. 2013. Effect of inlet ozone concentration on the performance of a micro-bubble ozonation system for inactivation of *Bacillus subtilis* spores. *Separation and Purification Technology*, **114**, 126-133.
- Zhu, H., Imai, T., Tani, K., Ukita, M., Sekine, M., Higuchi, T. & Zhang, Z. 2007a. Enhancement of oxygen transfer efficiency in diffused aeration systems using liquid-film-forming apparatus. *Environmental technology*, **28** (5), 511-519.
- Zhu, H., Imai, T., Tani, K., Ukita, M., Sekine, M., Higuchi, T. & Zhang, Z. 2007b. Development of high efficient oxygen supply method by using contacting water-liquid film with air. *Journal of Water and Environment Technology*, **5** (2), 57-69.

## CHAPTER 3

### PERFORMANCE OF A CARBON DIOXIDE REMOVAL PROCESS USING A WATER SCRUBBER WITH THE AID OF A WATER-FILM-FORMING-UNIT

#### 3.1 Introduction

Greenhouse gases are commonly considered major contributors to global warming and climate change, which can lead to several undesirable and long-lasting effects on the environment and human beings, such as rising sea levels, frequent hurricanes, the spread of tropical diseases, and extinction of several species. Among greenhouse gases, carbon dioxide (CO<sub>2</sub>) is widely believed to be mostly responsible for global warming because of its great abundance in the atmosphere, accounting for approximately 80% of worldwide greenhouse gases (Sumida *et al.*, 2011). Specifically, CO<sub>2</sub> is believed to contribute more than 60% to the global warming effect (Mondal *et al.*, 2012, Yu *et al.*, 2012).

The combustion of fossil fuels is the major source of high concentrations of CO<sub>2</sub> in the atmosphere. Despite the development of advanced technologies to identify alternative energy sources and reduce CO<sub>2</sub> emissions, the world still relies on fossil fuels to satisfy 80% of its energy demands (Olah *et al.*, 2008). From human activities, 24 Gt of atmospheric CO<sub>2</sub> is emitted per year, and this number is predicted to increase continuously in the coming decades (Mikkelsen *et al.*, 2010). **Table 3.1** shows typical CO<sub>2</sub> concentrations in the exhaust gas of various sources. CO<sub>2</sub> removal could not only reduce CO<sub>2</sub> emissions into the atmosphere but also upgrade biogas or landfill gas to achieve high methane concentrations for use as a renewable energy source and substitute for fossil fuels (Pettersson & Wellinger, 2009). To address this and mitigate the effects of global warming and climate change, there has been an increased focus on controlling CO<sub>2</sub> emissions and removing CO<sub>2</sub> from exhausted gas.

Over the past several decades, absorption has become the most developed and practical method for CO<sub>2</sub> sequestration on an industrial scale (Bhown & Freeman, 2011, Mondal *et al.*, 2012, Olajire, 2010, Rahmadoost *et al.*, 2014). There are two absorption methods, namely, physical and chemical absorption. Chemical absorption using aqueous-amine or alkaline solutions has been proposed as the most promising means of removing CO<sub>2</sub> from gas streams



owing to its high absorption efficiency, simple operation, and potential to regenerate liquid sorbents through heating and/or depressurization (Leung *et al.*, 2014, Yu *et al.*, 2012). However, there are several limitations of this method: high corrosion rate, solvent loss, production of volatile degradation compounds, and notably, the high cost and amount of energy required for the regeneration of the solvent (Bhown & Freeman, 2011, González-Salazar, 2015, Leung *et al.*, 2014, Mondal *et al.*, 2012, Olajire, 2010, Yu *et al.*, 2012). It is estimated that more than half of the capture cost is utilized in sorbent regeneration (Chowdhury *et al.*, 2011); therefore, finding and using a solvent that can reduce the cost of regeneration is essential and urgent. The use of a physical absorption process can solve these problems.

**Table 3.1** Typical CO<sub>2</sub> content in exhausted gas

Source	CO <sub>2</sub> content (vol. %)
a. Power plant flue gas	
Coal-fired power plant	10 – 15 (Bhown & Freeman, 2011, Mondal <i>et al.</i> , 2012, Car <i>et al.</i> , 2008)
Natural gas-fired power plant	7 – 8 (Mondal <i>et al.</i> , 2012, Car <i>et al.</i> , 2008)
b. Industrial flue gas	
Blast furnace gas (before combustion)	20 (Mondal <i>et al.</i> , 2012, Car <i>et al.</i> , 2008)
Blast furnace gas (after combustion)	27 (Mondal <i>et al.</i> , 2012, Car <i>et al.</i> , 2008)
Cement kiln off-gas	14 – 33 (Mondal <i>et al.</i> , 2012, Car <i>et al.</i> , 2008)
Oil refineries and petrochemical plant fired heater	8 (Mondal <i>et al.</i> , 2012, Car <i>et al.</i> , 2008)
c. Other	
Biogas	15 – 60 (Ryckebosch <i>et al.</i> , 2011)
Landfill gas	15 – 50 (Pettersson & Wellinger, 2009)

Differing from chemical absorption, physical absorption is based on Henry's Law, meaning that it is temperature- and pressure-dependent and the removal of CO<sub>2</sub> depends on its solubility in the liquid phase (Olajire, 2010). Common processes for this technique comprise the use of dimethyl ether with polyethylene glycol, methanol, propylene carbonate, and N-methyl-2-pyrrolidone via the Selexol process, Rectisol process, Purisol process, or Fluor process, respectively (Yu *et al.*, 2012, Olajire, 2010). These processes do not require re-boiler heat for solvent recovery and do not lead to corrosion, but they involve high costs for solvents or refrigerating solvents (Olajire, 2010). For these reasons, using water as the physical sorbent is an alternative approach with many potentially positive effects. For example, using tap water as the solvent in a packed-column scrubber, Yong Xiao *et al.* were able to attain CO<sub>2</sub> removal

rates of 24.4–94.2% under various conditions of pressure (0.8–1.2 MPa), initial CO<sub>2</sub> concentration (25–45%), liquid-to-gas ratio (0.15–0.5), and temperature (10–40°C) (Xiao *et al.*, 2014). Meanwhile, Läntelä *et al.* concluded that 53.1–88.9% of CO<sub>2</sub> could be removed from landfill gas using water scrubbing at various pressures (2.0–2.5 MPa), temperatures (10–25°C), and water flow rates (5.5–11.0 L min<sup>-1</sup>) (Läntelä *et al.*, 2012). Because the water scrubber method does not rely on chemical reactions, the interaction between CO<sub>2</sub> and water is weak, leading to a decreased energy requirement for the reversal of the combination of CO<sub>2</sub> and water; therefore, water can be easily regenerated and reused in the removal process. Moreover, absorption and desorption can be accomplished in water, resulting in greater stability without undesirable byproducts and expanding the opportunities to use the effluent water containing high CO<sub>2</sub> concentrations for other purposes, such as carbon source for the cultivation of microalgae to produce biomass for the production of biofuels, medications, or foods (Ho *et al.*, 2011). Nevertheless, because this method is based on the physical solubility of a gas in the liquid phase, the process is slow and has a low removal efficiency. To increase the absorption rate, the process must be carried out at high pressures and low temperatures and, consequently, high levels of energy are required.

To overcome these restrictions, it is necessary to promote mass transfer in a two-phase gas-liquid flow, which increases the physical solubility of the gas (in this case, CO<sub>2</sub>) and then its removal rate. Various studies have already demonstrated that the use of devices producing water-films or fine bubbles can increase the mass transfer coefficient and gas solubility remarkably because the interfacial area is greater in the presence of fine bubbles and a thin water-films. Therefore, the interaction between gas molecules and liquids is enhanced, and the absorption rate increases (Bang *et al.*, 2014, Imai & Zhu, 2011, Kawahara *et al.*, 2009, Parmar & Majumder, 2013, 2014). Furthermore, compared with other scrubbers, such as packed-bed or spray scrubbers, a simply constructed bubble-column scrubber can attain a higher removal efficiency and mass transfer coefficient (Chen *et al.*, 2015, Cheng *et al.*, 2013, Li *et al.*, 2014). Thus, utilizing such a scrubber along with a water-film enhanced with fine bubble-forming device is the most promising means of accelerating CO<sub>2</sub> capture at a reasonable cost.

In the present water absorption study, a water-film-forming device which can generate large quantities of water-film and fine bubbles was used to stimulate the dissolution of CO<sub>2</sub> in tap

water and then promote the CO<sub>2</sub> removal process. In this study, the effect of numerous factors, including pressure, temperature, gas flow rate, liquid-to-gas ratio, and initial CO<sub>2</sub> concentration, on the removal and absorption rates of CO<sub>2</sub> is evaluated.

### 3.2 Materials and Methods

In this study, a pilot apparatus was used with the setup shown in **Figure 3.1**. The absorption process was carried out in a reactor with a diameter of 220 mm and height of 160 mm. The feed gases, which comprised a mixture of N<sub>2</sub> and CO<sub>2</sub>, were prepared using flow rate controllers. The inlet compressed gas at the differential conditions of pressure (0.30, 050, and 0.70 MPa) was entered to flow rate controllers. This mixed gas (CO<sub>2</sub> and N<sub>2</sub>) moved into the water-film-forming device connected to the inside of the absorption tank after blending with tap water pumped from the pump. Tap water was directly used as the once-through physical absorbent without any purification. The absorption tank was designed to connect with the water-film-forming device, which had an interior height of 170 mm and diameter of 80 mm and produced a large number of fine bubbles and water-film to enhance the solubility of CO<sub>2</sub> in water.

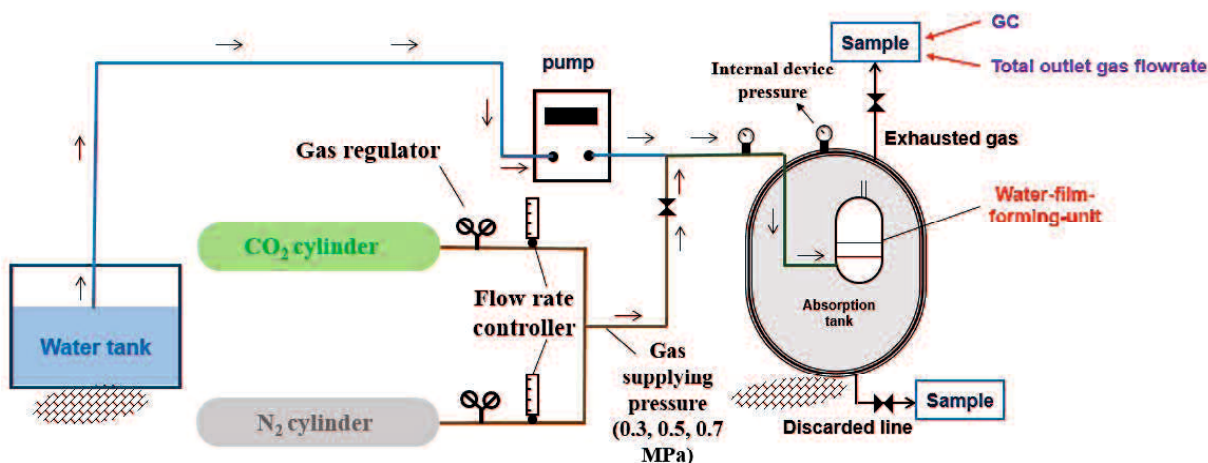


**Figure 3.1** Experimental apparatus used for CO<sub>2</sub> absorption.

The structure of the WFFU has been described in **Figures 3.2(a)** and **3.2(b)**. It consists of two main parts: a fine-bubble generator (Part A) and an enhanced mixing and water film generator (Part B) (**Figure 3.2(a)**). The mechanism in this device can provide three times contacting between water and gas phase. First, the mixture of gas and water is introduced to

the fine-bubble generator. The shape of the fine-bubble generator and high speed of water and gas flow can create centripetal force inside the generator. The centripetal force forms the reduction in pressure (negative pressure zone) in the central axis of the generator. The gas is automatically pulled into this negative pressure zone; here, upon impact with the rotating flow, numerous fine bubbles are produced and escape from exit 1 and exit 2 (see **Figure 3.2(b)** and **3.2(c)**). Next, fine-bubbles which escape from exit 1 with extremely high speed impact on the wall of water-film generator (Part B). This impact can stimulate the mixing of the gas and the surrounding water and produces water films. Finally, when these water films and the fine bubbles move from the water body to its surface, they remain in contact with the water phase, enhancing the gas-bubble and surface transfer.

The experiments were conducted at varying gas supplying pressures, temperatures, gas flow rates, and initial CO<sub>2</sub> concentrations. The internal device pressure is the pressure inside the absorption tank while the experiments are being conducted. This pressure, along with the volume and speed of the outlet water, varied with adjustments in the position of the blowdown valve on the discarded water line (See **Figure 3.1**) For example, when the valve is adjusted to the low position (a small hole at the exit), the internal pressure and speed of outlet water increase while the output volume decreases. To investigate the impact of internal pressure, the gas flow rate, water flow rate, gas compressed pressure, and temperature were kept at 20 L min<sup>-1</sup>, 14 L min<sup>-1</sup>, 0.50 MPa, and 20°C, respectively, while the internal pressure was set at two different points, 0.06 and 0.10 MPa. Herein, three mixed inlet gases containing varying levels of CO<sub>2</sub> were applied: gas G<sub>1</sub> (15% CO<sub>2</sub> and 85% N<sub>2</sub>), gas G<sub>2</sub> (25% CO<sub>2</sub> and 75% N<sub>2</sub>), and gas G<sub>3</sub> (35% CO<sub>2</sub> and 65% N<sub>2</sub>).

The concentration of CO<sub>2</sub> in the induced gas with N<sub>2</sub> was adjusted from 10% to 100% using flow rate controllers to change the proportions of the two gases. Meanwhile, the G/Lratio was controlled in the manner that the liquid flow rate was maintained at 14 L min<sup>-1</sup>, while the total gas flow rate was adjusted from 5 to 25 L min<sup>-1</sup> (these values can be seen and controlled by flow rate controllers). To determine the effects of temperature, the three gases were again utilized as feed gases, while the temperature was adjusted from 10°C to 30°C, corresponding to the normal range of temperatures in Japan throughout the year.

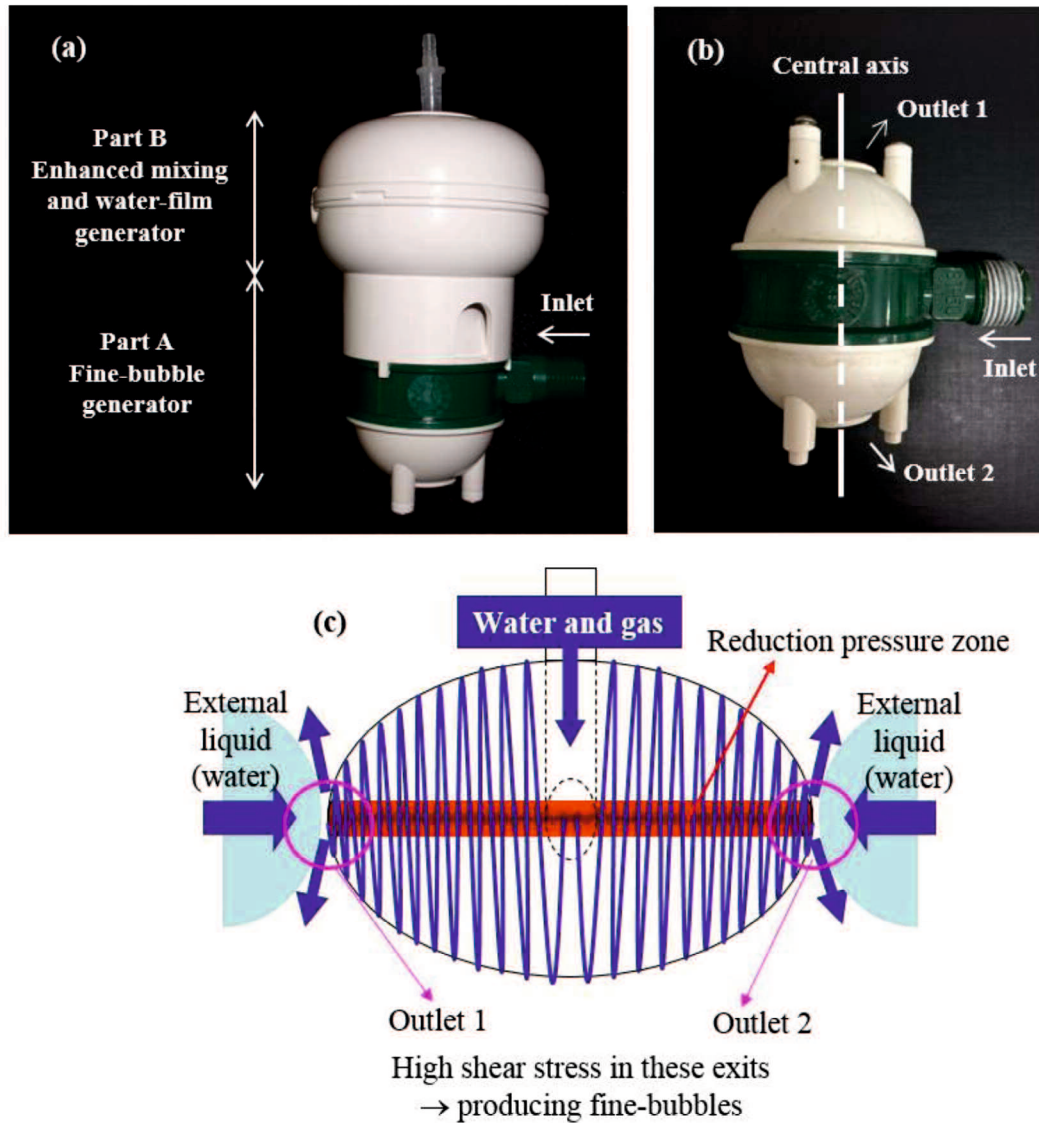


**Figure 3.2** (a) Structure of WFFU, (b) a fine-bubble generator (Part A) and (c) theory of making fine-bubbles.

To evaluate the CO<sub>2</sub> removal efficiency and absorption rate, the outlet gas at the exit (exhaust gas valve) was collected and then analyzed using gas chromatography (GC-8APT, Shimadzu). The CO<sub>2</sub> concentration in water was measured by a CO<sub>2</sub> meter (CGP-31, DKK-TOA Co.). According to (Chen, 2012), the absorption rate can be calculated by the following formula:

$$R = \frac{F_{\text{CO}_2}}{V} \left[ 1 - \left( \frac{1-x_{\text{CO}_2}^{\text{in}}}{x_{\text{CO}_2}^{\text{in}}} \right) \left( \frac{x_{\text{CO}_2}^{\text{out}}}{1-x_{\text{CO}_2}^{\text{out}}} \right) \right] \quad (3.1)$$

where  $R$  ( $\text{mol s}^{-1}\text{L}^{-1}$ ) is the absorption rate of  $\text{CO}_2$  in the liquid phase;  $F_{\text{CO}_2}$  ( $\text{mol s}^{-1}$ ) is the  $\text{CO}_2$  molar flow rate;  $V$  (L) is the volume of liquid phase in the chamber;  $x_{\text{CO}_2}^{\text{in}}$  is the molar fraction of  $\text{CO}_2$  at the inlet; and  $x_{\text{CO}_2}^{\text{out}}$  is the molar fraction of  $\text{CO}_2$  at the outlet.

### 3.3 Results and Discussion

#### 3.3.1 Effect of internal pressure in the absorption tank

The influence of internal pressure in the absorption tank on the removal efficiency of  $\text{CO}_2$  is presented in **Figure 3.3**. At 0.06 MPa of pressure, the  $\text{CO}_2$  removal rates were 44.6%, 47.4%, and 50.1% at 15%, 25%, and 35% initial  $\text{CO}_2$  concentration, respectively. Meanwhile, at the higher pressure of 0.10 MPa,  $\text{CO}_2$  removal was more effective with all three of the feed gases. Specifically, the  $\text{CO}_2$  removal efficiency for gases  $G_1$ ,  $G_2$ , and  $G_3$  were 47.5%, 50.3%, and 51.2%, respectively. These results suggest that the increase in pressure in the chamber improved  $\text{CO}_2$  removal efficiency, in accordance with Henry's law. According to Henry's law, the solubility of gas in water is the function of temperature and pressure (Olajire, 2010), and pressure has a positive effect on the absorption of  $\text{CO}_2$  in the aqueous phase, as shown in the equation  $C_i = K_H \cdot p_i$ , where  $p_i$  is the partial pressure of gaseous substance  $i$ ,  $K_H$  is Henry's constant (which depends on temperature and pressure), and  $C_i$  is the concentration of the dissolved gas  $i$ . Additionally, at a higher internal pressure corresponding with a lower volume of outlet water and higher exit speed, the retention time of liquid in the tank was longer, and the length of time that gas and water were in contact was prolonged. The resulting increased turbulence of liquid inside the chamber, prompted tangency between two phases and strengthened the potential for  $\text{CO}_2$  capture. This also explains how the accumulation of the dissolution of  $\text{CO}_2$  in water led to the escalation of absorption rate  $R$  ( $\text{mol s}^{-1}\text{L}^{-1}$ ) with increasing internal pressure due to the greater dissolution rate of  $\text{CO}_2$  in water at higher pressure. For instance, with the inlet mixed gas  $G_2$ , the absorption rate of  $\text{CO}_2$  in the water was  $17.5 \times 10^{-4}$  and  $18.3 \times 10^{-4} \text{ mol s}^{-1}\text{L}^{-1}$  at internal pressures of 0.06 and 0.10 MPa, respectively.

Accordingly, based on the data presented in **Figure 3.3**, the removal rate rose by around 3.0% when the internal pressure increased only 0.04 MPa, confirming that pressure was the

crucial factor affecting the solubility of CO<sub>2</sub> in water and the removal efficiency of CO<sub>2</sub> from the gas stream. Higher pressure in the absorption chamber was favorable for CO<sub>2</sub> removal.

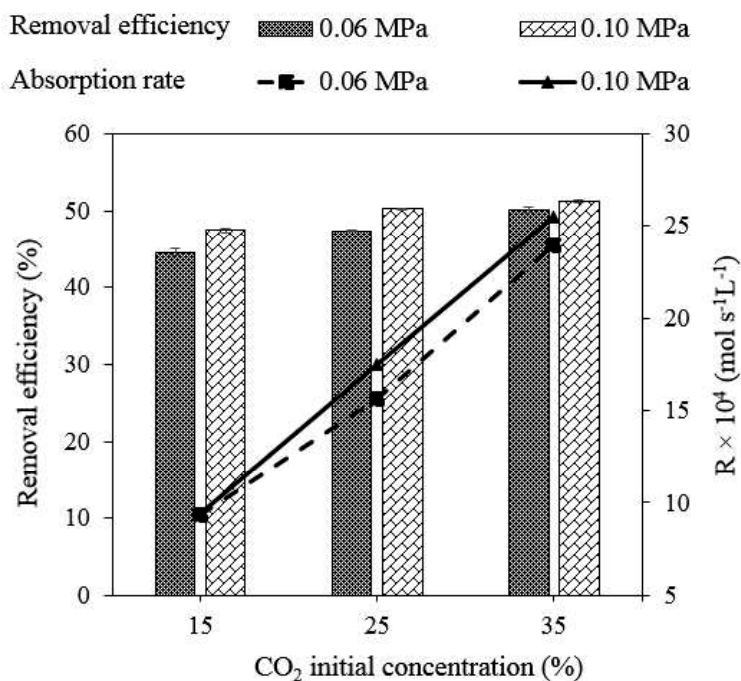


**Figure 3.3** CO<sub>2</sub> removal efficiency and absorption rate at different CO<sub>2</sub> concentrations of inlet gas (G<sub>1</sub>, G<sub>2</sub>, and G<sub>3</sub>) under internal pressure conditions of 0.06 and 0.10 MPa. Water flow rate: 14 L min<sup>-1</sup>; total gas flow rate: 20 L min<sup>-1</sup>; total inlet gas supplying pressure: 0.50 MPa; and temperature: 20°C.

### 3.3.2 Effect of inlet gas supplying pressure

The effect of induced gas pressure on the CO<sub>2</sub> removal and absorption rates is plotted in **Figure 3.4**. Interestingly, with all three inlet gases (G<sub>1</sub>, G<sub>2</sub>, and G<sub>3</sub>), once the total gas flow rate was set at 10 and 20 L min<sup>-1</sup>, the removal efficiency generally exhibited a slightly downward trend as gas supplying pressure was adjusted from 0.30 to 0.50 MPa but increased again when the gas supplying pressure was continuously increased to 0.70 MPa. Meanwhile, the absorption rate spiked more than twice as gas supplying pressure was increased from 0.30 to 0.70 MPa.

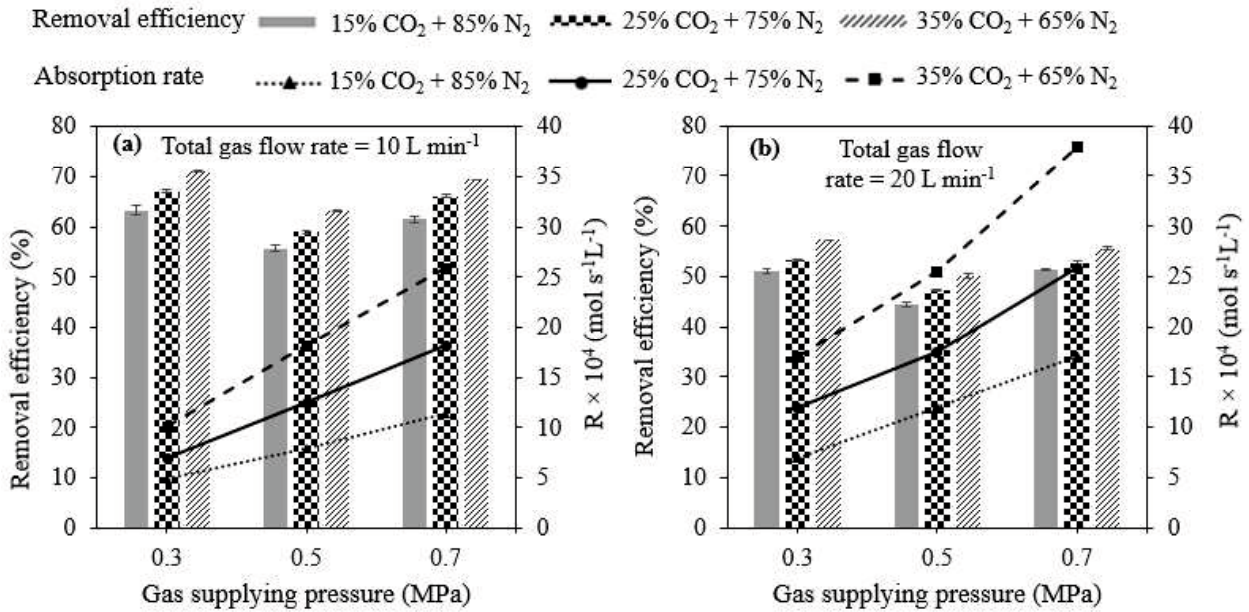


**Figure 3.4** Removal efficiency and absorption rate of CO<sub>2</sub> at different compositions of inlet gas under various total inlet gas supplying pressures. Water flow rate: 14 L min<sup>-1</sup>; internal pressure: 0.06 MPa; and temperature: 20°C. (a) Total gas flow rate: 10 L min<sup>-1</sup>; (b) Total gas flow rate: 20 L min<sup>-1</sup>.

Normally, similar to gas solubility, removal efficiency increases with gas pressure, as dictated by Henry's law. This may elucidate the reason for the surge of absorption rate with gas supplying pressure in the range from 0.30 to 0.70 MPa. However, the removal rate at 0.30 MPa of gas supplying pressure in these experiments was greater than at 0.50 MPa. The effect of gas supplying pressure on the absorption of CO<sub>2</sub> and the CO<sub>2</sub> removal capacity from the stimulated gas is very complicated and governed by a combination of various factors and phenomena. The joining and adjusting influences which are resulted by these phenomena decide the trend of removal efficiency. With an increase of pressure, the theoretical solubility of CO<sub>2</sub> in water increases. However, when the inlet gas at differential compressed pressure was introduced to the WFFU in order to complete the contacting and mixing between two phases of gas and liquid, some phenomena or some factors of the gas phase can be changed in the WFFU and the absorption chamber. That might be the change in interfacial area of the fine bubble, contacting area between two phases of gas and water or mixing capacity in the WFFU. It is suggested that one or some of the phenomena could improve significantly the capture of CO<sub>2</sub> at the condition of low pressure of 0.30 MPa. And also, it can be seen that, in term of



removal efficiency, the removal efficiency underwent the minor change as an increase of gas supplying pressure from 0.30 to 0.70 MPa. The good removal performance can be achieved at both low (0.30 MPa) and high pressure (0.70 MPa) condition. This may subsequently allow CO<sub>2</sub> to be dissolved in tap water at low inlet pressures and provide a means of reducing operating energy and cost.

### 3.3.3 Effect of gas-to-liquid ratio

Gas flow rate and the ratio of the inlet gas flow rate to water flow rate (G/L) are important parameters influencing the efficiency of CO<sub>2</sub> capture from the mixed gases. **Figure 3.5(a)** presents the performance of different G/L ratios on the removal of CO<sub>2</sub> from the three gas streams: G<sub>1</sub>, G<sub>2</sub> and G<sub>3</sub>. As shown in **Figure 3.5(a)**, the increase in gas flow rate from 5 to 25 L min<sup>-1</sup> (equivalent to a growth in G/L from 0.36 to 1.79) led to the notable abatement of the CO<sub>2</sub> separation capability. More specifically, the removal rates at the flow rates of 10, 15, 20, and 25 L min<sup>-1</sup> were 55.7%, 49.7%, 44.6%, and 38.2%, respectively, for inlet gas G<sub>1</sub>. In the same way, with the flow rate adjusted from 5 to 25 L min<sup>-1</sup>, the removal rate experienced a downward trend from 69.2% to 41.9% and from 73.7% to 46.3% at the initial CO<sub>2</sub> concentrations of 25% and 35%, respectively. This effect of the different set values of the G/L ratio can be primarily attributed to the change in the turbulence of the liquid and gas retention times in the water-film-forming unit. Because of acceleration in the gas transfer rate, a larger amount of CO<sub>2</sub> entered the device and reduced the contact time between the gas and aqueous phases (Chai & Zhao, 2012, Lin & Chu, 2015, Xiao *et al.*, 2014). In addition, the increase in gas flow rate and constant water flow rate contributed to an increase in the G/L ratio. This was followed by a loss of the liquid turbulence in the chamber, impeding the contact between gas and water. Accordingly, the removal efficiency of CO<sub>2</sub> decrease with the increase of G/L ratio.

Conversely, at higher initial CO<sub>2</sub> volume, greater amounts of CO<sub>2</sub> made contact with each unit volume of the liquid phase; thus, the absorption rate increased noticeably, as shown in **Figure 3.5(b)**. However, the rise in the absorption rate occurred at different speeds at various concentrations of CO<sub>2</sub>. After the flow rate was adjusted from 10 to 25 L min<sup>-1</sup>, the absorption rate slightly increased from  $7.0 \times 10^{-4}$  to  $9.8 \times 10^{-4}$  mol s<sup>-1</sup>L<sup>-1</sup> with an initial CO<sub>2</sub> concentration of 15% (G<sub>1</sub>). Meanwhile, with this same change in flow rate, the speed of CO<sub>2</sub> absorption surged dramatically from  $7.5 \times 10^{-4}$  to  $18.1 \times 10^{-4}$  mol s<sup>-1</sup>L<sup>-1</sup> and from  $10.7 \times 10^{-4}$  to  $27.4 \times 10^{-4}$

$4 \text{ mol s}^{-1}\text{L}^{-1}$  for inlet gases  $G_2$  and  $G_3$ , respectively. It was also confirmed that the absorption rate surged more rapidly when the amount of  $\text{CO}_2$  moved into the bubble tank was increased. Consequently, although a decrease in gas flow rate along with a decline in the G/L ratio was expected to improve the  $\text{CO}_2$  removal capacity, it instead led to the decline of the absorption level. This would make the application of this capturing process may not satisfy the requirement of polluted gas treatment speed in a larger scale of removing  $\text{CO}_2$  from flue gas. Note that in selecting a suitable G/L ratio, it is recommended that the demand and requirements of the  $\text{CO}_2$  separating process be considered.

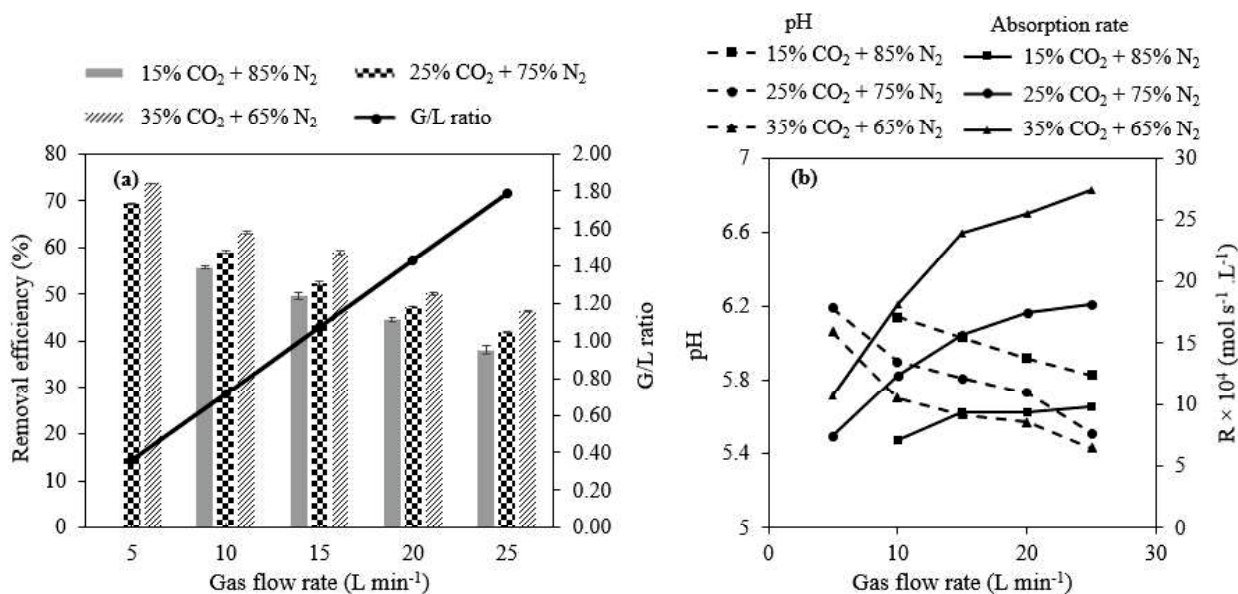


**Figure 3.5** (a) Removal efficiency of  $\text{CO}_2$  at different compositions of inlet gas with a changing G/L ratio. (b) Absorption rate of  $\text{CO}_2$  and pH of outlet water at different compositions of inlet gas with a changing G/L ratio. Water flow rate:  $14 \text{ L min}^{-1}$ ; internal device pressure:  $0.06 \text{ MPa}$ ; total inlet gas supplying pressure:  $0.50 \text{ MPa}$ ; and temperature:  $20^\circ\text{C}$ .

### 3.3.4 Effect of $\text{CO}_2$ partial pressure and initial $\text{CO}_2$ concentration

Due to normal variations in  $\text{CO}_2$  concentration in the exhaust gas (**Table 3.1**), the effect of the inlet gas  $\text{CO}_2$  concentration on the removal efficiency was examined within a range of 10–100% (equivalent to a  $\text{CO}_2$  partial pressure range of  $0.05\text{--}0.50 \text{ MPa}$ ). The proportion of  $\text{CO}_2$  in the mixed gas with  $\text{N}_2$  was adjusted by changing the flow rate ratio between  $\text{CO}_2$  and  $\text{N}_2$ . The degree of  $\text{CO}_2$  removal increased continuously from 50.1% to 97.8% at a gas flow rate of  $15 \text{ L min}^{-1}$  and from 41.9% to 93.5% at a gas flow rate of  $20 \text{ L min}^{-1}$  as the  $\text{CO}_2$  partial pressure

increased from 0.05 to 0.50 MPa (**Figure 3.6(a)**). In contrast, the pH decreased from 6.0 to 5.0 under both total gas flow rates (15 and 20 L min<sup>-1</sup>), suggesting that increasing the CO<sub>2</sub> partial pressure as increasing the inlet CO<sub>2</sub> concentration in the inlet mixed gas accelerated the dissolution of CO<sub>2</sub> in water. These results demonstrate that the variation in CO<sub>2</sub> partial pressure was related strongly and proportionally to the CO<sub>2</sub> absorption ability and removal rate in the liquid phase. This process was described by Henry's Law, in that the gas partial pressure directly affected the gas dissolution rate. When the gas partial pressure increased, the concentration of the gas phase increased, leading to a reduction in the resistance between the two-phase liquid and gas and enable for CO<sub>2</sub> to dissolve greatly into water. In general, an increase in partial pressure quickly accelerated the dissolution of CO<sub>2</sub> in water, followed by an increase in removal efficiency. Moreover, higher inlet CO<sub>2</sub> gas partial pressures resulted in higher initial CO<sub>2</sub> concentrations; therefore, the CO<sub>2</sub> removal efficiency results indicated that the potential for CO<sub>2</sub> molecules to pass through the gas bulk to the gas-liquid interface increased with higher initial CO<sub>2</sub> concentrations in the gas mixture.

A similar trend was observed in the response of the CO<sub>2</sub> absorption rate. This rate increased from  $6.0 \times 10^{-4}$  to approximately  $35.0 \times 10^{-4}$  mol s<sup>-1</sup>L<sup>-1</sup> when the CO<sub>2</sub> partial pressure increased from 0.05 to 0.50 MPa and the CO<sub>2</sub> proportion in the inlet gas increased from 10% to 100%. (**Figure 3.6(b)**). At higher initial CO<sub>2</sub> concentrations, the partial pressure was accelerated, enhancing the solubility of CO<sub>2</sub> in water.

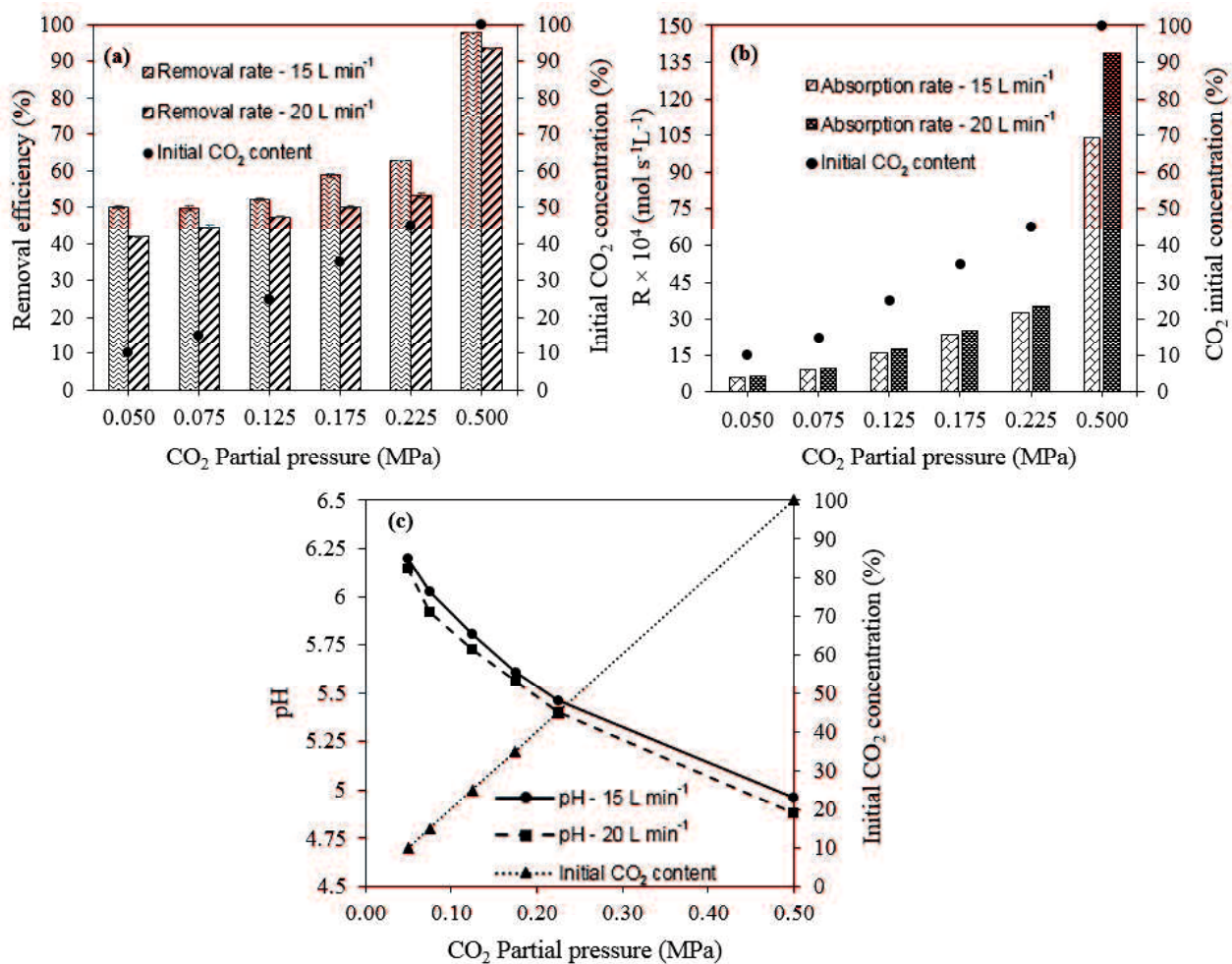


**Figure 3.6** Removal efficiency of CO<sub>2</sub>, (b) absorption rate of CO<sub>2</sub>, and (c) pH of the absorbed water at different initial CO<sub>2</sub> partial pressures with a total gas flow rate of 15 L min<sup>-1</sup> and 20 L min<sup>-1</sup>; Water flow rate: 14 L min<sup>-1</sup>; internal device pressure: 0.06 MPa; total inlet gas supplying pressure: 0.50 MPa; and temperature: 20°C.

### 3.3.5 Effect of temperature

**Figure 3.7** depicts the CO<sub>2</sub> removal ability and absorption rate at numerous temperatures. At the condition of a gas flow rate of 20 L min<sup>-1</sup> and a gas supplying pressure of 0.50 MPa, the removal rate exhibited a noticeable drop from around 65.0% to 30.0% as the temperature increased from 10°C to 30°C. Similarly, with the same change in temperature, the absorption rate dropped from  $12.8 \times 10^{-4}$  to  $7.5 \times 10^{-4}$  mol s<sup>-1</sup>L<sup>-1</sup> for inlet gas G<sub>1</sub>, from  $21.9 \times 10^{-4}$  to  $13.7 \times 10^{-4}$  mol s<sup>-1</sup>L<sup>-1</sup> for gas G<sub>2</sub>, and from  $31.3 \times 10^{-4}$  to  $20.4 \times 10^{-4}$  mol s<sup>-1</sup>L<sup>-1</sup> for gas G<sub>3</sub>. Because the absorption of CO<sub>2</sub> in water is a physical process, the CO<sub>2</sub> solubility in water is temperature- and pressure-dependent, as described by Henry's law. Based on this, as pressure and inlet gas

composition remained constant, increasing temperature had an adverse effect on removal efficiency and the absorption capacity (Carroll *et al.*, 1991, Murray & Riley, 1971, Weiss, 1974). Temperature additionally acted upon the bubble diameter, rise velocity, and gas holdup. Increasing temperature was responsible for the enhancement of the bubble rising velocity (Van Le *et al.*, 2013). It is widely accepted that the gas holdup and total bubble surface area decline with a surge in temperature (Pérez-Garibay *et al.*, 2012). Because of these properties, increasing temperature restrains the dissolution rate of CO<sub>2</sub>, and in this experiment, lower temperature in the chamber provided optimal conditions for the sequestration of CO<sub>2</sub> from the feed gases.

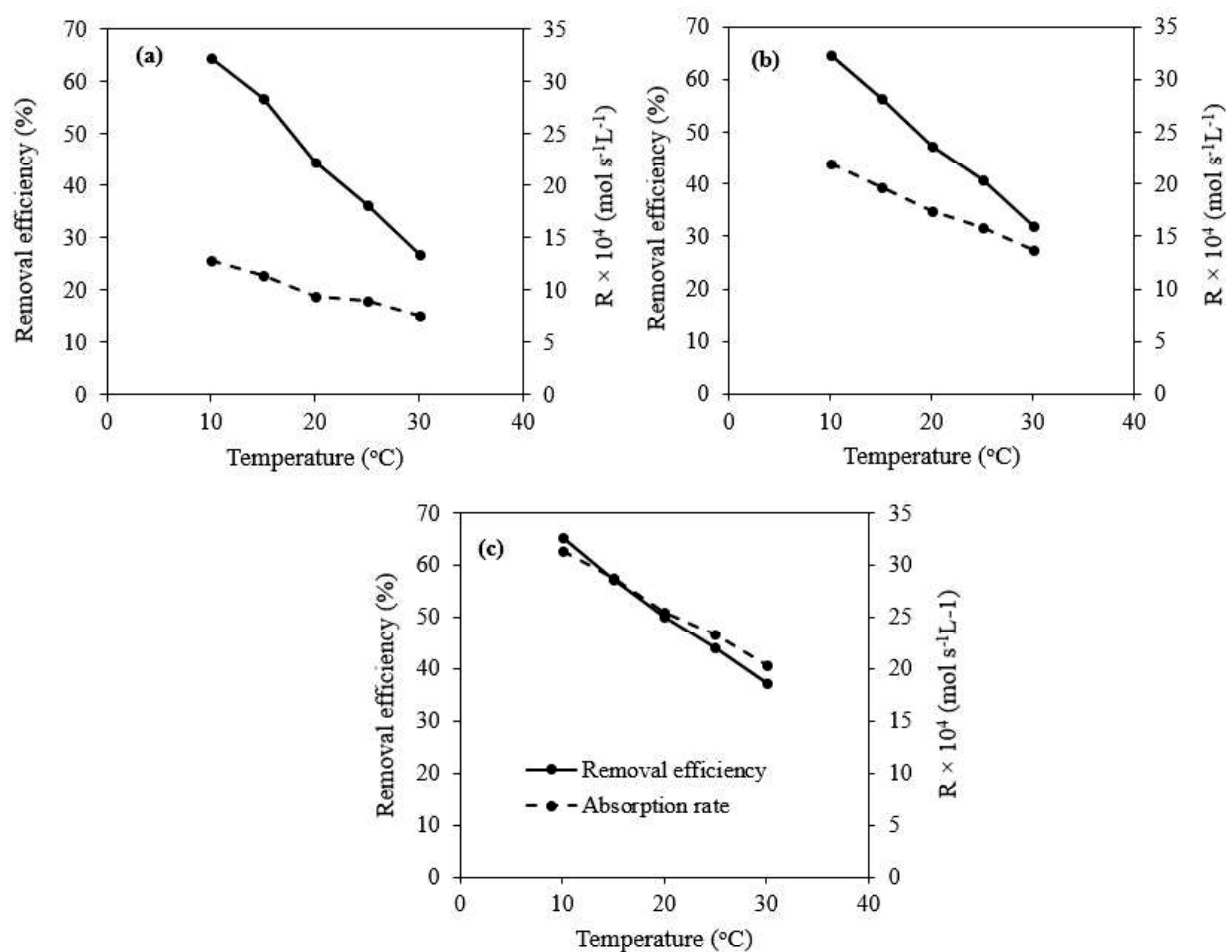


**Figure 3.7** Removal efficiency and absorption rate of CO<sub>2</sub> in water at different gas compositions: (a) 15% CO<sub>2</sub>-85% N<sub>2</sub>, (b) 25% CO<sub>2</sub>-75% N<sub>2</sub>, and (c) 35% CO<sub>2</sub>-65% N<sub>2</sub>. Total gas flow rate: 20 L min<sup>-1</sup>; water flow rate: 14 L min<sup>-1</sup>; internal device pressure: 0.06 MPa; total inlet gas supplying pressure: 0.50 MPa.

### 3.4 Conclusions

For the physical absorption of CO<sub>2</sub> with tap water used as the solvent, an apparatus that could intensify the mass transfer between a two-phase liquid and gas via the generation of water-film as well as fine bubbles was employed to reduce the levels of CO<sub>2</sub> in the exhaust gases. The effect of various operating factors on the removal efficiency and absorption rate of CO<sub>2</sub> in water was established in this study. At a gas supplying pressure of 0.50 MPa and temperature of 20°C and with CO<sub>2</sub> concentrations in the mixed gas fluctuating from 15% to 35%, removal efficiency increased from 38.2 to 73.7% when the G/L ratio also reduced from 1.79 to 0.36 in accordance with gas flow rate decreasing from 25 to 5 L min<sup>-1</sup>. Meanwhile, under the same conditions of gas supplying pressure, temperature, and gas flow rate range, the absorption rate decreased from  $27.4 \times 10^{-4}$  to  $10.7 \times 10^{-4}$  mol s<sup>-1</sup>L<sup>-1</sup> when using the mixed gas comprising 35% CO<sub>2</sub> and 65% N<sub>2</sub>. Temperature also played an essential role in improving the removal rates since the removal rate grew from 30.0% to 65.0% with the drop of temperature from 30°C to 10°C at the gas supplying pressure of 0.50 MPa, 1.43 of G/L ratio and with the range from 15% to 35% of CO<sub>2</sub> in the feed gas.

According to the experimental results, the optimum conditions comprise a high internal pressure in the chamber, 0.30 MPa of total gas supplying pressure, high inlet gas CO<sub>2</sub> concentration, and low temperature. However, although a low G/L ratio can lead to high efficacy of CO<sub>2</sub> removal, it reduces the absorption rate, corresponding to a low rate of CO<sub>2</sub> absorption from a large quantity of exhaust gas; therefore, it lowers the performance of the absorption process and limits the application of this procedure at the industrial scale. To resolve this issue, a suitable G/L ratio should be carefully considered and selected in order to not only meet the standard requirement of removal efficiency but also reach an acceptable absorption rate to treat a huge amount of industrial released gas. Another solution for this, which will be addressed in further research, is to develop the design of water-film-forming-unit as well as the apparatus, for example, increasing the number of the water-film generators inside the apparatus, with an aim to obtain high removal rates at high G/L ratios.

### 3.5 References

- Bang, J.-H., Kim, W., Song, K. S., Jeon, C. W., Chae, S. C., Cho, H.-J., Jang, Y. N. & Park, S.-J. 2014. Effect of experimental parameters on the carbonate mineralization with  $\text{CaSO}_4 \cdot 2\text{H}_2\text{O}$  using  $\text{CO}_2$  microbubbles. *Chemical Engineering Journal*, **244**, 282-287.
- Bhown, A. S. & Freeman, B. C. 2011. Analysis and status of post-combustion carbon dioxide capture technologies. *Environmental science & technology*, **45** (20), 8624-8632.
- Car, A., Stropnik, C., Yave, W. & Peinemann, K.-V. 2008. Pebax®/polyethylene glycol blend thin film composite membranes for  $\text{CO}_2$  separation: Performance with mixed gases. *Separation and Purification Technology*, **62** (1), 110-117.
- Carroll, J. J., Slupsky, J. D. & Mather, A. E. 1991. The solubility of carbon dioxide in water at low pressure. *Journal of Physical and Chemical Reference Data*, **20** (6), 1201-1209.
- Chai, X. & Zhao, X. 2012. Enhanced removal of carbon dioxide and alleviation of dissolved oxygen accumulation in photobioreactor with bubble tank. *Bioresource technology*, **116**, 360-365.
- Chen, P.-C. 2012. Absorption of carbon dioxide in a bubble-column scrubber, INTECH Open Access Publisher.
- Chen, P.-C., Huang, C.-H., Su, T., Chen, H.-W., Yang, M.-W. & Tsao, J.-M. 2015. Optimum conditions for the capture of carbon dioxide with a bubble-column scrubber. *International Journal of Greenhouse Gas Control*, **35**, 47-55.
- Cheng, L., Li, T., Keener, T. & Lee, J.-Y. 2013. A mass transfer model of absorption of carbon dioxide in a bubble column reactor by using magnesium hydroxide slurry. *International Journal of Greenhouse Gas Control*, **17**, 240-249.
- Chowdhury, F. A., Okabe, H., Yamada, H., Onoda, M. & Fujioka, Y. 2011. Synthesis and selection of hindered new amine absorbents for  $\text{CO}_2$  capture. *Energy Procedia*, **4**, 201-208.
- González-Salazar, M. A. 2015. Recent developments in carbon dioxide capture technologies for gas turbine power generation. *International Journal of Greenhouse Gas Control*, **34**, 106-116.
- Ho, S.-H., Chen, C.-Y., Lee, D.-J. & Chang, J.-S. 2011. Perspectives on microalgal  $\text{CO}_2$ -emission mitigation systems—a review. *Biotechnology advances*, **29** (2), 189-198.

- Imai, T. & Zhu, H. 2011. Improvement of Oxygen Transfer Efficiency in Diffused Aeration Systems Using Liquid-Film-Forming Apparatus, INTECH Open Access Publisher.
- Kawahara, A., Sadatomi, M., Matsuyama, F., Matsuura, H., Tominaga, M. & Noguchi, M. 2009. Prediction of micro-bubble dissolution characteristics in water and seawater. *Experimental Thermal and Fluid Science*, **33** (5), 883-894.
- Läntelä, J., Rasi, S., Lehtinen, J. & Rintala, J. 2012. Landfill gas upgrading with pilot-scale water scrubber: performance assessment with absorption water recycling. *Applied energy*, **92**, 307-314.
- Leung, D. Y., Caramanna, G. & Maroto-Valer, M. M. 2014. An overview of current status of carbon dioxide capture and storage technologies. *Renewable and Sustainable Energy Reviews*, **39**, 426-443.
- Li, T., Keener, T. C. & Cheng, L. 2014. Carbon dioxide removal by using Mg(OH)<sub>2</sub> in a bubble column: Effects of various operating parameters. *International Journal of Greenhouse Gas Control*, **31**, 67-76.
- Lin, C.-C. & Chu, C.-R. 2015. Feasibility of carbon dioxide absorption by NaOH solution in a rotating packed bed with blade packings. *International Journal of Greenhouse Gas Control*, **42**, 117-123.
- Mikkelsen, M., Jørgensen, M. & Krebs, F. C. 2010. The teraton challenge. A review of fixation and transformation of carbon dioxide. *Energy & Environmental Science*, **3** (1), 43-81.
- Mondal, M. K., Balsora, H. K. & Varshney, P. 2012. Progress and trends in CO<sub>2</sub> capture/separation technologies: A review. *Energy*, **46** (1), 431-441.
- Murray, C. & Riley, J. 1971. The solubility of gases in distilled water and sea water—IV. Carbon dioxide. *Deep Sea Research and Oceanographic Abstracts*, **18** (5), 533-541.
- Olah, G. A., Goeppert, A. & Prakash, G. S. 2008. Chemical recycling of carbon dioxide to methanol and dimethyl ether: from greenhouse gas to renewable, environmentally carbon neutral fuels and synthetic hydrocarbons. *The Journal of organic chemistry*, **74** (2), 487-498.
- Olajire, A. A. 2010. CO<sub>2</sub> capture and separation technologies for end-of-pipe applications – A review. *Energy*, **35** (6), 2610-2628.



- Parmar, R. & Majumder, S. K. 2013. Microbubble generation and microbubble-aided transport process intensification—A state-of-the-art report. *Chemical Engineering and Processing: Process Intensification*, **64**, 79-97.
- Parmar, R. & Majumder, S. K. 2014. Hydrodynamics of microbubble suspension flow in pipes. *Industrial & Engineering Chemistry Research*, **53** (9), 3689-3701.
- Petersson, A. & Wellinger, A. 2009. Biogas upgrading technologies—developments and innovations. *IEA Bioenergy*, **20**, 1-19.
- Rahmandoost, E., Roozbehani, B. & Maddahi, M. H. 2014. Experimental Studies of CO<sub>2</sub> Capturing from the Flue Gases. *Iranian Journal of Oil & Gas Science and Technology*, **3** (4), 1-15.
- Ryckebosch, E., Drouillon, M. & Vervaeren, H. 2011. Techniques for transformation of biogas to biomethane. *Biomass and bioenergy*, **35** (5), 1633-1645.
- Sumida, K., Rogow, D. L., Mason, J. A., McDonald, T. M., Bloch, E. D., Herm, Z. R., Bae, T.-H. & Long, J. R. 2011. Carbon dioxide capture in metal–organic frameworks. *Chemical reviews*, **112** (2), 724-781.
- Van Le, T., Imai, T., Higuchi, T., Yamamoto, K., Sekine, M., Doi, R., Vo, H. T. & Wei, J. 2013. Performance of tiny microbubbles enhanced with “normal cyclone bubbles” in separation of fine oil-in-water emulsions. *Chemical Engineering Science*, **94**, 1-6.
- Weiss, R. F. 1974. Carbon dioxide in water and seawater: the solubility of a non-ideal gas. *Marine chemistry*, **2** (3), 203-215.
- Xiao, Y., Yuan, H., Pang, Y., Chen, S., Zhu, B., Zou, D., Ma, J., Yu, L. & Li, X. 2014. CO<sub>2</sub> removal from biogas by water washing system. *Chinese Journal of Chemical Engineering*, **22** (8), 950-953.
- Yu, C.-H., Huang, C.-H. & Tan, C.-S. 2012. A review of CO<sub>2</sub> capture by absorption and adsorption. *Aerosol and Air Quality Research*, **12** (5), 745-769.

## CHAPTER 4

# RESPONSE SURFACE METHOD FOR MODELING THE REMOVAL OF CARBON DIOXIDE FROM A SIMULATED GAS USING WATER ABSORPTION ENHANCED WITH A WATER-FILM-FORMING-UNIT

### 4.1 Introduction

With the rapid growth of commerce and modern civilization, the world has ever-increasing energy demands that result in large CO<sub>2</sub> emissions. The atmospheric concentration of CO<sub>2</sub> has increased more than 40% since the beginning of the industrial revolution (270–400 ppmV) and has been rising annually by 2 ppmV (Moreira & Pires, 2016, Singh & Ahluwalia, 2013). With industrial activities such as fossil fuel burning and industrial production, 30 billion tons of CO<sub>2</sub> are released to the atmosphere each year (Moreira & Pires, 2016, Li *et al.*, 2013). In addition, according to the International Panel on Climate Change (IPCC), the atmospheric CO<sub>2</sub> concentration is predicted to increase to 936 ppmV before 2100 and lead to a rise in the mean global temperature of approximately 1.0–3.0 °C (Chou, 2013, Lee *et al.*, 2012). Therefore, the removal of CO<sub>2</sub> from the atmosphere has recently become an urgent issue that has gained global attention, in order to mitigate global warming and the subsequent negative consequences.

Absorption is the most widely used method to capture CO<sub>2</sub> from gas streams because it is a well-established technique that has been in use for nearly 60 years (Babu, 2014, Rao & Rubin, 2002). The main principle of this method is to transfer one or more substances from a gas stream into a liquid phase through the vapor–liquid phase boundary. There are two main types of absorption processes: physical absorption and chemical absorption. This classification is based on whether or not a chemical reaction occurs after the dissolution of substances into a liquid absorbent (Aresta, 2013). In this research, it focuses on the application of water scrubbing – classified as physical absorption – on the removal of CO<sub>2</sub>. In contrast to chemical absorption, the operation of physical absorption is based on Henry’s Law, which implies that the absorption process is temperature and pressure dependent and the removal of CO<sub>2</sub> depends on its solubility in the liquid phase (Olajire, 2010). Water absorption is one of the most popular processes for physical absorption. The fundamental principle of this method relies on the solubility of CO<sub>2</sub> in water. The separation of CO<sub>2</sub> from a gas stream occurs due to the difference

in the solubility between CO<sub>2</sub> and other gases. CO<sub>2</sub> is more soluble in water than other gases, such as N<sub>2</sub>, O<sub>2</sub>, H<sub>2</sub>, and CH<sub>4</sub> (Weiss, 1974). As a consequence, it can be absorbed in water more easily and thus removed from the feed streams. Through this method, absorption and desorption can be accomplished using water, which results in lower cost (for solvents and regeneration) and higher stability, all with an environmentally friendly process (resulting in no unexpected toxic by-products) (Xiao *et al.*, 2014). However, this scheme retains the challenge of improving the CO<sub>2</sub> removal efficiency because of the lower interaction between CO<sub>2</sub> and water than when organic solvents are used for physical or chemical absorption. This method has not been applied widely and is in need of more research and development. In order to augment the solubility of gases in the aqueous phase, it is possible to form a liquid-film through the use of gas bubbles—especially fine bubbles or microbubbles—to produce a high interfacial area and enhance the interaction between gas molecules and liquids (Bang *et al.*, 2014, Parmar & Majumder, 2013, Xu *et al.*, 2008, Imai & Zhu, 2011).

Microbubbles are defined as tiny bubbles with diameter below 100 μm (Parmar & Majumder, 2013). Tiny bubbles have a high surface tension, small buoyancy, and low slip velocity, all of which leads to a longer residence time for gas bubbles in an aqueous solution. Microbubbles also have a high gas dissolution rate because the surface area and internal pressure of the bubble rise notably, resulting in an increase in the partial pressure of the dissolving gas and a decrease in the bubble rising speed (Parmar & Majumder, 2013). In addition, a large surface area can be provided per unit volume of gas. These properties of microbubbles support their use as a potential solution for improving the dissolution of CO<sub>2</sub> in a liquid phase.

The aim of this study is to implement our method of utilizing tap water as a solvent in conjunction with a water-film-forming-unit (WFFU) that is able to form water-films and microbubbles to promote the dissolution of CO<sub>2</sub> in the tap water. The general objective of this study is, therefore, to remove CO<sub>2</sub> from a mixed gas at high removal efficiency via an eco-friendly method to prevent the release of hazardous by-products. With the investigation of various factors, the response surface method (RSM) was used to build models for this absorption process that can be used as a beneficial tool in predicting and selecting optimum conditions. Owing to the utilization of RSM, it provides several benefits when conducting

experiments such as time-saving, reducing experimental trials and availability for observing the interactions among factors.

## **4.2 Materials, experimental apparatus and methods**

### **4.2.1 Materials and experimental apparatus**

The simulated gas consisted of a mixture of nitrogen and CO<sub>2</sub> mixed by using gas flow meters. The CO<sub>2</sub> (99.99%) and N<sub>2</sub> (99.99%) gases were purchased from Iwatani Corporation (Japan). Tap water was employed directly as the once-through physical absorbent without any purification process.

The apparatus used in this study are shown in **Figure 4.1**. The reactor is the main component of this system (represented as number 5 in **Figure 4.1**), with 22 cm diameter and 16 cm height. The absorption reactor was designed to connect with the liquid-film-forming device inside it, which has a 17 cm height and an 8 cm diameter, to generate large quantities of microbubbles.

The experiments were carried out at differing conditions of gas supplying pressure, temperature, gas to liquid ratio (G/L), and initial CO<sub>2</sub> concentration. In this study, the inlet gas supplying pressure was examined in the range of 0.25–0.75 MPa. The concentration of CO<sub>2</sub> mixed with N<sub>2</sub> was adjusted from 10% to 45% using a gas flow rate controller. Meanwhile, the G/L ratio was controlled by holding the liquid flow rate at 14 L min<sup>-1</sup> while changing the gas flow rate from 5 to 25 L min<sup>-1</sup>. Temperature was investigated in the range of 10 °C to 30 °C, which corresponds to the normal annual temperature range in Japan.

In order to evaluate the absorption rate and the removal efficiency of CO<sub>2</sub>, the outlet gas from the exhaust gas valve was collected into a sampling gas bag and then analyzed by gas chromatography (GC-8A, Shimadzu, Japan). The GC-8A is equipped with a thermal conductivity detector (TCD) and an activated carbon 60/80 column (1.5 m × 3.0 mm ID). Argon was used as the carrier gas. The operation temperatures for the injector, the column, and the detector were 50, 60, and 50 °C, respectively. The CO<sub>2</sub> concentration in water was measured with a CO<sub>2</sub> meter (CGP- 31, DKK-TOA Co., Japan).

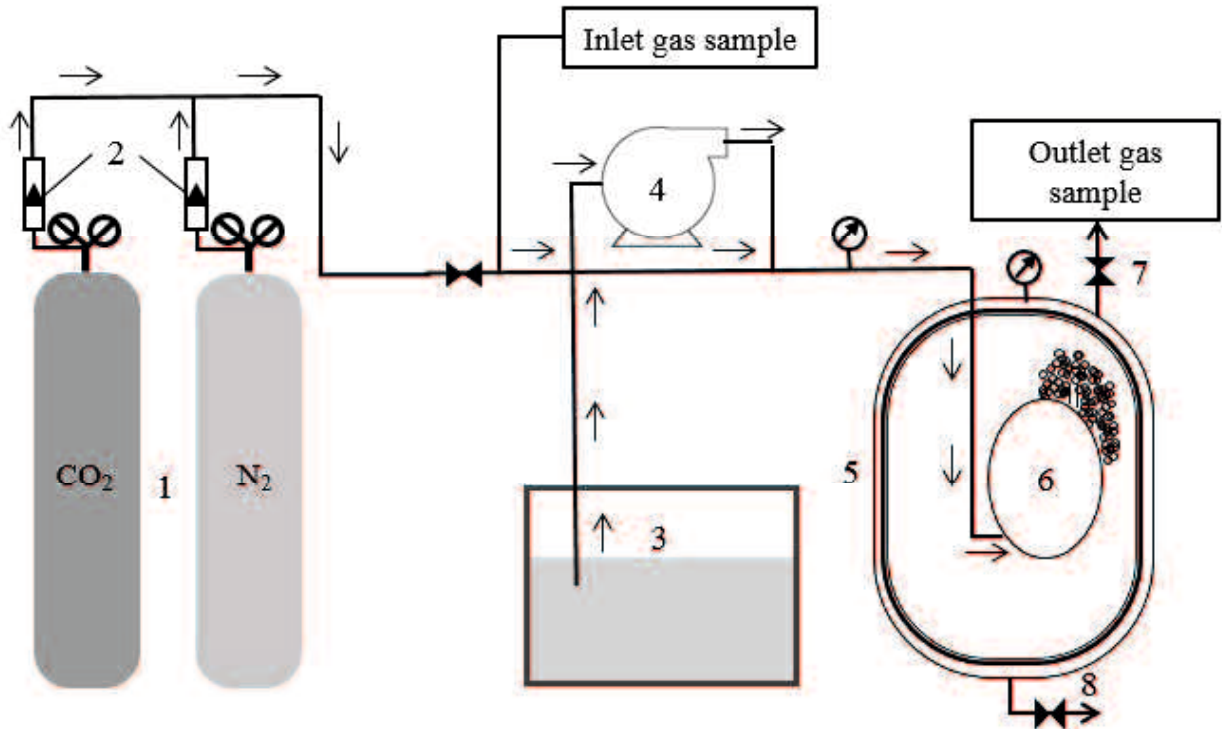


**Figure 4.1** Experimental apparatus used for CO<sub>2</sub> absorption: (1) CO<sub>2</sub> and N<sub>2</sub> cylinders; (2) gas flow rate controllers; (3) water tank; (4) pump; (5) reactor; (6) liquid-film-forming device; (7) exhaust gas valve; and (8) blowdown valve.

According to Pao Chi Chen's study (Chen, 2012), the absorption rate can be calculated by the following formula:

$$R = \frac{F_{\text{CO}_2}}{V} \left[ 1 - \left( \frac{1-x_{\text{CO}_2}^{\text{in}}}{x_{\text{CO}_2}^{\text{in}}} \right) \left( \frac{x_{\text{CO}_2}^{\text{out}}}{1-x_{\text{CO}_2}^{\text{out}}} \right) \right] \quad (4.1)$$

where  $R$  (mol s<sup>-1</sup>L<sup>-1</sup>) is the absorption rate of CO<sub>2</sub> in the liquid phase;  $F_{\text{CO}_2}$  (mol s<sup>-1</sup>) is the CO<sub>2</sub> molar flow rate;  $V$  (L) is the volume of liquid phase in the chamber;  $x_{\text{CO}_2}^{\text{in}}$  is the molar fraction of CO<sub>2</sub> at the inlet; and  $x_{\text{CO}_2}^{\text{out}}$  is the molar fraction of CO<sub>2</sub> at the outlet.

#### 4.2.2 Plackett–Burman design

The Plackett–Burman design was used to screen and select the factors significantly affecting CO<sub>2</sub> removal and absorption rate. Generally, Plackett–Burman design is applied to reduce the number of factors in case of the initial factors are several (more than 7 factors). In this research, due to only four initial factors, it is not necessary to screen and reduce the number of factors.

However, in order to follow all steps of the RSM procedure, Plackett–Burman design was used to accomplish the step of selecting and determining significant factors.

The four factors investigated were gas supplying pressure (GSP) ( $X_1$ ), CO<sub>2</sub> initial concentration (CO<sub>2</sub> conc.) ( $X_2$ ), gas/liquid ratio (G/L) ( $X_3$ ), and temperature (Temp.) ( $X_4$ ). According to the Plackett–Burman design, each parameter was set at two levels: -1 for a low level and +1 for a high level. With these parameters, the program Minitab 14 was used to design the experimental matrix and determine the important factors. The levels of each factor, their values, and their effects as used in the experimental design matrix are given in **Table 4.1**. The effect of each parameter was estimated by **Eq 4.2**:

$$E_{X_i} = \frac{\sum M_{i+}}{N/2} - \frac{\sum M_{i-}}{N/2} \quad (4.2)$$

where  $E_{X_i}$  is the effect of the tested variables ( $X_i$ );  $M_{i+}$  and  $M_{i-}$  are the responses (CO<sub>2</sub> removal efficiency  $E$  and absorption rate  $R$ ) collected from trials where the variable ( $X_i$ ) was measured at high and low levels, respectively; and  $N$  is the number of experiments.

The factors having a  $P$ -value  $\leq 0.1$  at the confidence level of 90% were considered as the key factors that acted significantly on the removal rate. These factors were then used in the modeling step utilizing the response surface method (RSM).

**Table 4.1** Levels of the experimental variables, estimated effects, and P-value studied in the Plackett-Burman design

Code	Variable	Low level (-1)	High level (+1)	Removal efficiency <sup>a</sup>		Absorption rate <sup>b</sup>	
				Effect ( $E_{X_i}$ )	$P$ -value	Effect ( $E_{X_i}$ )	$P$ -value
$X_1$	Gas supplying pressure (GSP) (MPa)	0.30	0.50	-8.18 <sup>f</sup>	0.003 <sup>c</sup>	5.12 <sup>e</sup>	0.028 <sup>c</sup>
$X_2$	CO <sub>2</sub> initial concentration (CO <sub>2</sub> conc.) (%)	15	35	3.84 <sup>e</sup>	0.078 <sup>d</sup>	11.41 <sup>e</sup>	0.000 <sup>c</sup>
$X_3$	Gas/Liquid ratio (G/L)	0.71	1.43	-16.79 <sup>f</sup>	0.000 <sup>c</sup>	4.70 <sup>e</sup>	0.038 <sup>c</sup>
$X_4$	Temperature (Temp.) (°C)	10	25	-23.68 <sup>f</sup>	0.000 <sup>c</sup>	-3.03 <sup>f</sup>	0.144

<sup>a</sup>  $R^2 = 0.9744$ ; adj  $R^2 = 0.9598$

<sup>b</sup>  $R^2 = 0.8872$ ;  $\text{adj } R^2 = 0.8227$

<sup>c</sup>  $P$ -value  $< 0.05$  (Significant at 95% confidence level)

<sup>d</sup>  $P$ -value  $< 0.1$  (Significant at 90% confidence level)

<sup>e</sup> Positive effect; <sup>f</sup> Negative effect

### 4.2.3 Response surface method (RSM)

After screening the key factors, the next step in the experiment was to determine the model regressions and optimum conditions by using a response surface method. Central composite design (CCD) is popularly applied to design experiments for RSM. The design composes of three parts: (1) a full factorial or fractional factorial design; (2) an additional design, often a star design where experimental points are at a distance  $\alpha$  from its center; and (3) a central point (Bezerra *et al.*, 2008).

Responses obtained by experiments are represented by quadratic models using the polynomial equation (Phummala *et al.*, 2015):

$$y = \beta_0 + \sum_{i=1}^k \beta_i x_i + \sum_{i=1}^k \beta_{ii} x_i^2 + \sum_{i=1}^k \sum_{j=1}^k \beta_{ij} x_i x_j \quad (4.3)$$

where  $y$  is the predicted response;  $\beta_0$  is the constant;  $\beta_i$  is the linear effect term;  $\beta_{ii}$  is the quadratic effect term;  $\beta_{ij}$  is the interaction effect term;  $x_i$  is the variable  $i$ ; and  $x_j$  is the variable  $j$ . The quality of fit for the quadratic models was expressed by the coefficient of determination ( $R^2$ ) and the adjusted coefficient of determination ( $\text{adj-}R^2$ ).

The RSM with CCD was employed in this work to evaluate the impact of the independent and significant variables obtained from the Plackett–Burman design: gas supplying pressure (GSP) ( $X_1$ ), initial  $\text{CO}_2$  concentration ( $\text{CO}_2$  conc.) ( $X_2$ ), gas/liquid ratio (G/L) ( $X_3$ ), and temperature (Temp.) ( $X_4$ ). Based on CCD, each parameter was assessed at five coded levels (-2, -1, 0, 1, 2), with the corresponding values enumerated in **Table 4.3**.

## 4.3 Results and discussion

### 4.3.1 Screening key factors affecting the removal of CO<sub>2</sub> using tap water as the absorbent

The parameters of gas supplying pressure (GSP) ( $X_1$ ), initial CO<sub>2</sub> concentration (CO<sub>2</sub> conc.) ( $X_2$ ), gas/liquid ratio (G/L) ( $X_3$ ), and temperature (Temp.) ( $X_4$ ) were investigated using the Plackett–Burman design to identify how they affected the removal rate  $E$  and absorption rate  $R$ . The levels for each factor and the resulting analysis data of estimated effects and probability values ( $P$ -value) are given in **Table 4.1**. The experimental range for gas supplying pressure (GSP) ( $X_1$ ), initial CO<sub>2</sub> concentration (CO<sub>2</sub> conc.) ( $X_2$ ), gas/liquid ratio (G/L) ( $X_3$ ), and temperature (Temp.) ( $X_4$ ) are 0.30 – 0.50 MPa, 15% – 35%, 0.71 – 1.43, and 10 °C – 25 °C, respectively. Particular, based on the results obtained from **chapter 3**, for the factor of gas supplying pressure, the experimental range should be from 0.30 to 0.70 MPa. However, because the removal efficiencies at the condition of 0.30 MPa and 0.70 MPa were nearly same if the low level and high level were set at 0.30 MPa and 0.70 MPa, respectively, the effect of this factor would be zero and this would not reflect the actual phenomenon. Therefore, in Plackett – Burman, the experimental range for gas supplying factor was chosen from 0.30 to 0.50 MPa. The experimental matrix comprising 12 experiments was designed using Minitab 14 software and is given in **Table 4.2**. According to the data obtained from **Table 4.1**, factors with a  $P$ -value  $< 0.1$  were considered the key factors affecting the removal and absorption rates.



**Table 4.2** Plackett-Burman design matrix for evaluating influent factors with removal efficiency and absorption rate as responses

Run	$X_1$	$X_2$	$X_3$	$X_4$	Removal efficiency $E$		Absorption rate $R \times 10^4$	
					(%)		$(\text{mol s}^{-1}\text{L}^{-1})$	
					Observed	Predicted	Observed	Predicted
1	1	-1	-1	-1	79.47	77.15	7.85	9.17
2	1	1	-1	1	57.43	57.30	17.47	17.54
3	1	1	1	-1	61.86	64.19	30.76	25.27
4	1	1	-1	1	57.59	57.30	17.59	17.54
5	1	-1	1	-1	58.50	60.36	12.55	13.87
6	1	-1	1	1	38.11	36.67	8.01	10.83
7	-1	-1	-1	-1	88.69	85.33	5.21	4.05
8	-1	1	1	-1	71.33	72.38	19.64	20.152
9	-1	-1	-1	1	55.99	61.65	4.71	1.02
10	-1	1	1	1	52.10	48.69	15.67	17.12
11	-1	1	-1	-1	88.71	89.17	11.96	15.46
12	-1	-1	1	1	45.24	44.86	6.33	5.72

Using a  $P$ -value  $< 0.1$  (with the 90% confidence level), the initial  $\text{CO}_2$  concentration exerted significant and positive effects on the removal rate  $E$ , while the gas supplying pressure, gas/liquid ratio and temperature were found to have a negative influence. Additionally, the parameters of gas supplying pressure,  $\text{CO}_2$  initial concentration, and gas/liquid ratio impacted the absorption rate  $R$  at high rank, with  $P$ -value  $< 0.1$ , and showed a positive effect. Only did temperature have an insignificant influence on the absorption rate at the 90% confidence level. However, temperature was identified as a strongly significant factor for the response of  $E$ . Therefore, the four factors of gas supplying pressure, inlet  $\text{CO}_2$  concentration, G/L ratio, and temperature were found to have the significant influence on both the removal and absorption rates. Ultimately, gas supplying pressure ( $X_1$ ),  $\text{CO}_2$  initial concentration ( $X_2$ ), gas/liquid ratio ( $X_3$ ), and temperature ( $X_4$ ) were selected for further optimization in the next step using an RSM design.

**Table 4.3** Central composite design matrix for the experimental design and predicted responses for removal efficiency  $E$  (%) and absorption rate  $R$  ( $\text{mol s}^{-1}\text{L}^{-1}$ )

Run	Gas supplying pressure ( $X_1$ ) (MPa)		CO <sub>2</sub> initial concentration ( $X_2$ ) (%)		Gas/Liquid ratio ( $X_3$ )		Temperature ( $X_4$ ) (°C)		Removal efficiency $E$ (%)		Absorption rate $R \times 10^4$ ( $\text{mol s}^{-1}\text{L}^{-1}$ )	
	Actual	Code	Actual	Code	Actual	Code	Actual	Code	Observed	Predicted	Observed	Predicted
1	0.50	0	25	0	1.07	0	30	2	41.30	40.83	13.25	12.13
2	0.50	0	25	0	1.07	0	20	0	52.38	52.17	15.83	15.58
3	0.70	1	15	-1	0.71	-1	25	1	54.40	54.62	9.64	8.68
4	0.50	0	25	0	1.07	0	20	0	51.88	52.17	15.56	15.58
5	0.50	0	25	0	1.07	0	20	0	52.59	52.17	15.88	15.58
6	0.70	1	35	1	0.71	-1	15	-1	78.00	77.41	29.35	30.89
7	0.50	0	10	-2	1.07	0	20	0	50.12	50.90	6.13	6.34
8	0.50	0	25	0	1.07	0	20	0	52.28	52.17	15.76	15.58
9	0.30	-1	35	1	0.71	-1	25	1	64.64	65.55	10.98	11.15
10	0.30	-1	15	-1	1.43	1	15	-1	61.03	61.23	7.70	6.82
11	0.70	1	15	-1	1.43	1	25	1	45.47	44.69	13.06	13.04
12	0.25	-2	25	0	1.07	0	20	0	64.88	63.50	8.98	8.82
13	0.50	0	45	2	1.07	0	20	0	62.71	62.54	32.48	33.10
14	0.70	1	35	1	0.71	-1	25	1	63.08	62.74	25.14	24.90
15	0.70	1	15	-1	1.43	1	15	-1	60.97	59.92	21.07	21.29
16	0.70	1	35	1	1.43	1	15	-1	62.44	62.24	51.31	47.06
17	0.30	-1	35	1	1.43	1	25	1	52.10	52.08	15.67	14.99
18	0.50	0	25	0	1.79	2	20	0	41.90	42.56	18.11	19.81
19	0.70	1	15	-1	0.71	-1	15	-1	73.10	72.98	12.05	11.61
20	0.30	-1	35	1	0.71	-1	15	-1	79.87	80.52	11.64	10.54
21	0.30	-1	15	-1	0.71	-1	15	-1	75.98	75.70	5.04	4.15
22	0.70	1	35	1	1.43	1	25	1	50.54	50.69	34.47	35.75
23	0.30	-1	35	1	1.43	1	15	-1	64.29	63.93	18.36	19.70
24	0.50	0	25	0	1.07	0	10	-2	70.30	71.04	17.90	19.76

25	0.30	-1	15	-1	1.43	1	25	1	45.24	45.70	6.33	5.17
26	0.50	0	25	0	1.07	0	20	0	52.13	52.17	15.70	15.58
27	0.50	0	25	0	1.07	0	20	0	52.48	52.17	15.85	15.58
28	0.50	0	25	0	1.07	0	20	0	52.23	52.17	15.72	15.58
29	0.50	0	25	0	0.36	-2	20	0	69.19	68.79	7.45	6.46
30	0.30	-1	15	-1	0.71	-1	25	1	56.99	57.05	4.71	7.83
31	0.75	2	25	0	1.07	0	20	0	58.85	60.93	24.39	26.45

---

### 4.3.2 Effect of operating factors on the removal of CO<sub>2</sub> using tap water as the absorbent

The 31 experimental trials conducted in this work were targeted to assess the effects of the four variables and construct quadratic models. The experimental matrix, along with the corresponding results of the CCD, is presented in **Table 4.3**.

The regression equation coefficients were calculated and listed in **Table 4.4**. The significance of each coefficient was determined by the Student's *t*-test. In terms of actual units, the responses in removal efficiency *E* (%) and absorption rate *R* (mol s<sup>-1</sup>L<sup>-1</sup>) were fitted with second-order polynomial equations as expressed below:

$$E = 186.21 - 171.32X_1 - 0.54X_2 - 40.90X_3 - 3.98X_4 + 160.65X_1^2 + 0.01X_2^2 + 7.03X_3^2 + 0.04X_4^2 - 0.05X_1X_2 + 4.91X_1X_3 + 0.07X_1X_4 - 0.15X_2X_3 + 0.02X_2X_4 + 0.43X_3X_4 \quad (4.4)$$

$$R \times 10^4 = -8.71 - 30.87X_1 - 0.63X_2 + 11.16X_3 + 1.47X_4 + 32.82X_1^2 + 0.01X_2^2 - 4.88X_3^2 + 1.61X_1X_2 + 24.34X_1X_3 - 1.65X_1X_4 + 0.45X_2X_3 - 0.02X_2X_4 - 0.74X_3X_4 \quad (4.5)$$

**Table 4.4** Significance of regression coefficients for removal efficiency *E* (%) and absorption rate *R* (mol s<sup>-1</sup>L<sup>-1</sup>)

Terms	Regression coefficient	Standard error	<i>t</i> -value	<i>P</i> -value
<b>Removal efficiency <i>E</i> (%)</b>				
Constant	186.207	6.108	30.487	0.000*
<i>X</i> <sub>1</sub>	-171.323	9.811	-17.462	0.000*
<i>X</i> <sub>2</sub>	-0.536	0.163	-3.289	0.005*
<i>X</i> <sub>3</sub>	-40.900	4.333	-9.438	0.000*
<i>X</i> <sub>4</sub>	-3.976	0.337	-11.806	0.000*
<i>X</i> <sub>1</sub> <sup>2</sup>	160.650	7.543	21.299	0.000*
<i>X</i> <sub>2</sub> <sup>2</sup>	0.012	0.002	6.163	0.000*
<i>X</i> <sub>3</sub> <sup>2</sup>	7.031	1.292	5.443	0.000*
<i>X</i> <sub>4</sub> <sup>2</sup>	0.038	0.007	5.690	0.000*
<i>X</i> <sub>1</sub> <i>X</i> <sub>2</sub>	-0.048	0.111	-0.433	0.671
<i>X</i> <sub>1</sub> <i>X</i> <sub>3</sub>	4.913	3.085	1.593	0.131
<i>X</i> <sub>1</sub> <i>X</i> <sub>4</sub>	0.074	0.222	0.332	0.744
<i>X</i> <sub>2</sub> <i>X</i> <sub>3</sub>	-0.147	0.062	-2.380	0.030*
<i>X</i> <sub>2</sub> <i>X</i> <sub>4</sub>	0.018	0.004	4.147	0.001*
<i>X</i> <sub>3</sub> <i>X</i> <sub>4</sub>	0.433	0.123	3.506	0.003*
<b>Absorption rate <i>R</i> (mol s<sup>-1</sup>L<sup>-1</sup>)</b>				
Constant	-8.707	12.513	-0.696	0.496
<i>X</i> <sub>1</sub>	-30.866	20.100	-1.536	0.144
<i>X</i> <sub>2</sub>	-0.625	0.334	-1.872	0.080

$X_3$	11.164	8.878	1.258	0.227
$X_4$	1.474	0.690	2.136	0.048*
$X_1^2$	32.824	15.452	2.124	0.050*
$X_2^2$	0.007	0.004	1.803	0.090
$X_3^2$	-4.875	2.646	-1.842	0.084
$X_4^2$	0.004	0.014	0.268	0.792
$X_1X_2$	1.612	0.228	7.084	0.000*
$X_1X_3$	24.34	6.320	3.851	0.001*
$X_1X_4$	-1.651	0.455	-3.629	0.002*
$X_2X_3$	0.451	0.126	3.568	0.003*
$X_2X_4$	-0.015	0.009	-1.687	0.111
$X_3X_4$	-0.740	0.253	-2.925	0.010*

\*  $P$ -value < 0.05 (Significant for 95% confidence level)

The results of analysis of variance (ANOVA) for the regression models are given in **Table 4.5**. The probability values of the regression model in both the  $E$  and  $R$  cases equaled 0.000, demonstrating that the models were significant. The high determination coefficients ( $R^2$ ) of 0.996 and 0.982, together with adjusted determination coefficients (adj  $R^2$ ) of 0.993 and 0.966, for the responses of removal efficiency and absorption rate, respectively, indicate that the models explained 96.6%–99.6% of the variability in the response variable. **Figure 4.2** further confirms that there is a good agreement and correlation between the experimental and predicted values of the responses in both models.

**Table 4.5** Analysis of variance (ANOVA) for the parameters of central composite design (CCD) for removal efficiency  $E$  (%) and absorption rate  $R$  ( $\text{mol s}^{-1}\text{L}^{-1}$ )

Removal efficiency $E$ (%)					
Sources of variations	DF	Sum of Squares	Mean Square	$F$ -value	$P$ -value
Regression	14	3156.97	225.50	285.63	0.000
Linear	4	2614.20	87.08	110.30	0.000
Square	4	512.77	128.19	162.38	0.000
Interaction	6	29.99	5.00	6.33	0.001
Residual Error	16	12.63	0.79		
Total	30	3169.60			
Coefficient of determination ( $R^2$ ) = 0.996					
Adjusted determination coefficient (adj $R^2$ ) = 0.993					
Absorption rate $R \times 10^4$ ( $\text{mol s}^{-1}\text{L}^{-1}$ )					
Sources of variations	DF	Sum of Squares	Mean Square	$F$ -value	$P$ -value
Regression	14	2912.57	208.04	62.79	0.000
Linear	4	2531.14	12.07	3.64	0.027
Square	4	42.42	10.61	3.20	0.041
Interaction	6	339.01	56.50	17.05	0.000

Residual Error	16	53.01	3.31
Total	30	2965.59	
Coefficient of determination ( $R^2$ ) = 0.982			
Adjusted determination coefficient ( $adj R^2$ ) = 0.966			

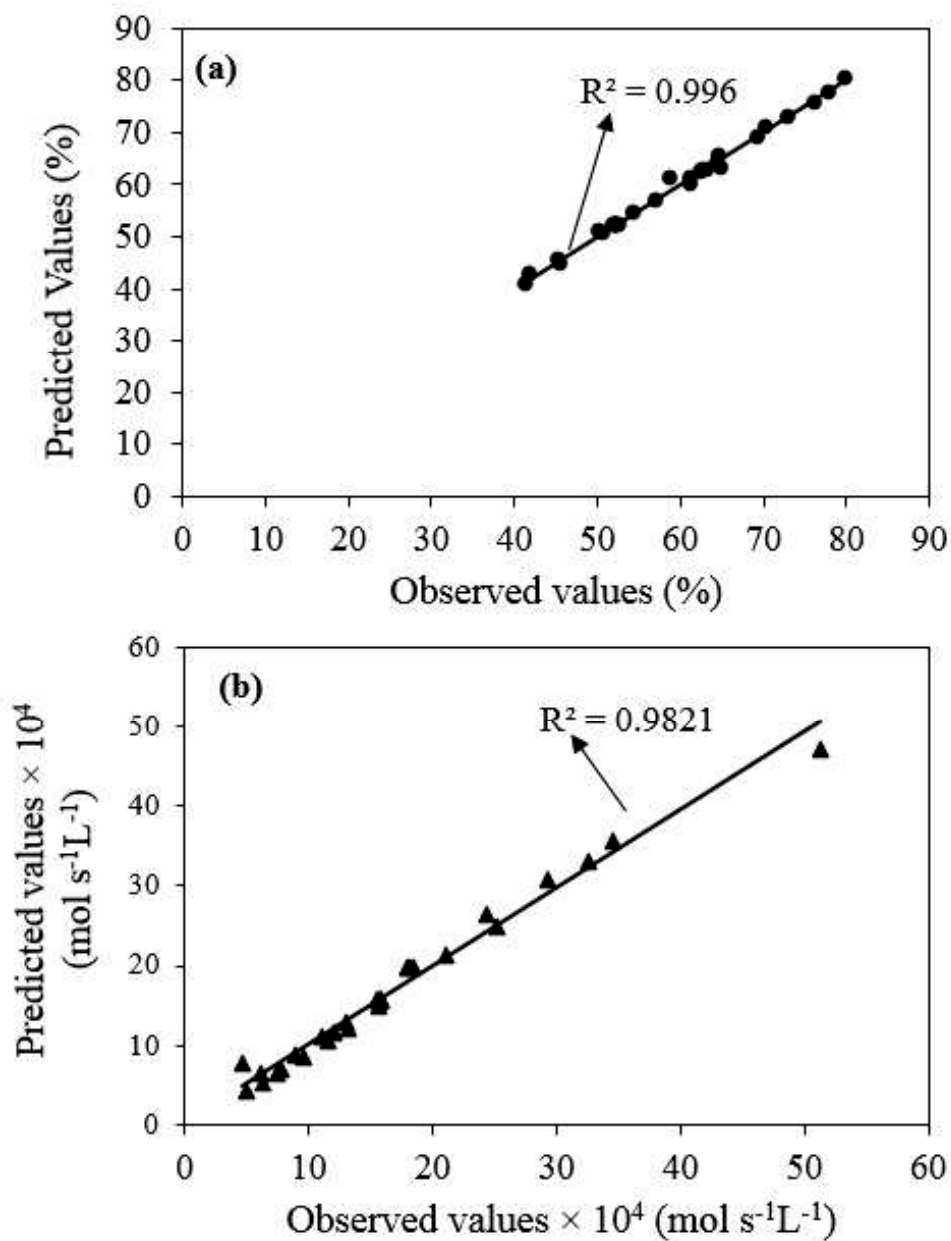


**Figure 4.2** Correlation between observed and predicted values for (a) removal efficiency and (b) absorption rate.

The 3D surface plots and contour plots in **Figures 4.3** and **4.4** were drawn to clarify the main and interactive effects of the independent variables on the responses. The plots were generated by varying two variables as a function of two significant factors at the same time within the experimental range, while the two other variables were kept constant at the center point.

**Figures 4.3(a)** and **4.4(a)** present the interaction effects between gas supplying pressure ( $X_1$ ) and G/L ratio ( $X_3$ ) on the removal capacity  $E$  and absorption rate  $R$ . In terms of gas supplying pressure, the removal rate fluctuated and reached the lowest point at 0.50 MPa, when gas supplying pressure was adjusted between 0.25 MPa and 0.75 MPa. Specifically, after a drop in CO<sub>2</sub> removal efficiency that occurred with the rise in gas supplying pressure from 0.25 to 0.50 MPa, the CO<sub>2</sub> capture increased again when the gas supplying pressure moved up to 0.75 MPa. Meanwhile, the absorption rate increased steadily with the growth in pressure. Based on Henry's law, pressure normally has a direct influence on the absorption of CO<sub>2</sub> in water, which would explain the strong augmentation in the absorption rate in the pressure range of 0.25 to 0.75 MPa. Interestingly, the CO<sub>2</sub> removal capacity declined with a change in gas supplying pressure from 0.25 to 0.50 MPa. The reason for this odd behavior is presented in **Section 3.3.2**.

The G/L ratio had a negative effect on the removal capacity and a positive effect on the absorption rate. Due to an increase in the inlet gas flow rate from 5 to 25 L min<sup>-1</sup> while keeping the water flow rate at a constant of 14 L min<sup>-1</sup> (equivalent to G/L range of 0.36 to 1.79), a large amount of CO<sub>2</sub> passed through the device and caused a turbulent liquid phase inside the absorption tank, which reduced the contact time between the gas and liquid phase (Chai & Zhao, 2012, Lin & Chu, 2015, Xiao *et al.*, 2014), and ultimately led to a decline in the removal rate. However, according to Eq. (4.1), a higher gas flow rate stimulates the relative CO<sub>2</sub> molar flow rate per unit of liquid phase, effectively increasing the absorption rate.

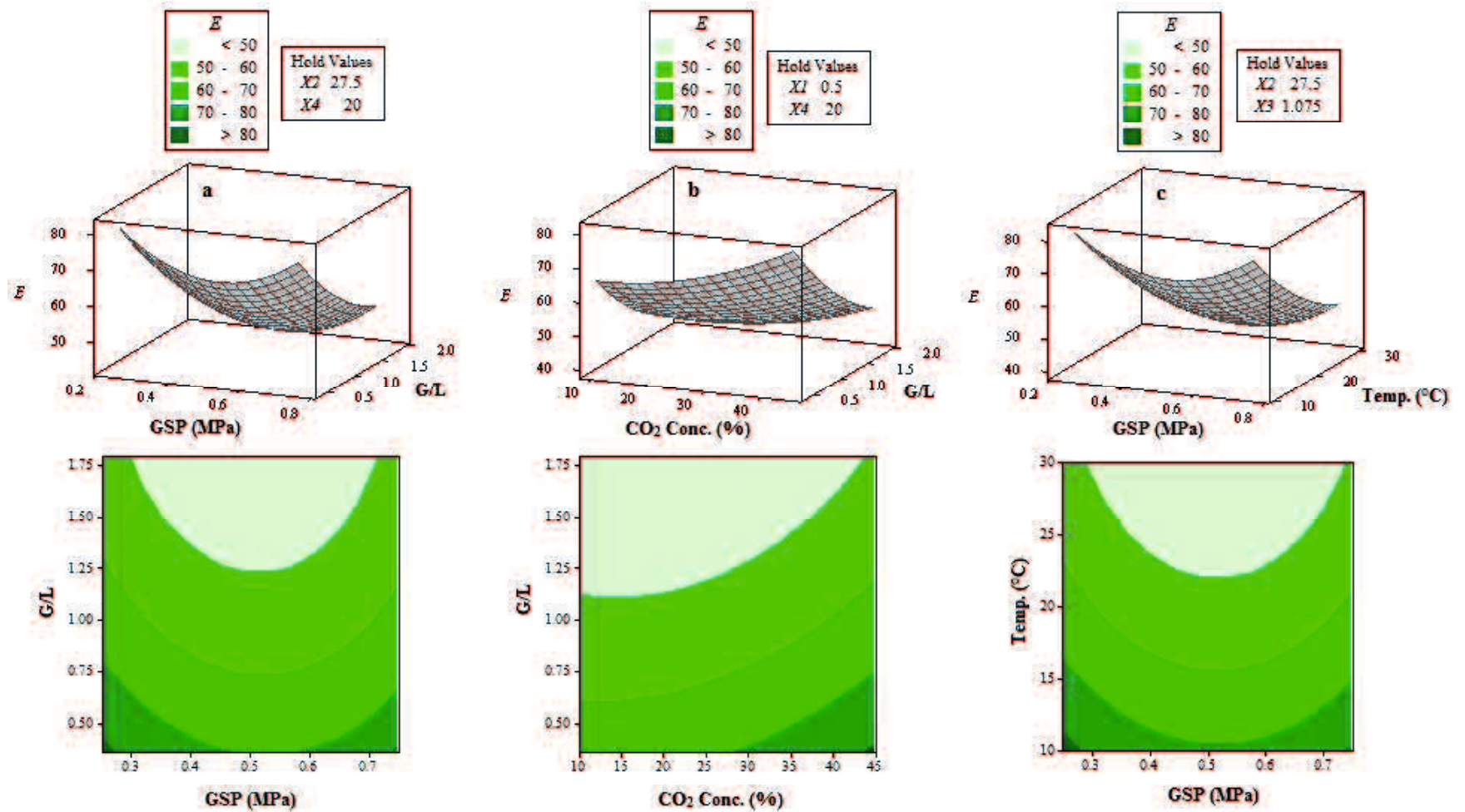


**Figure 4.3** Three-dimensional response surface plots and contour plots of removal efficiency interactions between: (a) gas supplying pressure and G/L ratio; (b) CO<sub>2</sub> initial concentration and G/L ratio; (c) gas supplying pressure and temperature.



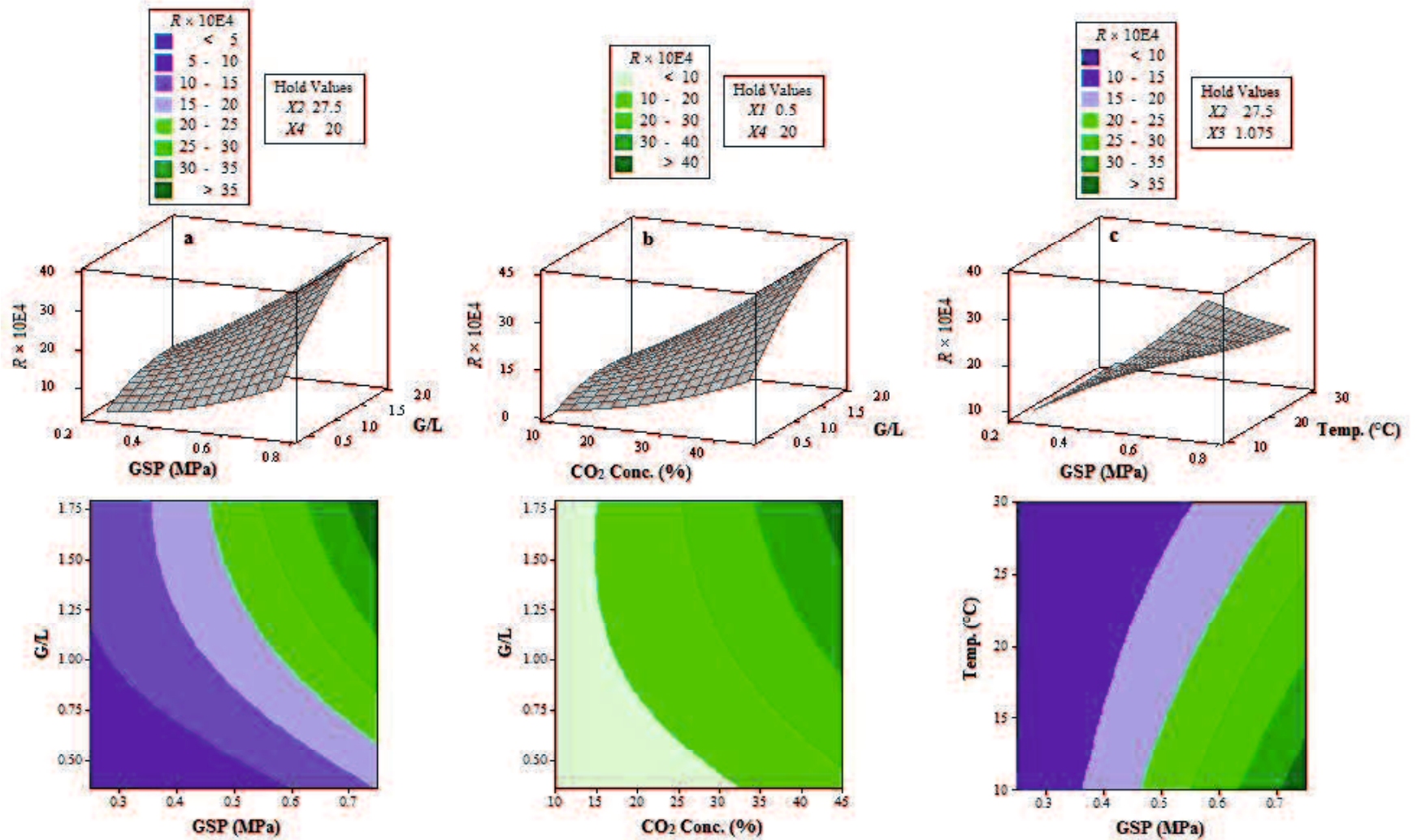


**Figure 4.4** Three-dimensional response surface plots and contour plots of absorption rate interaction between: (a) gas supplying pressure and G/L ratio; (b)  $CO_2$  initial concentration and G/L ratio; (c) gas supplying pressure and temperature.

The interaction effects between the inlet CO<sub>2</sub> concentration and the gas/liquid flow ratio on CO<sub>2</sub> capture of and absorption rate are illustrated in **Figures 4.3(b)** and **4.4(b)**, respectively. As shown in these figures, an increase in the inlet CO<sub>2</sub> concentration improves the sequestration of CO<sub>2</sub> into water. At higher initial CO<sub>2</sub> concentrations, the gas partial pressure increased and lowered the resistance between the gas and liquid phases, which caused an accumulation of dissolved CO<sub>2</sub> in the tap water, as indicated by Henry's Law. As a result of this, not only the removal efficiency but also the CO<sub>2</sub> absorption rate improved directly and remarkably with the accumulation of CO<sub>2</sub> when increasing the concentration in the mixed gas from 10% to 45%

**Figures 4.3(c)** and **4.4(c)** illustrate the interactive influences between temperature and gas supplying pressure. The range of temperature investigated was 10 °C to 30 °C. The solubility of gas is dependent on temperature, and an increase in temperature leads to an increase in the gas dissolution rate (Carroll *et al.*, 1991). Therefore, CO<sub>2</sub> removal efficiency and absorption level decreased with increasing temperature. Furthermore, temperature also had an effect on the bubble diameter, rise velocity, and gas holdup. Increasing temperature resulted in a reduction in the gas holdup and total bubble surface area due to an increase in the bubble rise velocity (Pérez-Garibay *et al.*, 2012). For these reasons, increased temperature had a negative effect on the dissolution rate of CO<sub>2</sub>.

### **4.3.3 Evaluation of the models and experiment**

In order to verify the reliability of our results and to determine the validity of our statistical models and regression equations, 5 additional experiments were conducted under different experimental conditions. The results, including the observed values, predicted values, and % errors between the observed and predicted values for the two responses are listed in **Table 4.6**.

In each run, the predicted values for removal efficiency and absorption rate calculated from **Eqs 4.4** and **4.5**, respectively, were compared to the observed values. The % error between predicted and observed values fluctuated in the range of 0.46% and 3.69% for the removal efficiency and 3.59% and 8.28% for the absorption rate. The fact that % errors were less than 9% confirmed again that the statistical models obtained from this study are both accurate and reliable. These results, when combined with a high correlation coefficient  $R^2 > 0.98$  (shown in **section 4.3.2**), show that the use of the polynomial equations (**Eqs 4.4** and **4.5**) to estimate the CO<sub>2</sub> removal efficiency and absorption rate is concise and reliable. With the aid of statistical

models and second-order polynomial equations, the CO<sub>2</sub> removal efficiency and absorption rate could be calculated precisely without conducting experiments. Therefore, it is possible to determine the appropriate or optimum conditions for controlling the absorption process to meet the standard requirements of CO<sub>2</sub> removal and absorption rate in a cost effective and timely manner. This approach provides the means to employ this water absorption system in real-time.

**Table 4.7** shows a comparison of the CO<sub>2</sub> removal performance in this study with that of other methods, including conventional water scrubbing (packed column scrubber), amine absorption, adsorption, and membrane techniques. Compared to amine absorption, water scrubbing has some special benefits, i.e., it reduces corrosion problems, it does not release toxic by-products, and the process control is simple. In addition, using water as the absorbent leaves many choices for the disposal of solvents. The disposed water containing high concentrations of CO<sub>2</sub> can also be used for other purposes, such as a carbon source for the cultivation of microalgae (Wang *et al.*, 2008, Singh & Ahluwalia, 2013). Therefore, due to the environmentally friendly advantages, water scrubbing can be considered a better choice for the environment in the comparison with the other technologies (Cozma *et al.*, 2013).

On the other hand, the disadvantage of conventional water scrubbing is that because water is a weak absorbent, high amounts of energy are required for maintaining the high pressure (1.0–2.0 MPa) required during the absorption process in order to achieve a high mass transfer between the two phases of liquid and gas and high dissolution rate. To solve this problem, this study used tap water as the CO<sub>2</sub> absorbent in the apparatus outfitted with the water-film-forming-unit (WFFU) to remove carbon dioxide from the gas stream effectively at a low gas supplying pressure of 0.30 MPa. In the scrubber connected to the WFFU, a large number of liquid-films and fine bubbles were formed, promoting the effective and strong pathway for a high gas transfer efficiency and dissolution rate into water (Imai & Zhu, 2011). **Figure 4.5** indicates that with the aid of the WFFU, CO<sub>2</sub> dissolved into water faster with a concentration three times higher than in the case of without the WFFU. The reasons for the high CO<sub>2</sub> dissolution rate are that fine bubbles enable large interfacial contact area between the gas and water and have a long residence time in the liquid phase due to their low buoyancy and low slip velocity (Parmar & Majumder, 2013). Therefore, a high CO<sub>2</sub> removal efficiency can be achieved without the use of high pressure. This can be demonstrated by comparison with the

results of previous studies. Läntelä *et al.* (2012) concluded that in an absorption column packed with a pall-ring ( $4 \times 4$  cm) filling material for high internal surface area, the removal of CO<sub>2</sub> from the raw landfill gas by water absorption can reach 88.9% under high pressure conditions (2.5 MPa), a CO<sub>2</sub> inlet concentration of 37.8%–43.6%, a temperature of 10–15 °C, and a water flow rate of 11 L min<sup>-1</sup>. Meanwhile, with the aid of a WFFU in enhancing the CO<sub>2</sub> dissolution rate, at the initial conditions of low gas supplying pressure (0.25 MPa), CO<sub>2</sub> inlet concentration (40%), temperature (12 °C), and gas/liquid ratio (0.71), the water absorption process can achieve a CO<sub>2</sub> removal efficiency of about 92.0%. However, one remaining limitation in this study is the low performance of this process under high gas-to-liquid ratio conditions or a high load of induced gas. This can be explained by the lack of capacity in producing fine bubbles with only one WFFU. Hence, this problem can be solved by increasing the number of WFFUs used in the apparatus. When the number of WFFU increases, the amount of and the speed with which the liquid-films and microbubbles are produced increases. This increase in effectiveness enhances the mass transfer as well as increasing the contact area between the gas and liquid phases, supporting the use of this type of apparatus under conditions with high loads of inlet gas.

**Table 4.6** Experimental confirmation for removal efficiency  $E$  (%) and absorption rate  $R$  ( $\text{mol s}^{-1}\text{L}^{-1}$ )

Run	Gas supplying pressure (MPa) (X1)	CO <sub>2</sub> initial concentration (%) (X2)	Gas/Liquid ratio (X3)	Temperature (°C) (X4)	Removal efficiency $E$ (%)			Absorption rate $R \times 10^4$ ( $\text{mol s}^{-1}\text{L}^{-1}$ )		
					Observed	Predicted	% Error	Observed	Predicted	% Error
1	0.70	25	0.71	15	76.24	73.65	-3.46	18.86	20.49	8.28
2	0.30	15	1.07	20	56.46	58.01	2.71	6.29	6.52	3.59
3	0.30	35	0.71	30	58.24	60.31	-3.49	11.32	10.67	-5.91
4	0.50	35	0.36	10	92.86	93.29	0.46	10.96	11.71	6.61
5	0.50	45	1.43	25	48.92	50.76	3.69	32.14	34.27	6.41

% Error is the percentage of error between observed value and predicted value; % Error =  $\frac{\text{Predicted value} - \text{Observed value}}{(\text{Predicted value} + \text{Observed value})/2} \times 100\%$ .

**Table 4.7** Comparison of different CO<sub>2</sub> removal technologies

Parameter	This study	Conventional water scrubbing	Amine absorption	Adsorption	Membrane
Working pressure	< 0.30 MPa	1.0 – 2.0 MPa <sup>(1)</sup>	Low pressure <sup>(1)</sup>	0.7 – 0.8 MPa (Pressure Swing Adsorption) <sup>(7)</sup>	2.5 – 4.0 MPa <sup>(1)</sup>
Operation and maintain cost	Low	Low <sup>(4)(7)</sup>	High <sup>(6)</sup>	High <sup>(7)</sup>	High membrane cost <sup>(1)</sup>
Energy requirement	1.5 – 4.5 MJ/kgCO <sub>2</sub>	–	4 – 6 MJ/kgCO <sub>2</sub> <sup>(3)</sup>	2 – 3 MJ/kgCO <sub>2</sub> <sup>(3)</sup>	0.5 – 6 MJ/kgCO <sub>2</sub> <sup>(3)</sup>
Toxic by-product	Low	Low <sup>(4)</sup>	High <sup>(2)(6)</sup>	Low <sup>(1)(6)</sup>	Low <sup>(3)(6)</sup>
Corrosion rate	Moderate	Moderate <sup>(1)</sup>	High <sup>(1)(2)(5)</sup>	Low <sup>(1)</sup>	Low <sup>(5)</sup>
Control requirement	Low	–	High <sup>(3)</sup>	High <sup>(3)</sup>	Low <sup>(3)</sup>
Other	Less environmental impact because no chemical is required in the scrubbing process. However, the process is slow and requires a lot of water <sup>(1)(4)</sup> .		High environmental impact due to sorbent degradation, generation of volatile degradation compounds and the disposal of solvent <sup>(2)</sup> .	High temperature is required in the adsorption process <sup>(2)</sup> .	Operational problems include low flux and fouling <sup>(2)</sup> .

List of references used in **Table 4.7**

<sup>1</sup> Andriani *et al.* (2014)

<sup>2</sup> Leung *et al.* (2014)

<sup>3</sup> Mondal *et al.* (2012)

<sup>4</sup> Ofori-Boateng and Kwofie (2009)

<sup>5</sup> Olajire (2010)

<sup>6</sup> Shimekit and Mukhtar (2012)

<sup>7</sup> Zhao *et al.* (2010)

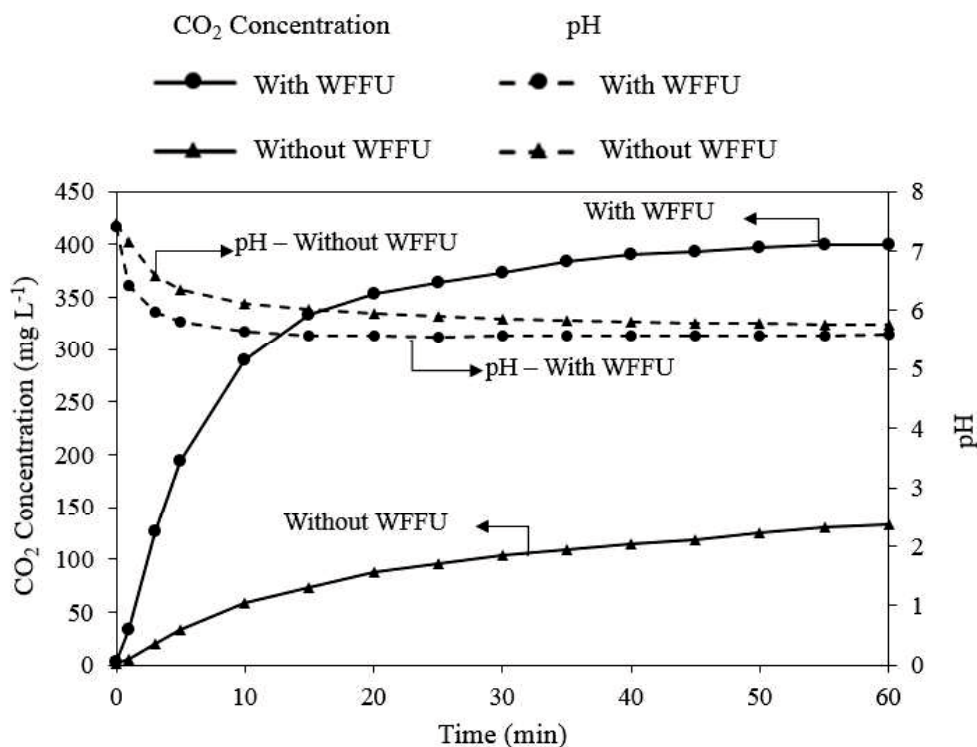


**Figure 4.5** CO<sub>2</sub> Concentration dissolving into 60 L of water and the change of pH during 60 minutes in two cases of with and without using liquid-film-forming-device (WWFU). Inlet gas supplying pressure: 0.50 MPa; inlet gas composition: 15% CO<sub>2</sub>–85% N<sub>2</sub>; G/L ratio: 1.43; and temperature: 20 °C.

#### 4.4 Conclusions

This study provided evidence that using an RSM in connection with CCD statistical experimental design could successfully construct models identifying the effects of various independent variables, including gas supplying pressure, initial CO<sub>2</sub> concentration, G/L ratio, and temperature, on the CO<sub>2</sub> removal efficiency and the degree of absorption. Good agreements between the predicted values obtained from the two models with the experimentally observed values were achieved, with the coefficient of determination  $R^2$  being more than 0.98 in both cases. The models can be used as useful tools to predict the CO<sub>2</sub> removal efficiency and absorption rate accurately without carrying out a large number of experiments.

In order to achieve high efficiency of CO<sub>2</sub> capture from the mixed gas, the water scrubbing process was designed with gas supplying pressure set under 0.30 MPa or over 0.70 MPa. However, for the aim of reducing operating cost, the lower the gas supplying pressure,



the lower expenditure is. In addition, higher inlet CO<sub>2</sub> concentrations, lower temperatures, and lower G/L ratios improved the solubility of CO<sub>2</sub> in water. However, due to the low G/L ratio, the absorption rate of the absorption process was low, and was thus uneconomical. Accordingly, to achieve not only a high removal rate but also a satisfactory absorption rate, it is suggested to consider the mass flow of the feed gas, efficacy demand, and required CO<sub>2</sub> separation process before selecting the optimal conditions. Eventually, further research will be needed to further develop an apparatus design for connecting several liquid-film generators, which is expected to enable not only a high removal rate but also a great absorption rate. In future studies, measurements of the bubble sizes and mass transfer coefficients will be carried out to comprehensively assess the absorption process.

#### 4.5 References

- Aresta, M. 2013. Carbon dioxide recovery and utilization, Springer Science & Business Media. Germany.
- Babu, P. V. 2014. Hydrate based gas separation (HBGS) technology for precombustion capture of carbon dioxide. PhD thesis. National University of Singapore, Singapore.
- Bang, J.-H., Kim, W., Song, K. S., Jeon, C. W., Chae, S. C., Cho, H.-J., Jang, Y. N. & Park, S.-J. 2014. Effect of experimental parameters on the carbonate mineralization with CaSO<sub>4</sub>·2H<sub>2</sub>O using CO<sub>2</sub> microbubbles. *Chemical Engineering Journal*, **244**, 282-287.
- Bezerra, M. A., Santelli, R. E., Oliveira, E. P., Villar, L. S. & Escaleira, L. A. 2008. Response surface methodology (RSM) as a tool for optimization in analytical chemistry. *Talanta*, **76** (5), 965-977.
- Carroll, J. J., Slupsky, J. D. & Mather, A. E. 1991. The solubility of carbon dioxide in water at low pressure. *Journal of Physical and Chemical Reference Data*, **20** (6), 1201-1209.
- Chai, X. & Zhao, X. 2012. Enhanced removal of carbon dioxide and alleviation of dissolved oxygen accumulation in photobioreactor with bubble tank. *Bioresource technology*, **116**, 360-365.
- Chen, P.-C. 2012. Absorption of carbon dioxide in a bubble-column scrubber, INTECH Open Access Publisher.

- Chou, C. 2013. Carbon dioxide separation and capture for global warming mitigation. *J. Adv. Eng. Technol.*, **1**, 1-4.
- Cozma, P., Ghinea, C., Mămăligă, I., Wukovits, W., Friedl, A. & Gavrilesco, M. 2013. Environmental impact assessment of high pressure water scrubbing biogas upgrading technology. *CLEAN–Soil, Air, Water*, **41** (9), 917-927.
- Imai, T. & Zhu, H. 2011. Improvement of oxygen transfer efficiency in diffused aeration systems using liquid-film-forming apparatus, INTECH Open Access Publisher.
- Läntelä, J., Rasi, S., Lehtinen, J. & Rintala, J. 2012. Landfill gas upgrading with pilot-scale water scrubber: performance assessment with absorption water recycling. *Applied energy*, **92**, 307-314.
- Lee, Z. H., Lee, K. T., Bhatia, S. & Mohamed, A. R. 2012. Post-combustion carbon dioxide capture: Evolution towards utilization of nanomaterials. *Renewable and Sustainable Energy Reviews*, **16** (5), 2599-2609.
- Li, B., Duan, Y., Luebke, D. & Morreale, B. 2013. Advances in CO<sub>2</sub> capture technology: a patent review. *Applied Energy*, **102**, 1439-1447.
- Lin, C.-C. & Chu, C.-R. 2015. Feasibility of carbon dioxide absorption by NaOH solution in a rotating packed bed with blade packings. *International Journal of Greenhouse Gas Control*, **42**, 117-123.
- Moreira, D. & Pires, J. C. 2016. Atmospheric CO<sub>2</sub> capture by algae: negative carbon dioxide emission path. *Bioresource technology*, **215**, 371-379.
- Olajire, A. A. 2010. CO<sub>2</sub> capture and separation technologies for end-of-pipe applications – A review. *Energy*, **35** (6), 2610-2628.
- Parmar, R. & Majumder, S. K. 2013. Microbubble generation and microbubble-aided transport process intensification—A state-of-the-art report. *Chemical Engineering and Processing: Process Intensification*, **64**, 79-97.
- Pérez-Garibay, R., Martínez-Ramos, E. & Rubio, J. 2012. Gas dispersion measurements in microbubble flotation systems. *Minerals Engineering*, **26**, 34-40.
- Phummala, K., Imai, T., Reungsang, A., Higuchi, T., Sekine, M., Yamamoto, K. & Kanno, A. 2015. Optimization of enzymatic hydrolysis for pretreated wood waste by response surface methodology in fermentative hydrogen production. *Journal of Water and Environment Technology*, **13** (2), 153-166.

- Rao, A. B. & Rubin, E. S. 2002. A technical, economic, and environmental assessment of amine-based CO<sub>2</sub> capture technology for power plant greenhouse gas control. *Environmental science & technology*, **36** (20), 4467-4475.
- Singh, U. B. & Ahluwalia, A. S. 2013. Microalgae: a promising tool for carbon sequestration. *Mitigation and Adaptation Strategies for Global Change*, **18** (1), 73-95.
- Wang, B., Li, Y., Wu, N. & Lan, C. Q. 2008. CO<sub>2</sub> bio-mitigation using microalgae. *Applied microbiology and biotechnology*, **79** (5), 707-718.
- Weiss, R. F. 1974. Carbon dioxide in water and seawater: the solubility of a non-ideal gas. *Marine chemistry*, **2** (3), 203-215.
- Xiao, Y., Yuan, H., Pang, Y., Chen, S., Zhu, B., Zou, D., Ma, J., Yu, L. & Li, X. 2014. CO<sub>2</sub> removal from biogas by water washing system. *Chinese Journal of Chemical Engineering*, **22** (8), 950-953.
- Xu, Q., Nakajima, M., Ichikawa, S., Nakamura, N. & Shiina, T. 2008. A comparative study of microbubble generation by mechanical agitation and sonication. *Innovative food science & emerging technologies*, **9** (4), 489-494.

## CHAPTER 5

# INFLUENCE OF WATER-FILM-FORMING-UNIT ON THE ENHANCED REMOVAL OF CARBON DIOXIDE FROM MIXED GAS USING WATER ABSORPTION APPARATUS

### 5.1 Introduction

The major contributor to global warming is anthropogenic greenhouse gas emissions. The increased concentration of greenhouse gases, primarily including carbon dioxide, methane, nitrous oxide, and hydrofluorocarbons, have endangered the Earth and humankind through global climate change, damage to global ecosystems, glacier melting, and enhanced health risks. As 77% of greenhouse gases emissions are carbon dioxide (CO<sub>2</sub>), CO<sub>2</sub> is the primary cause of global warming (Alonso *et al.*, 2017). According to the Emission Database for Global Atmospheric Research, global emissions of CO<sub>2</sub> were 36.2 billion tonnes in 2015, compared to 33.4 billion tonnes in 2011 (Olivier *et al.*, 2016). While CO<sub>2</sub> emissions continue to grow, determining an effective and economic way to control the release of carbon dioxide to the atmosphere is currently one of the most important aims of global research.

In general, the most popular method for removing CO<sub>2</sub> from mixed gas is absorption. There are two types of absorption methods; chemical absorption and physical absorption. Chemical absorption using amine-based solvents is the most mature and widespread method owing to its high CO<sub>2</sub> removal efficiency and the potential for regenerating sorbents. However, this method involves some problems relating to the high equipment corrosion rate, amine degradation, the significant amount of heat required for regenerating absorbents, and the generation of toxic by-products (Leung *et al.*, 2014, Olajire, 2010). Compared to amine absorption, physical water scrubbing has some unique benefits, such as reduced corrosion problems, no toxic by-products, and an easily controlled process. As it does not use chemicals or produce toxic by-products, water scrubbing is a more environmentally friendly method of absorbing carbon dioxide from exhaust gas; therefore, it is a promising technology for controlling carbon dioxide emissions in an environmentally conscious manner (Cozma *et al.*, 2013).

However, few studies focus on the absorption of CO<sub>2</sub> using water without chemical reactions. The greatest limitation of this method is the lack of interaction between carbon dioxide and water, which results in low removal efficiency and the need to operate at high pressure (1.0 - 2.0 MPa). Maintaining high pressure throughout operation leads to energy consumption and costs. To combat this problem, we employed a water scrubber apparatus connected to a water-film-forming-unit (WFFU), with the aim of promoting mass transfer and contact between the gas and liquid phases, thereby improving the effectiveness of this method. In the apparatus, the formation of many water films and small bubbles effectively promotes gas transfer efficiency and dissolution rate (Imai & Zhu, 2011). The small bubbles supply a large available interfacial contact area between the gas and water, and have a long residence time in the liquid phase due to low buoyancy and low slip velocity (Parmar & Majumder, 2013). Therefore, high CO<sub>2</sub> removal efficiency can be achieved without the need for high pressure. A previous study demonstrated that utilizing a WFFU in the absorption system could improve CO<sub>2</sub> removal capacity under low pressure (0.30 MPa) conditions (Nguyen *et al.*, 2017). Despite this, however, there were still limitations caused by the low removal efficiency under a high feed gas load and a lack of results that could clearly illuminate the role of the WFFU in enhancing CO<sub>2</sub> removal. Therefore, further research is needed on the differences in the removal process with and without a WFFU, the potential for improving removal efficiency by using more than one WFFU, and the manner in which a WFFU can improve the absorption process. This research will need to comprehensively assess the effects of using a WFFU to improve the CO<sub>2</sub> removal process. Furthermore, to scale up this water absorption method and apply it in the apparatus outfitted with several WFFUs, the removal performance and phenomena occurring after the apparatus outfitted with several WFFU must be investigated.

Furthermore, the Taguchi method was applied to thoroughly evaluate the effect of various factors on the CO<sub>2</sub> removal capacity, and explore optimum conditions for the absorption process. These findings can be used to design protocols for capturing carbon dioxide from mixed gas using water as the absorption solvent.

## 5.2 Materials and Methods

### 5.2.1 Experimental setup and methods

In this absorption system, the inlet gas was a mixture of CO<sub>2</sub> and N<sub>2</sub>. The ratio of CO<sub>2</sub> to N<sub>2</sub> was adjusted using flow meters. Tap water was used as the non-circulated absorbent without any purification process. The experimental setup used for removing CO<sub>2</sub> is illustrated in **Figure 5.1**. Before introducing the gas to the absorption chamber, the inlet gas was mixed with the water pumped from the water tank. The main part of this system is the absorption chamber. This chamber was a stainless steel, pressurized chamber, with an interior volume of 5 L and equipped with a water-film-forming-unit (WFFU) inside. The WFFU can support the generation of a large number of water films and small bubbles in order to enhance the interfacial area between the water and the gas (**Figure 5.2**).

The operational variables investigated in this study are the number of WFFUs outfitted inside the absorption chamber, gas supplying pressure, initial CO<sub>2</sub> concentration, gas-to-liquid (G/L) ratio, and temperature. The effect of the number of WFFUs on the removal rate was examined by assessing the CO<sub>2</sub> removal performance in three models of absorption system equipped with zero, one, and two WFFUs (non-WFFU, 1-WFFU, and 2-WFFUs, respectively), as shown in **Figure 5.1**. The investigated range of gas supplying pressure was from 0.25 to 0.70 MPa. The influence of CO<sub>2</sub> initial concentration was analyzed by setting the CO<sub>2</sub> initial concentration in the mixture with N<sub>2</sub> at 10%, 15%, 25%, 35%, and 45% using flow meters. The G/L ratio was set by controlling the gas flow rate from 5 L min<sup>-1</sup> to 25 L min<sup>-1</sup>, and maintaining the water flow rate of 14 L min<sup>-1</sup> (equivalent to a G/L ratio range of 0.36 – 1.79). To correspond to the annual range of temperature in Japan, the impact of temperature was assessed in the range of 10 °C to 30 °C.

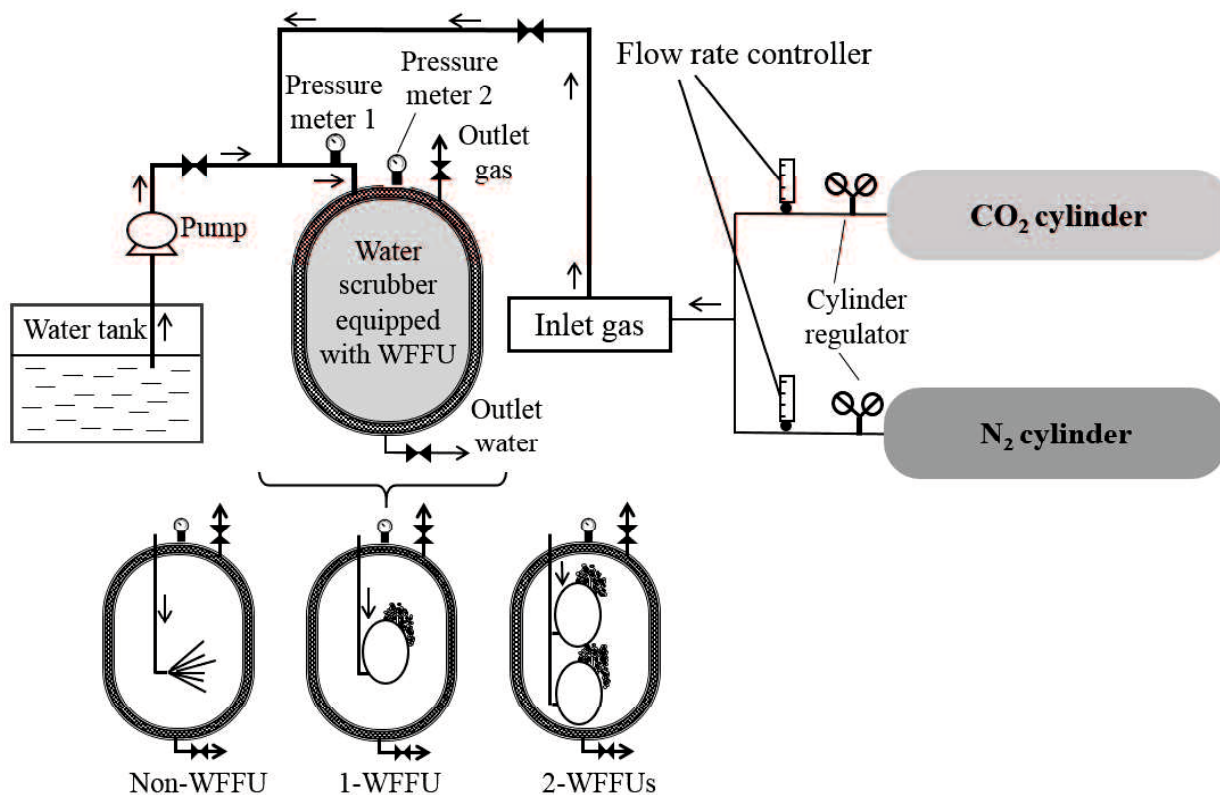


**Figure 5.1** Schematic diagram of the apparatus used for the removal of carbon dioxide in this study.

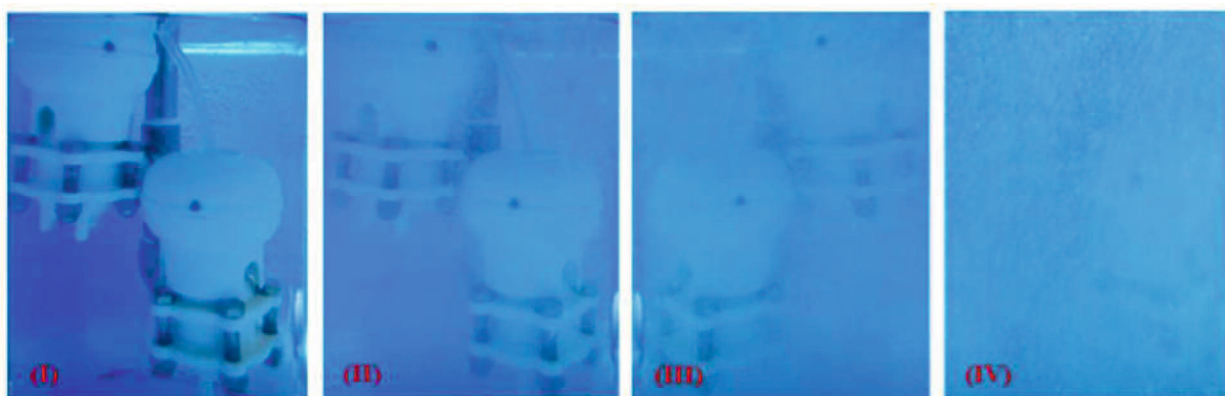


**Figure 5.2** Snapshots of the production of water-films and fine bubbles in the absorption tank.

The outlet gas was collected in the gas sample bag and used to measure the removal efficiency and absorption rate. Gas samples were analyzed by gas chromatography (GC-8APT, Shimadzu). The GC-8APT was equipped with a thermal conductivity detector (TCD) and an activated carbon 60/80 mesh column (1.5m × 3.0mm ID). The carrier gas was argon. The operational temperature of the injector, column, and detector were 50 °C, 60 °C, and 50 °C,

respectively. The absorption rate was computed by the following equation, introduced by Chen (2012):

$$R = \frac{F_{\text{CO}_2}}{V} \left[ 1 - \left( \frac{1-x_{\text{CO}_2}^{\text{in}}}{x_{\text{CO}_2}^{\text{in}}} \right) \left( \frac{x_{\text{CO}_2}^{\text{out}}}{1-x_{\text{CO}_2}^{\text{out}}} \right) \right] \quad (5.1)$$

where  $R$  ( $\text{mol s}^{-1}\text{L}^{-1}$ ) is the absorption rate of  $\text{CO}_2$  in the liquid phase;  $F_{\text{CO}_2}$  ( $\text{mol s}^{-1}$ ) is the  $\text{CO}_2$  molar flow rate;  $V$  (L) is the volume of liquid phase in the chamber;  $x_{\text{CO}_2}^{\text{in}}$  is the molar fraction of  $\text{CO}_2$  at the inlet; and  $x_{\text{CO}_2}^{\text{out}}$  is the molar fraction of  $\text{CO}_2$  at the outlet.

### 5.2.2 Taguchi analysis method

The Taguchi method is a useful and effective statistical tool for designing experiments, developed in 1986 (Taguchi, 1986). The aim of this method is to decrease the number of experiments in order to decrease operational time and costs, identify significant factors affecting the response, and maintain quality of the design phase (Asiltürk & Akkuş, 2011).

Based on the number of parameters and the number of levels within each parameter, the Taguchi method creates a standard orthogonal array and experimental matrix. In order to evaluate parameters, the experimental data are transformed into a statistical measure of performance called the signal-to-noise ratio (S/N). This ratio is the ratio of the mean (signal) to the standard deviation (noise). The S/N ratio depends on the quality characteristics of the product or process to be optimized (Datta *et al.*, 2008). The best level of each parameter is the level which achieves the highest S/N ratio. The S/N ratio can be calculated using three concepts: nominal is best, smaller is better, and larger is better (Asiltürk & Akkuş, 2011).

$$\text{Nominal is best: } S/N = 10 \log \frac{\bar{y}}{s_y^2}; \quad (5.2)$$

$$\text{smaller is better: } S/N = -10 \log \frac{1}{n} (\sum y^2); \quad (5.3)$$

$$\text{and larger is better: } S/N = -10 \log \frac{1}{n} (\sum \frac{1}{y^2}); \quad (5.4)$$

where  $\bar{y}$  is the average of observed data,  $s_y^2$  is the variance of  $y$ ,  $y$  is the observed data, and  $n$  is the quantity of observations.

In this study, software MINITAB 14 was used to create the Taguchi experimental matrix and analyze the results. We assessed the effects of five controlling factors, including the



number of WFFUs, gas supplying pressure, CO<sub>2</sub> inlet concentration, the G/L ratio, and water temperature, on CO<sub>2</sub> removal and absorption rates. Except for the number of WFFUs, which had two levels (“1” and “2”), each factor was investigated at three levels (labelled as “1”, “2”, and “3”, **Table 5.1**). Normally, for a combination of one factor with two levels and four factors with three levels, the total number of experiments would be  $2^1 \times 3^4$  (=162). However, utilizing the Taguchi method not only greatly reduces the number of experiments to 18 trials, but also increases the efficiency and quality of the analysis process. **Table 5.2** presents the total matrix of 18 trials, the observed CO<sub>2</sub> removal rates, and the transformed S/N ratios for each trial.

**Table 5.1** Controlling factors and their levels

Factor	Unit	Level		
		1	2	3
Number of WFFUs	Piece	1	2	-
Inlet gas supplying pressure	MPa	0.30	0.50	0.70
Initial CO <sub>2</sub> concentration	%	15	25	35
G/L ratio	-	0.71	1.07	1.43
Temperature	°C	15	20	25

**Table 5.2** Taguchi's L<sub>18</sub> orthogonal design and CO<sub>2</sub> removal efficiency, absorption rate and S/N ratio results

Trial	Number of WFFUs		Gas supplying pressure (MPa)		CO <sub>2</sub> initial concentration (%)		G/L ratio		Temperature (°C)		Removal efficiency (%)	S/N ratio <sup>a</sup>	Absorption rate (× 10 <sup>4</sup> ) (mol s <sup>-1</sup> L <sup>-1</sup> )	S/N ratio <sup>b</sup>
	Level	Actual	Level	Actual	Level	Actual	Level	Actual	Level	Actual				
1	1	1	1	0.30	1	15	1	0.71	1	15	75.98	37.61	5.33	14.53
2	1	1	1	0.30	2	25	2	1.07	2	20	60.86	35.69	11.80	21.44
3	1	1	1	0.30	3	35	3	1.43	3	25	52.10	34.34	20.00	26.02
4	1	1	2	0.50	1	15	1	0.71	2	20	55.72	34.92	7.91	17.96
5	1	1	2	0.50	2	25	2	1.07	3	25	46.79	33.4	17.54	24.88
6	1	1	2	0.50	3	35	3	1.43	1	15	56.00	34.96	32.17	30.15
7	1	1	3	0.70	1	15	2	1.07	1	15	64.03	36.13	15.14	23.60
8	1	1	3	0.70	2	25	3	1.43	2	20	52.81	34.45	31.53	29.97
9	1	1	3	0.70	3	35	1	0.71	3	25	63.08	36.00	28.78	29.18
10	2	2	1	0.30	1	15	3	1.43	3	25	63.28	36.03	8.91	19.00
11	2	2	1	0.30	2	25	1	0.71	1	15	97.68	39.80	9.43	19.49
12	2	2	1	0.30	3	35	2	1.07	2	20	80.51	38.12	18.82	25.49
13	2	2	2	0.50	1	15	2	1.07	3	25	63.91	36.11	11.13	20.93
14	2	2	2	0.50	2	25	3	1.43	1	15	77.20	37.75	26.84	28.58
15	2	2	2	0.50	3	35	1	0.71	2	20	85.08	38.60	21.54	26.66
16	2	2	3	0.70	1	15	3	1.43	2	20	67.45	36.58	21.25	26.55
17	2	2	3	0.70	2	25	1	0.71	3	25	74.65	37.46	21.14	26.50
18	2	2	3	0.70	3	35	2	1.07	1	15	83.31	38.41	43.64	32.80

Note:

S/N ratio<sup>a</sup>: transformed data to S/N ratios for removal efficiency (Larger is better)S/N ratio<sup>b</sup>: transformed data to S/N ratios for absorption rate (Larger is better)

## 5.3 Results and Discussion

### 5.3.1 Effect of water-film-forming-unit (WFFU)

The effect of WFFU on the removal of CO<sub>2</sub> from the feed gas was investigated by evaluating the CO<sub>2</sub> removal rate and absorption rate in the apparatus under three conditions: non-WFFU, 1-WFFU, and 2-WFFUs (see **Figure 5.1**). The removal and absorption rates at a gas supplying pressure of 0.30 MPa, a total inlet gas flow rate of 15 L min<sup>-1</sup>, and a temperature of 15 °C are shown in **Figures 5.3(a)** and **5.3(b)**. Using WFFUs revealed an improvement in the CO<sub>2</sub> capture ability; the CO<sub>2</sub> removal efficiency for 2-WFFUs was approximately 20% higher than that for non-WFFU. Similarly, with a feed gas composition (CO<sub>2</sub> to N<sub>2</sub> ratio) of 15:85, 25:75, and 35:65, the absorption rate increased from  $7.22 \times 10^{-4}$  to  $7.89 \times 10^{-4}$  mol s<sup>-1</sup>L<sup>-1</sup>, from  $12.54 \times 10^{-4}$  to  $13.46 \times 10^{-4}$  mol s<sup>-1</sup>L<sup>-1</sup>, and from  $18.24 \times 10^{-4}$  to  $19.16 \times 10^{-4}$  mol s<sup>-1</sup>L<sup>-1</sup>, respectively, when comparing that rate in two circumstances of non-using WFFU and using 2-WFFUs in the absorption apparatus. These results prove that WFFU significantly promotes the dissolution and absorption capacity of CO<sub>2</sub> in water. This is due to generation of a very large number of water films that stimulate the supply of CO<sub>2</sub> in two directions, so that CO<sub>2</sub> transfer can occur across the inner interface (gas bubble and water film) and the outer interface (surrounding environment and water film). This substantially increases the interfacial contact area between the two phases (Nguyen *et al.*, 2017, Zhu *et al.*, 2007).

**Figure 5.3(a)** also shows that the CO<sub>2</sub> absorption capability of non-WFFU is higher than that of 1-WFFU. The first explanation for this phenomenon is that the use of only one WFFU leads to a low ability to produce small bubbles and water films, which leads to a minimal improvement of CO<sub>2</sub> sequestration. The second reason is that, compared to the internal pressure of 0.10 MPa in the non-WFFU apparatus, the internal pressure in the chamber is lower when using a WFFU (0.06 MPa) because of pressure consumption by the WFFU. Internal pressure has a positive influence on CO<sub>2</sub> removal efficiency as well as the dissolution rate, i.e. an increase of internal pressure leads to an increase of absorption potential and CO<sub>2</sub> removal rate (Nguyen *et al.*, 2017). Therefore, due to lower internal pressure in the absorption chamber in the 1-WFFU apparatus, more of the trapped gas breaks through the water film and is released to the environment, decreasing the removal rate. A combination of these reasons explains the lower removal and absorption rate for 1-WFFU conditions. This proves that the internal

pressure of the WFFU is an important factor that can improve CO<sub>2</sub> removal performance. If the addition of one WFFU results in an increased removal efficiency in the 1-WFFU and 2-WFFU conditions, the higher value of the internal pressure leads to the high removal efficiency in the non-WFFU condition. Thus, there are two approaches by which to increase the removal efficiency: increasing the number of WFFUs and increasing internal pressure. However, given by the structure of our apparatus, it is difficult to control and adjust the internal pressure. Furthermore, the absorption system could become unstable and unsafe at a high internal pressure. Therefore, increasing the number of WFFUs is a simpler, safer, more stable, and more effective approach to improving the performance of CO<sub>2</sub> removal process than increasing internal pressure.

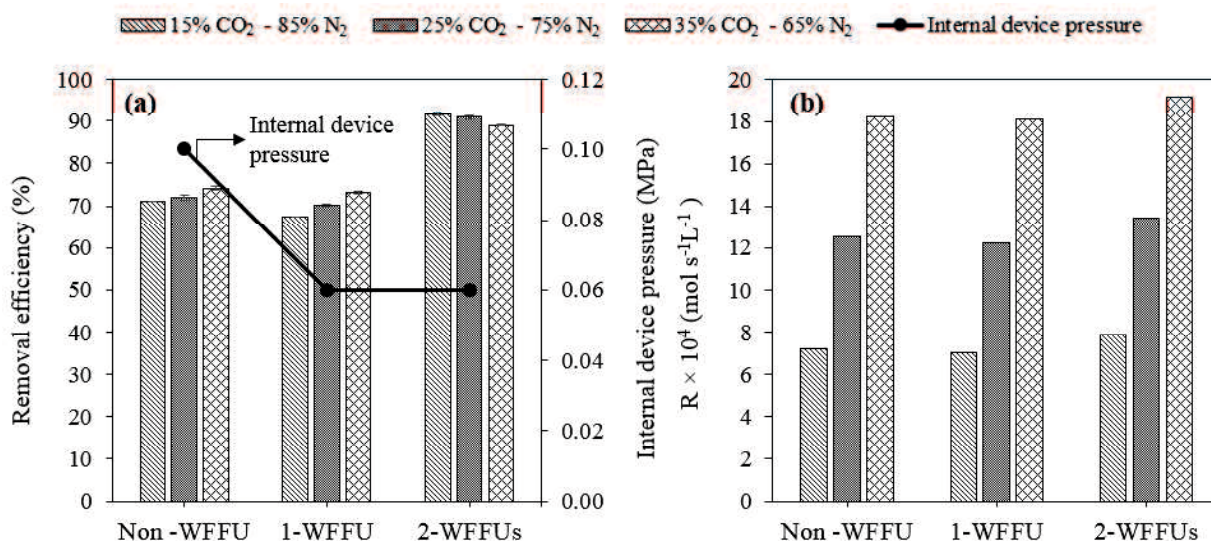


**Figure 5.3** Effect of the water-film-forming-unit (WFFU) on (a) CO<sub>2</sub> removal efficiency and (b) absorption rate. Operating conditions: gas supplying pressure = 0.30 MPa; G/L ratio = 1.07; total gas flow rate = 15 L min<sup>-1</sup>; water flow rate = 14 L min<sup>-1</sup>; and temperature = 15°C.

Accordingly, the WFFU has a notable impact on CO<sub>2</sub> capture from the mixed gas. With two WFFUs inside the chamber, the removal efficiency of CO<sub>2</sub> is greatly increased at a low gas supplying pressure of 0.30 MPa. Hence, we suggest that an increasing number of WFFUs can result in a significant improvement in the absorption process and more effective and cheaper CO<sub>2</sub> capture from the high feed gas load.

### 5.3.2 Effect of inlet gas supplying pressure

Normally, gas supplying pressure plays an important role when using physical water absorption to remove CO<sub>2</sub> from mixed gas. In order to evaluate and compare the influence of gas supplying pressure on the CO<sub>2</sub> removal process in both our novel absorption tank (equipped with 1 or 2 WFFUs) and a conventional tank (not equipped with a WFFU), the removal capacity and absorption rate were measured (**Figures 5.4(a)** and **(b)**). In the conventional apparatus, the removal efficiency and absorption rate increases with pressure at an initial gas composition of 25% CO<sub>2</sub> and 75% N<sub>2</sub>, a total gas flow rate of 15 L min<sup>-1</sup>, and a temperature of 15 °C. When pressure is increased from 0.25 to 0.70 MPa, the removal and absorption rate increases from 72.4% to 79.03% and from  $10.54 \times 10^{-4}$  to  $29.26 \times 10^{-4}$  mol s<sup>-1</sup>L<sup>-1</sup>, respectively. These results show that, if a WFFU is not installed inside the chamber, pressure has a direct effect on the absorption process, as dictated by Henry's law. Henry's law states that the solubility of gas in the aqueous phase is directly proportional to the gas pressure. Thus, an increase in gas supplying pressure improves CO<sub>2</sub> dissolution in water and CO<sub>2</sub> removal rate.

However, in the apparatus linked with 1- WFFU and 2-WFFUs, the removal efficiency generally decreased as pressure was adjusted from 0.25 to 0.50 MPa but increased again when the pressure was then increased to 0.70 MPa. Meanwhile, the absorption rate increased approximately three-fold as pressure was increased from 0.25 to 0.70 MPa. This can be explained by the fact that 0.50 MPa is the critical pressure point in the apparatus equipped with WFFU (Nguyen *et al.*, 2017). Moreover, there is a decrease in removal rate at conditions of 0.50 MPa. Generally, with the aid of WFFU, a high removal rate can be achieved at low gas supplying pressures below 0.30 MPa.

Furthermore, **Fig. 5.4 (a)** shows that in the apparatuses equipped with 1- and 2-WFFUs, increasing the number of WFFUs reduces the influence of gas supplying pressure on removal efficiency. In the former (1-WFFU), specifically, the removal efficiencies of 75.7% at a gas supplying pressure of 0.25 MPa, 61.3 at 0.50 MPa, and 67.3% at 0.70 MPa proved that although a high removal efficiency can be obtained at low pressure, increasing the pressure is still important for improving CO<sub>2</sub> removal performance. Meanwhile, in apparatuses outfitted with 2-WFFUs, there is a slight fluctuation in removal efficiency under different pressure conditions. This is especially true when the gas supplying pressure is increased from 0.50 MPa

to 0.70 MPa, as the removal efficiency remains nearly unchanged at 83.6% and 84.6%, respectively. These results illustrate that with the addition of only one more WFFU to the chamber, the effect of gas supplying pressure on removal efficiency tends to decrease. They also suggest that as the number of WFFUs inside the absorption chamber increase, the differences between CO<sub>2</sub> removal performance at low or high pressure conditions might become smaller.

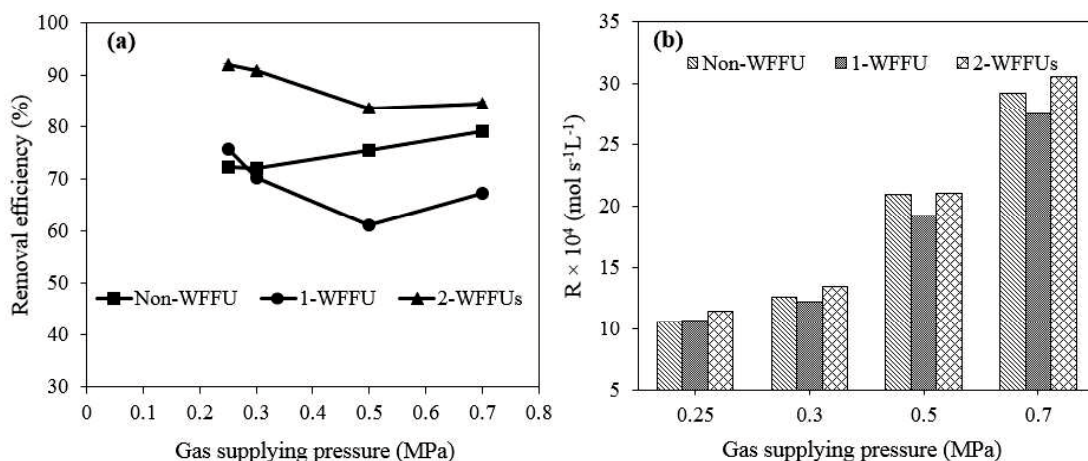


**Figure 5.4** Effect of gas supplying pressure on (a) CO<sub>2</sub> removal efficiency and (b) absorption rate. Operating conditions: G/L ratio = 1.07; total gas flow rate = 15 L min<sup>-1</sup>; water flow rate = 14 L min<sup>-1</sup>; feed gas composition = 25% CO<sub>2</sub> and 75% N<sub>2</sub>; and temperature = 15 °C.

Because a higher removal efficiency can be achieved at low gas supplying pressure (0.25 MPa), and it minimizes the effect of increasing pressure on removal efficiency, the application of several WFFUs to improve CO<sub>2</sub> capture from mixed gas can potentially solve the problem of the high pressure requirement (1.0–2.0 MPa) in conventional water absorption (packing absorption scrubber) (Andriani *et al.*, 2014, Läntelä *et al.*, 2012). Thus, CO<sub>2</sub> can be removed efficiently and cost-effectively.

### 5.3.3 Effect of CO<sub>2</sub> initial concentration

The influence of CO<sub>2</sub> initial concentration on CO<sub>2</sub> removal in the three types of absorption system was investigated by varying the CO<sub>2</sub> inlet concentration from 10% to 45%. The operational conditions involved a gas inlet pressure of 0.50 MPa, a total inlet gas flow rate of 15 L min<sup>-1</sup>, and a temperature of 15 °C. An increase in CO<sub>2</sub> concentration resulted in increased removal efficiency and absorption rate (**Figures 5.5(a) and (b)**). Specifically, in the non-WFFU

system, an increase of CO<sub>2</sub> intake concentration resulted in a CO<sub>2</sub> removal and absorption rate increase from 74.07% to 78.72% and from  $7.91 \times 10^{-4}$  to  $40.82 \times 10^{-4} \text{ mol s}^{-1}\text{L}^{-1}$ , respectively. For the 1-WFFU system, the removal and absorption rate experienced a dramatic increase of 60.89% to 69.93% and  $7.08 \times 10^{-4}$  to  $39.27 \times 10^{-4} \text{ mol s}^{-1}\text{L}^{-1}$ , respectively. In the 2-WFFUs absorption system, the removal efficiency increased slightly from 82.88% to 85.62%, while the absorption rate increased from  $8.00 \times 10^{-4}$  to  $41.01 \times 10^{-4} \text{ mol s}^{-1}\text{L}^{-1}$ .

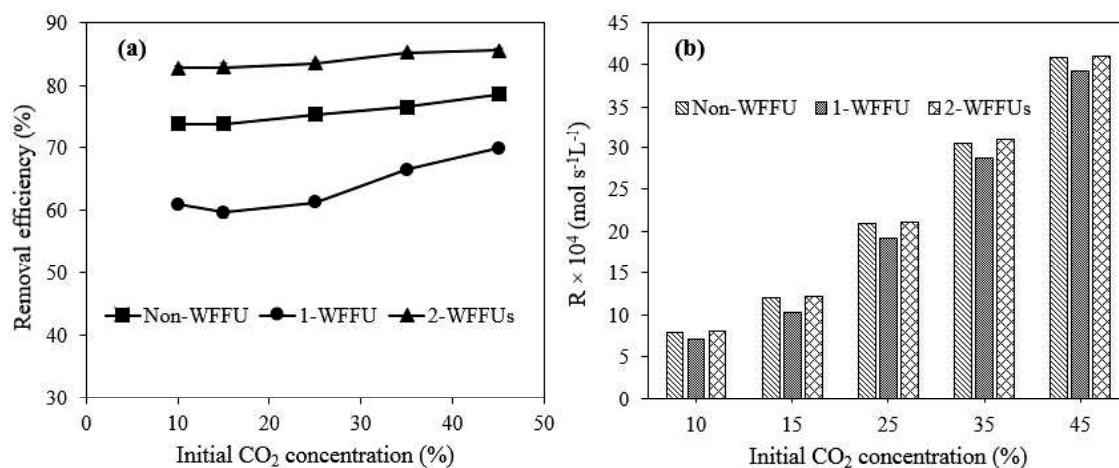


**Figure 5.5** Effect of CO<sub>2</sub> initial concentration on (a) CO<sub>2</sub> removal efficiency and (b) absorption rate. Operating conditions: gas supplying pressure = 0.50 MPa; G/L ratio = 1.07; total gas flow rate = 15 L min<sup>-1</sup>; water flow rate = 14 L min<sup>-1</sup>; and temperature = 15 °C.

Increasing the CO<sub>2</sub> initial concentration from 10% to 45% increases the number of CO<sub>2</sub> molecules per one unit of volume, as well as the CO<sub>2</sub> partial pressure, from 0.05 to 0.23 MPa. Gas partial pressure is the driving force of gas dissolution potential in the liquid phase. Therefore, with an increase of gas partial pressure and a reduction of mass transfer resistance of the gas phase, an increase of CO<sub>2</sub> concentration stimulates contact between the two phases (liquid and gas), as well as accelerating the dissolution rate of CO<sub>2</sub> in water (Zeng *et al.*, 2013). However, the effect of CO<sub>2</sub> initial concentration and CO<sub>2</sub> partial pressure on the removal process was smaller in the 2-WFFUs system. This phenomenon also occurred when investigating the effect of total gas supplying pressure on CO<sub>2</sub> removal performance (**section 5.3.2**). This indicates that both total inlet gas supplying pressure and gas partial pressure have a minor influence on the removal rate when using several WFFUs in the absorption system. Generally, because a WFFU can reduce the effect of pressure on gas capture during physical

absorption, the addition of WFFUs makes it possible to use water as the solvent and avoid the issue of pressure.

#### 5.3.4 Effect of gas-to-liquid ratio

The performance of the three water absorption systems with different gas-to-liquid (G/L) ratios is described in **Figures 5.6(a)** and **(b)**. The G/L ratio varied from 0.36 to 1.79 as the gas flow rate was adjusted from 5 to 25 L min<sup>-1</sup> and the water flow rate was controlled at 14 L min<sup>-1</sup> by flow meter controllers. Other factors including gas supplying pressure, temperature were kept constant at 0.30 MPa, and 15 °C, respectively. As mentioned above, the 2-WFFUs system clearly promotes CO<sub>2</sub> absorption in water because the CO<sub>2</sub> removal and absorption rates were substantially greater than in the other two systems. In the 2-WFFUs system, with a feed gas composition of 15% CO<sub>2</sub> and 85% N<sub>2</sub>, the removal efficiency reached a maximum of 95.78% at a G/L ratio of 0.71. Meanwhile, at the same G/L ratio, the removal efficiency of the 1-WFFU and non-WFFU systems also achieved maximum values of 67.59% and 81.6%, respectively. In contrast, maximum absorption rates:  $17.88 \times 10^{-4}$  mol s<sup>-1</sup>L<sup>-1</sup> for 2-WFFU,  $13.16 \times 10^{-4}$  mol s<sup>-1</sup>L<sup>-1</sup> for 1-WFFU, and  $16.99 \times 10^{-4}$  mol s<sup>-1</sup>L<sup>-1</sup> for non-WFFU, were achieved at a G/L ratio of 1.79.

Therefore, when the G/L ratio increases, the removal efficiency decreases but the absorption rate increases. The same trends are observed with a feed gas composition of 35% CO<sub>2</sub> and 65% N<sub>2</sub> (**Figure 5.6(b)**). Because the G/L ratio is controlled by maintaining a constant water flow rate of 14 L min<sup>-1</sup>, the increase of G/L ratio from 0.36 to 1.79 was equivalent to an increase of the gas flow rate from 5 to 25 L min<sup>-1</sup>. Thus, an increase in gas flow rate leads to a decrease in removal efficiency (Choi *et al.*, 2009). This may be because an increasing G/L ratio increases the load of CO<sub>2</sub> and reduces liquid turbulence inside the chamber (Xiao *et al.*, 2014). This leads to a smaller contact area and time between the gas and liquid phases, and prevents production of a water film (Chai & Zhao, 2012, Lin & Chu, 2015). However, the increase of G/L ratio with an increase of gas flow rate results in a larger amount of CO<sub>2</sub> entering 1 unit of water volume within 1 unit of time; thus, the amount of CO<sub>2</sub> absorbed by the water in 1 unit of time is higher. Moreover, a higher mass transfer coefficient is achieved with an increased gas flow rate (Zeng *et al.*, 2013). Therefore, the absorption rate increases with a higher G/L ratio or gas flow rate.



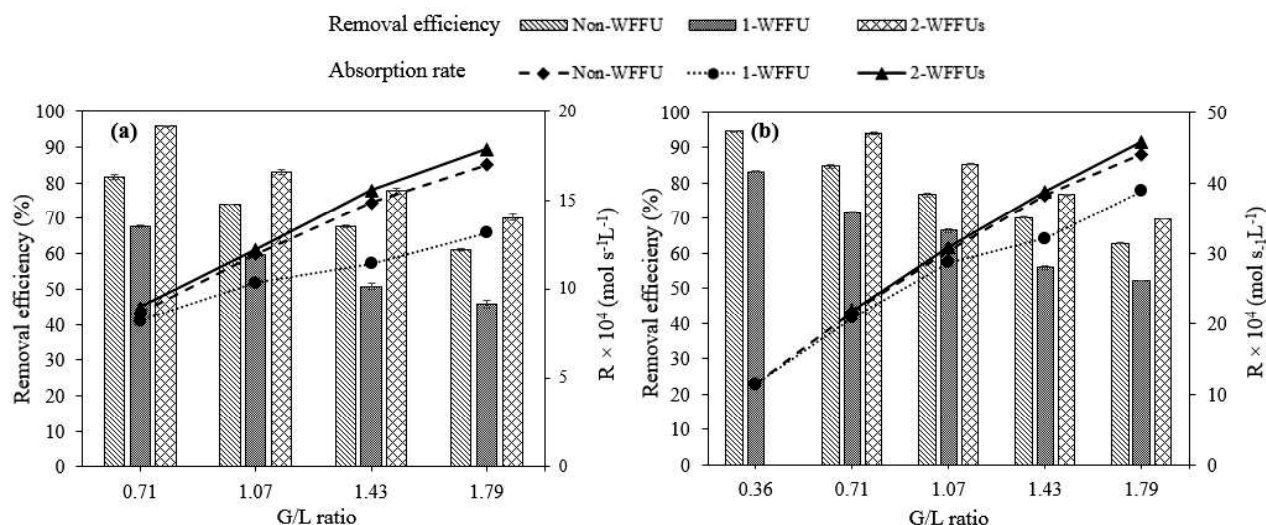


**Figure 5.6** Effect of G/L ratio on CO<sub>2</sub> removal efficiency and absorption rate with a feed gas composition of (a) 15% CO<sub>2</sub> and 85% N<sub>2</sub> and (b) 35% CO<sub>2</sub> and 65% N<sub>2</sub>. Operating conditions: gas supplying pressure = 0.50 MPa; water flow rate = 14 L min<sup>-1</sup>; and temperature = 15 °C.

### 5.3.5 Effect of temperature

When using tap water as the physical absorbent of CO<sub>2</sub> from mixed gas, the water temperature is an essential parameter. The role of temperature in CO<sub>2</sub> capture by WFFU-enhanced water absorption is shown in **Figure 5.7**. With an increase of temperature from 10 °C to 30 °C, the CO<sub>2</sub> removal percentage decreased remarkably from 82.31% to 45.93% (non-WFFU), 78.68% to 43.47% (1-WFFU), and 98.06% to 61.39% (2-WFFU). Correspondingly, the absorption rate decreased from  $7.53 \times 10^{-4}$  to  $6.32 \times 10^{-4}$  mol s<sup>-1</sup>L<sup>-1</sup>,  $7.36 \times 10^{-4}$  to  $6.05 \times 10^{-4}$  mol s<sup>-1</sup>L<sup>-1</sup>, and  $8.16 \times 10^{-4}$  to  $7.23 \times 10^{-4}$  mol s<sup>-1</sup>L<sup>-1</sup>, respectively.

Increasing temperature has a negative effect on CO<sub>2</sub> removal rate. In water-based physical absorption, separation of CO<sub>2</sub> from mixed gas is achieved by the difference in solubility between CO<sub>2</sub> and the other gases. The solubility of gas in the aqueous phase is a function of pressure and temperature (Carroll *et al.*, 1991, Murray & Riley, 1971). Heating the temperature of the solution promotes kinetic energy and causes more motion in the gas molecules trapped in the liquid phase. This finally breaks the bonds between the two phases and releases the gas into the environment. Hence, when temperature increases, the solubility of CO<sub>2</sub> decreases, resulting in a reduction of CO<sub>2</sub> removal efficiency, as described in **Figure 5.7**.

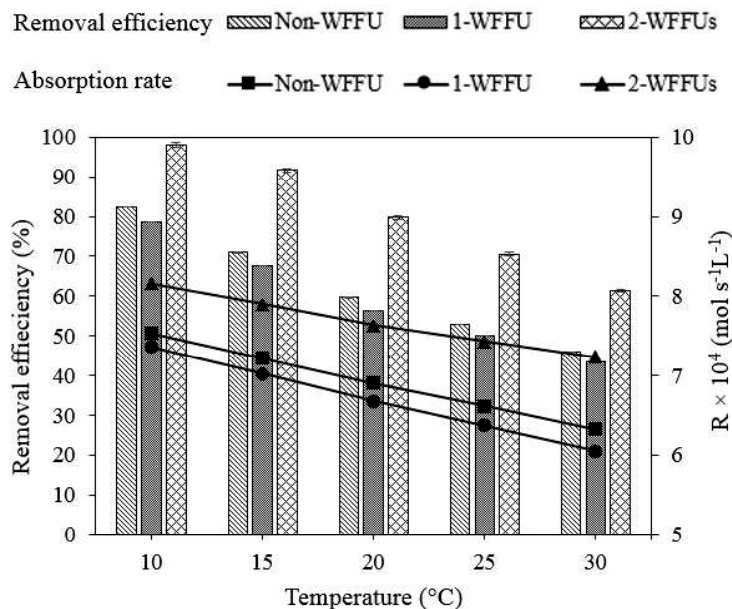


**Figure 5.7** Effect of liquid temperature on CO<sub>2</sub> removal efficiency and absorption rate. Operating conditions: gas supplying pressure = 0.30 MPa; G/L ratio = 1.07; total gas flow rate = 15 L min<sup>-1</sup>; water flow rate = 14 L min<sup>-1</sup>; and feed gas composition = 15% CO<sub>2</sub> and 85% N<sub>2</sub>.

### 5.3.6 Taguchi method results

Due to our aim of obtaining a high removal efficiency and absorption rate, the S/N ratio was transformed by the concept “Larger is better” (Eq 5.4). The higher the S/N ratio, the higher the impact of this level on the responses (i.e. removal efficiency and absorption rate). This means that, for each factor, the level with the maximum S/N ratio had the greatest effect on the responses. The S/N ratios for each level of the five parameters are shown in **Figure 5.8** and **Table 5.3**. For each parameter, the value of delta is the difference between the maximum (high effect) and minimum (low effect) S/N ratio. Furthermore, based on the analysis of variance (ANOVA), the contribution percentage (%) of all parameters to the removal efficiency and absorption rate were computed and presented in **Figure 5.9**. According to these results, it is possible to rank and evaluate the effect of each factor on the removal and absorption rates.

The Taguchi method results indicate that the number of WFFUs outfitted in the absorption apparatus was the most significant factor influencing the removal rate, with a contribution percentage of 50.65% and a delta value of 2.37. The second and third most significant factors were temperature and G/L ratio, with contribution percentages and delta values of 21.50% and 18.02%, and 1.89 and 1.71, respectively. The other factors consisting of gas supplying pressure

(delta = 0.97) and CO<sub>2</sub> initial concentration (delta = 0.51) had a minor effect on the removal rate, with a combined contribution percentage of only 7.27%. Accordingly, the highest removal efficiency of nearly 98% occurred in the 2-WFFUs system, at a temperature of 15 °C, a G/L ratio of 0.71, a CO<sub>2</sub> initial concentration of 35%, and a gas supplying pressure of 0.30 MPa (see **Table 5.4**).

In terms of absorption rate, the influence of each factors was ranked from largest to smallest as follows: CO<sub>2</sub> initial concentration, gas supplying pressure, G/L ratio, number of WFFUs, and temperature, with delta values of 7.96, 7.11, 4.32, 0.92, and 0.44, respectively. Among these factors, CO<sub>2</sub> initial concentration and gas supplying pressure showed a significant influence on absorption rate, with contribution proportions of 47.35% and 37.45%, respectively. Together, these two factors contributed 84.80% to the absorption rate. Meanwhile, 14.98% of the response came from the G/L ratio, the number of WFFUs, and temperature, which implies that these factors were insignificant. Based on the Taguchi statistical analysis, at optimum conditions of a CO<sub>2</sub> initial concentration of 35%, a gas supplying pressure of 0.70 MPa, a G/L ratio of 1.43, and a temperature of 15 °C, the absorption rate reached a maximum of  $55.05 \times 10^{-4} \text{ mol s}^{-1}\text{L}^{-1}$  with the aid of 2-WFFUs enhancing the absorption process (see **Table 5.4**).

**Table 5.3** S/N response table for CO<sub>2</sub> removal efficiency and absorption rate

S/N ratios – Removal efficiency						
Factors	Number of WFFUs	Gas supplying pressure	CO <sub>2</sub> initial concentration	G/L ratio	Temperature	
Level 1	35.28	36.93	36.23	37.40	37.44	
Level 2	37.65	35.96	36.43	36.31	36.39	
Level 3		36.51	36.74	35.69	35.56	
Delta	2.37	0.97	0.51	1.71	1.89	
Rank	1	4	5	3	2	
S/N ratios – Absorption rate						
Factors	Number of WFFUs	Gas supplying pressure	CO <sub>2</sub> initial concentration	G/L ratio	Temperature	
Level 1	24.19	21.00	20.43	22.39	24.86	
Level 2	25.11	24.86	25.14	24.86	24.68	
Level 3		28.10	28.38	26.71	24.42	
Delta	0.92	7.11	7.96	4.32	0.44	
Rank	4	2	1	3	5	

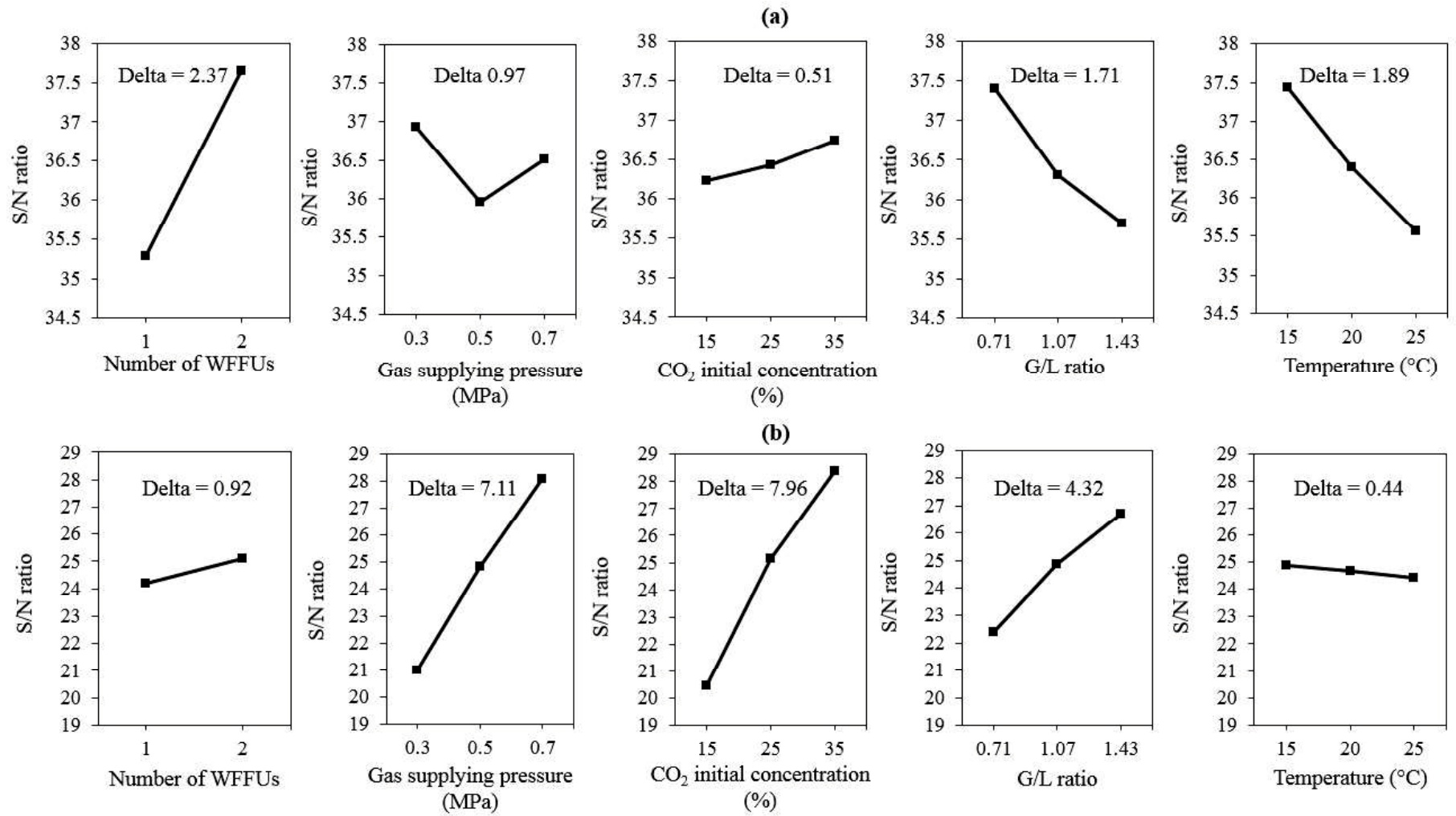


**Figure 5.8** S/N ratios and delta values for each factor influencing the (a) removal efficiency and (b) absorption rate.

■ Number of WFFUs   ▨ GSP   ■ CO<sub>2</sub> initial concentration   ▩ G/L ratio   ▤ Temperature   ▦ Error

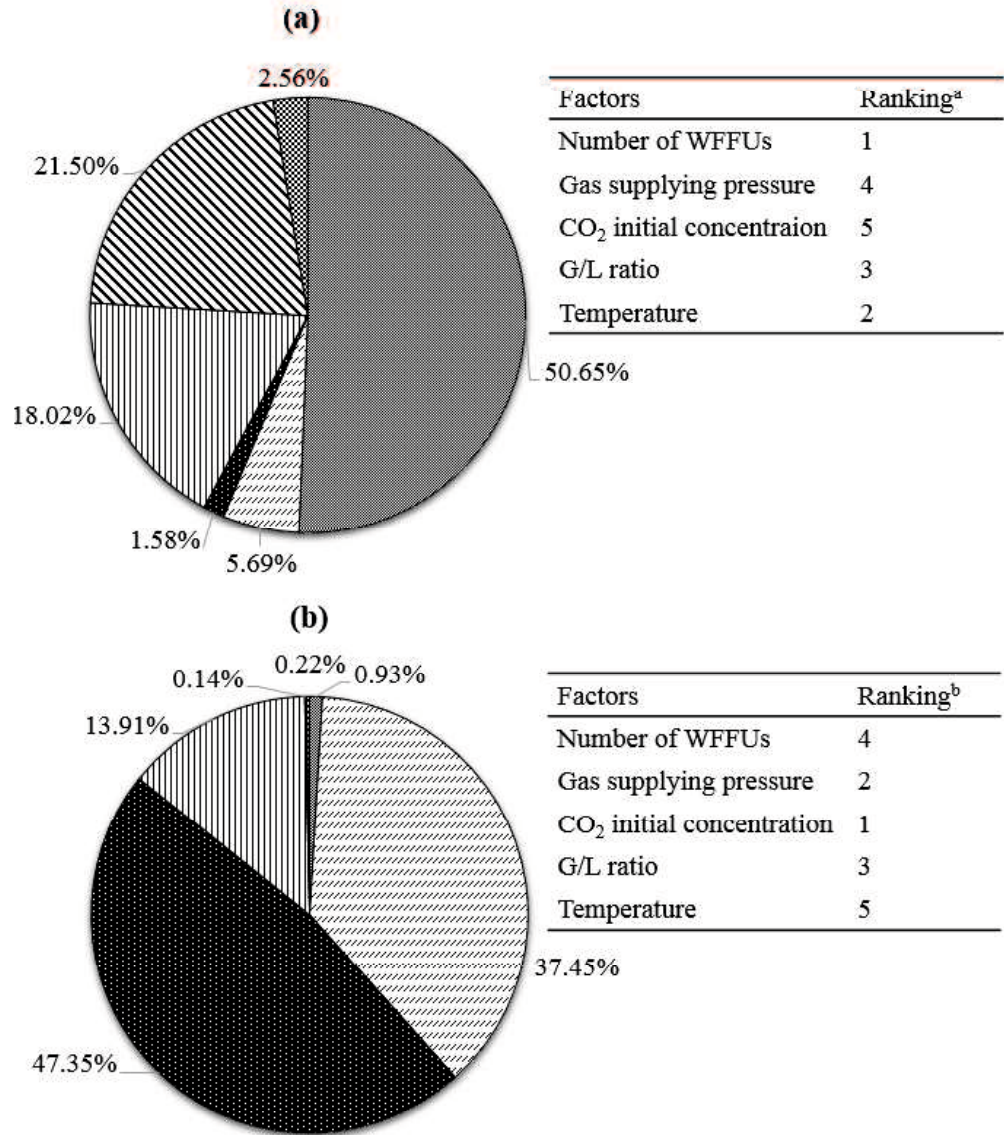


**Figure 5.9** Contribution percentages and ranking of five controlling factors on the (a) removal efficiency and (b) absorption rate of CO<sub>2</sub>.

**Table 5.4** Experimental verification under the optimum conditions

Run	Number of WFFUs	Gas supplying pressure (MPa)	CO <sub>2</sub> initial concentration (%)	G/L ratio	Temperature (°C)	<i>E</i> (%)	RSD <sup>a</sup> (%)	$R \times 10^4$ (mol s <sup>-1</sup> L <sup>-1</sup> )	RSD <sup>a</sup> (%)
Op. 1 <sup>b</sup>	1	2	0.30	35	0.71	15	97.3	13.44	
	2	2	0.30	35	0.71	15	97.5	13.46	0.2
	3	2	0.30	35	0.71	15	97.0	13.40	
Op. 2 <sup>b</sup>	1	2	0.70	35	1.43	15	76.5	55.06	
	2	2	0.70	35	1.43	15	76.5	55.03	0.1
	3	2	0.70	35	1.43	15	76.6	55.06	

Note:

<sup>a</sup> Relative standard deviation

<sup>b</sup> Op. 1, Op. 2: Optimum conditions for efficiency rate *E* (%) and absorption rate *R* (mol s<sup>-1</sup>L<sup>-1</sup>), respectively.

## 5.4 Conclusions

This study successfully investigated the influence of five factors on CO<sub>2</sub> capture from mixed gas in a water-based physical absorption system using water-film-forming-units. The results indicate that the number of WFFUs used in the absorption apparatus is the most important factor for improving CO<sub>2</sub> removal efficiency, with a contribution of over 50% to CO<sub>2</sub> removal performance. An increase in the number of WFFUs leads to a dramatic increase in the removal rate, indicating that WFFUs have a strong effect on promoting CO<sub>2</sub> solubility in the water phase. Solution temperature and G/L ratio have a significant influence on the removal rate, with contribution percentages of 21.50% and 18.02%, respectively. Furthermore, gas supplying pressure and CO<sub>2</sub> initial concentration show a minimal effect on the removal rate, with contribution percentages of 5.69% and 1.58%, respectively. It can be concluded that the effect of gas supplying pressure and partial pressure is minor. Therefore, the need to increase pressure in order to achieve a high gas dissolution rate becomes unimportant if a WFFU is used in the water scrubber. The use of WFFUs has advantages over conventional water scrubbers because high mass transfer and dissolution rates can be accomplished at low gas supplying pressures of 0.25 or 0.30 MPa. Generally, an apparatus with 2-WFFUs can achieve a maximum removal rate of 98% at the following optimum conditions: temperature = 15 °C, G/L ratio = 0.71, inlet CO<sub>2</sub> concentration = 35%, and gas supplying pressure = 0.30 MPa. A maximum absorption rate of  $55.05 \times 10^{-4} \text{ mol s}^{-1}\text{L}^{-1}$  can be achieved in an apparatus with two WFFUs at the same optimum inlet CO<sub>2</sub> concentration and temperature conditions, and at a G/L ratio of 1.43 and a gas supplying pressure of 0.70 MPa.

## 5.5 References

- Alonso, A., Moral-Vico, J., Markeb, A. A., Busquets-Fité, M., Komilis, D., Puentes, V., Sánchez, A. & Font, X. 2017. Critical review of existing nanomaterial adsorbents to capture carbon dioxide and methane. *Science of The Total Environment*, **595**, 51-62.
- Andriani, D., Wresta, A., Atmaja, T. D. & Saepudin, A. 2014. A review on optimization production and upgrading biogas through CO<sub>2</sub> removal using various techniques. *Applied biochemistry and biotechnology*, **172** (4), 1909-1928.

- Asiltürk, I. & Akkuş, H. 2011. Determining the effect of cutting parameters on surface roughness in hard turning using the Taguchi method. *Measurement*, **44** (9), 1697-1704.
- Carroll, J. J., Slupsky, J. D. & Mather, A. E. 1991. The solubility of carbon dioxide in water at low pressure. *Journal of Physical and Chemical Reference Data*, **20** (6), 1201-1209.
- Chai, X. & Zhao, X. 2012. Enhanced removal of carbon dioxide and alleviation of dissolved oxygen accumulation in photobioreactor with bubble tank. *Bioresource technology*, **116**, 360-365.
- Chen, P.-C. 2012. Absorption of carbon dioxide in a bubble-column scrubber, INTECH Open Access Publisher.
- Choi, W.-J., Seo, J.-B., Jang, S.-Y., Jung, J.-H. & Oh, K.-J. 2009. Removal characteristics of CO<sub>2</sub> using aqueous MEA/AMP solutions in the absorption and regeneration process. *Journal of Environmental Sciences*, **21** (7), 907-913.
- Cozma, P., Ghinea, C., Mămăligă, I., Wukovits, W., Friedl, A. & Gavrilescu, M. 2013. Environmental impact assessment of high pressure water scrubbing biogas upgrading technology. *CLEAN–Soil, Air, Water*, **41** (9), 917-927.
- Datta, S., Bandyopadhyay, A. & Pal, P. K. 2008. Grey-based Taguchi method for optimization of bead geometry in submerged arc bead-on-plate welding. *The International Journal of Advanced Manufacturing Technology*, **39** (11), 1136-1143.
- Imai, T. & Zhu, H. 2011. Improvement of oxygen transfer efficiency in diffused aeration systems using liquid-film-forming apparatus, INTECH Open Access Publisher.
- Läntelä, J., Rasi, S., Lehtinen, J. & Rintala, J. 2012. Landfill gas upgrading with pilot-scale water scrubber: performance assessment with absorption water recycling. *Applied energy*, **92**, 307-314.
- Leung, D. Y., Caramanna, G. & Maroto-Valer, M. M. 2014. An overview of current status of carbon dioxide capture and storage technologies. *Renewable and Sustainable Energy Reviews*, **39**, 426-443.
- Lin, C.-C. & Chu, C.-R. 2015. Feasibility of carbon dioxide absorption by NaOH solution in a rotating packed bed with blade packings. *International Journal of Greenhouse Gas Control*, **42**, 117-123.
- Murray, C. & Riley, J. 1971. The solubility of gases in distilled water and sea water—IV. Carbon dioxide. *Deep Sea Research and Oceanographic Abstracts*, **18** (5), 533-541.



- Nguyen, M. K. D., Imai, T., Yoshida, W., Dang, L. T. T., Higuchi, T., Kanno, A., Yamamoto, K. & Sekine, M. 2017. Performance of a carbon dioxide removal process using a water scrubber with the aid of a water-film-forming apparatus. *Waste and Biomass Valorization*, 1-13.
- Olajire, A. A. 2010. CO<sub>2</sub> capture and separation technologies for end-of-pipe applications – A review. *Energy*, **35** (6), 2610-2628.
- Olivier, J. G. J., Janssens-Maenhout, G., Muntean, M. & Peters, J. A. H. W. 2016. Trends in Global CO<sub>2</sub> Emissions: 2016 Report, PBL Netherlands Environmental Assessment Agency, <http://www.pbl.nl/en>.
- Parmar, R. & Majumder, S. K. 2013. Microbubble generation and microbubble-aided transport process intensification—A state-of-the-art report. *Chemical Engineering and Processing: Process Intensification*, **64**, 79-97.
- Taguchi, G. 1986. Introduction to quality engineering: designing quality into products and processes, Asian Productivity Organization. Tokyo.
- Xiao, Y., Yuan, H., Pang, Y., Chen, S., Zhu, B., Zou, D., Ma, J., Yu, L. & Li, X. 2014. CO<sub>2</sub> removal from biogas by water washing system. *Chinese Journal of Chemical Engineering*, **22** (8), 950-953.
- Zeng, Q., Guo, Y., Niu, Z. & Lin, W. 2013. The absorption rate of CO<sub>2</sub> by aqueous ammonia in a packed column. *Fuel processing technology*, **108**, 76-81.
- Zhu, H., Tsuyoshi, I., Tani, K., Ukita, M., Sekine, M., Higuchi, T. & Zhang, Z. 2007. Development of high efficient oxygen supply method by using contacting water-liquid film with air. *Journal of Water and Environment Technology*, **5** (2), 57-69.

## CHAPTER 6

### CONCLUSIONS AND FUTURE WORKS

#### 6.1 Conclusions

The utilization and effects of water-film-forming-unit (WFFU) in improving the capture of CO<sub>2</sub> from the mixed gas (CO<sub>2</sub> and N<sub>2</sub>) using water absorption is investigated completely and successfully in this research. The main findings are presented into three main categories in accordance with **chapter 3** to **chapter 5** as follows:

##### 6.1.1 Performance of CO<sub>2</sub> removal process using a water scrubber enhanced with a WFFU

The effects of five factors including internal pressure, gas supplying pressure, G/L ratio, initial CO<sub>2</sub> concentration and temperature on CO<sub>2</sub> removal and absorption rate were demonstrated fully and clearly. According to the experimental results, the optimum conditions comprise a high internal pressure in the chamber, 0.30 MPa of compressed gas supplying pressure, high inlet gas CO<sub>2</sub> concentration, and low temperature.

The increase of internal pressure (pressure inside absorption tank) from 0.06 MPa to 0.10 MPa leads to an increase of CO<sub>2</sub> removal rate by 3.0% as well as a sharp increase of CO<sub>2</sub> absorption rate.

Gas supplying pressure has a proportional influence on CO<sub>2</sub> absorption rate. However, the CO<sub>2</sub> removal efficiency firstly decreases since gas supplying pressure increases from 0.30 to 0.50 MPa and after that increases since gas supplying pressure increases from 0.50 to 0.70 MPa. It is hypothesized that in the surveying pressure range of 0.30 to 0.70 MPa, the effect of gas supplying pressure is minor and the fluctuation of removal efficiency with pressure is small. Therefore, good removal performance can happen at both condition of low and high pressure. For the aspect of economic, the operation of removal process at low pressure (0.30 MPa) is a better option with the manner of energy and cost-saving.

G/L ratio is an important factor of the CO<sub>2</sub> removal process. When the G/L ratio also reduced from 1.79 to 0.36 in accordance with gas flow rate decreasing from 25 to 5 L min<sup>-1</sup>, the removal rate surges dramatically while the absorption rate decreases.

The increasing of CO<sub>2</sub> inlet concentration is the reason for a growth of CO<sub>2</sub> partial pressure which is the driving force for gas dissolution in liquid phase. Therefore, this results in an increase of removal and absorption rate.

Temperature is an essential controlling factor when using water absorption. The removal efficiency and absorption rate experience a downward trend with an increase in temperature.

### **6.1.2 Response surface method (RSM) with central composite design (CCD) for modeling the removal of carbon dioxide using water absorption enhanced with a WWFU**

The RSM-CCD – statistical experimental design – successfully constructs models to identify the effects of various independent variables including gas supplying pressure, initial CO<sub>2</sub> concentration, G/L ratio, and temperature on the CO<sub>2</sub> removal efficiency and absorption rate.

The *p*-value of the regression model in both of the responses (removal efficiency and absorption rate) equaled to 0.000, representing that the models were significant. The high determination coefficients ( $R^2$ ) of 0.996 and 0.982, together with adjusted determination coefficients (adj  $R^2$ ) of 0.993 and 0.966, for the responses of removal efficiency and absorption rate, respectively, indicate that there are a good agreement and strong correlation between the experimental and predicted values of the responses in both models.

In order to verify the reliability of our results and to determine the validity of our statistical models and regression equations, 5 additional experiments were conducted under different experimental conditions. The % error between predicted and observed values fluctuated in the range of 0.46% and 3.69% for the removal efficiency and 3.59% and 8.28% for the absorption rate. The results prove that the statistical models obtained from this study are both accurate and reliable.

The combination of these results confirms that with statistical models and second-order polynomial equations, the CO<sub>2</sub> removal efficiency and absorption rate could be calculated precisely without conducting experiments. Hence, it is possible to determine the appropriate or optimum conditions for controlling the absorption process to meet the standard requirements of CO<sub>2</sub> removal and absorption rate in a cost-effective and timely manner. This approach provides the means to employ this water absorption system in real-time.

### **6.1.3 Influence of WFFU on the enhanced removal of carbon dioxide from mixed gas using water absorption apparatus**

With three cases of apparatus which equipped non-, 1-, and 2-WFFUs, under various conditions of gas supplying pressure of 0.30 MPa, G/L ratio (0.71 – 1.43), initial CO<sub>2</sub> concentration (10% – 35%) and temperature (10 °C – 30 °C), the CO<sub>2</sub> removal efficiency fluctuates from 42.6% to 92.0% (non-WFFU), from 39.4% to 88.7% (1-WFFU) and from 55% to 99.1% (2-WFFUs) while the CO<sub>2</sub> absorption rate were in range from  $5.03 \times 10^{-4}$  to  $23.37 \times 10^{-4}$  mol s<sup>-1</sup>L<sup>-1</sup> (non-WFFU), from  $4.97 \times 10^{-4}$  to  $22.57 \times 10^{-4}$  mol s<sup>-1</sup>L<sup>-1</sup> (1-WFFU), and from  $5.29 \times 10^{-4}$  to  $24.60 \times 10^{-4}$  mol s<sup>-1</sup>L<sup>-1</sup> (2-WFFUs).

The utilization of WFFUs revealed an improvement in the CO<sub>2</sub> capture ability; the CO<sub>2</sub> removal efficiency for 2-WFFUs was approximately 20% higher than that for non-WFFU and 25% higher than that for 1-WFFU. With 2-WFFUs inside the chamber, the removal efficiency of CO<sub>2</sub> is greatly increased at a low gas supplying pressure of 0.30 MPa.

The analysis results by statistical tool “Taguchi method” indicate that the number of WFFUs used in the absorption apparatus is the most important factor for improving CO<sub>2</sub> removal efficiency in the comparing with other factors containing variables including gas supplying pressure, initial CO<sub>2</sub> concentration, G/L ratio, and temperature, with a contribution of over 50% to CO<sub>2</sub> removal performance. Meanwhile, temperature and G/L ratio contribute 21.50% and 18.02%, respectively on the removal rate. Furthermore, gas supplying pressure and CO<sub>2</sub> initial concentration show a minor effect on the removal rate, with contribution percentages of 5.69% and 1.58%, respectively. The conclusion is that the effect of pressure and partial pressure is minor. Therefore, the need to increase pressure in order to achieve a high gas dissolution rate becomes unimportant if a WFFU is used in the water scrubber. The use of WFFUs has advantages over conventional water scrubbers because high mass transfer and dissolution rates can be accomplished at low gas supplying pressures of 0.25 or 0.30 MPa.

Generally, an apparatus with 2-WFFUs can achieve a maximum removal rate of 98% at the following optimum conditions: temperature = 15 °C, G/L ratio = 0.71, inlet CO<sub>2</sub> concentration = 35%, and gas supplying pressure = 0.30 MPa. A maximum absorption rate of  $55.05 \times 10^{-4}$  mol s<sup>-1</sup>L<sup>-1</sup> can be achieved in an apparatus with two WFFUs at the same optimum inlet CO<sub>2</sub>

concentration and temperature conditions, and at a G/L ratio of 1.43 and a gas supplying pressure of 0.70 MPa.

## **6.2 Future works**

It needs to develop the method to measure the bubble sizes, mass transfer coefficients and gas hold-up when conducting experiments in order to comprehensively assess the absorption process and fully understanding the effects of key factors on the CO<sub>2</sub> removal process.

Further research for the application of this advanced water absorption method in real-time with industrial exhausted gas is required. In order to take part in the reduction of CO<sub>2</sub> effect on the environment, it is necessary to practice this method as a part of the system “Carbon dioxide capture and storage” and extensively develop the combination with CO<sub>2</sub> utilization such as disinfection or microalga cultivation.

The next step of this research can focus on the utilization of the alternative cheap water such as sea water and sewage water as the solvent for the absorption process.

## LIST OF PUBLICATIONS AND PRESENTATIONS

### LIST OF PUBLICATIONS

1. **Diem-Mai Kim Nguyen**, Tsuyoshi Imai, Thanh-Loc Thi Dang, Takaya Higuchi, Ariyo Kanno, Koichi Yamamoto, and Masahiko Sekine (2018). Response surface method for modeling the removal of carbon dioxide from a simulated gas using water absorption enhanced with a liquid-film-forming device. *Journal of Environmental Sciences*. Vol. 65, 116 – 126. [DOI: 10.1016/j.jes.2017.03.026](https://doi.org/10.1016/j.jes.2017.03.026)
2. **Mai Kim Diem Nguyen**, Tsuyoshi Imai, Wataru Yoshida, Loc Thi Thanh Dang, Takaya Higuchi, Ariyo Kanno, Koichi Yamamoto, and Masahiko Sekine (2017). Performance of a carbon dioxide removal process using a water scrubber with the aid of a water-film-forming apparatus. *Waste and Biomass Valorization*, 1 – 13 (In Press). [DOI: 10.1007/s12649-017-9951-8](https://doi.org/10.1007/s12649-017-9951-8)
3. **Nguyen, D.-M. K.**, Imai, T., Aly, S. S., Higuchi, T., Kanno, A., Yamamoto, K. and Sekine, M (2018). Influence of water-film-forming-unit on the enhanced removal of carbon dioxide from mixed gas using water absorption apparatus. *Environmental Technology*, 1-29 (In Press). [DOI: 10.1080/09593330.2018.1512655](https://doi.org/10.1080/09593330.2018.1512655)
4. Shahira Said Aly, Tsuyoshi Imai, Mohamed Salah Hassouna, **Diem-Mai Kim Nguyen**, Takaya Higuchi, Ariyo Kanno, Koichi Yamamoto, Rinji Akada, and Masahiko Sekine (2018). Identification of factors that accelerate hydrogen production by *Clostridium butyricum* RAK25832 using casamino acids as a nitrogen source. *International Journal of Hydrogen Energy*. Vol. 43 (10), 5300 – 5313. [DOI: 10.1016/j.ijhydene.2017.08.171](https://doi.org/10.1016/j.ijhydene.2017.08.171)
5. Thanh-Loc Thi Dang, Tsuyoshi Imai, Tuan Van Le, **Diem-Mai Kim Nguyen**, Takaya Higuchi, Ariyo Kanno, Koichi Yamamoto, and Masahiko Sekine (2016). Synergistic effect of pressurized carbon dioxide and sodium hypochlorite on the inactivation of *Enterococcus* sp. in seawater. *Water research*. Vol. 106, 204 – 213. [DOI: 10.1016/j.watres.2016.10.003](https://doi.org/10.1016/j.watres.2016.10.003)
6. Loc T. T. Dang, Tsuyoshi Imai, Tuan V. Le, Satoshi Nishihara, Takaya Higuchi, **Mai K. D. Nguyen**, Ariyo Kanno, Koichi Yamamoto, and Masahiko Sekine (2016). Effects of pressure and pressure cycling on disinfection of *Enterococcus* sp. in seawater using

- pressurized carbon dioxide with different content rates. *Journal of Environmental Science and Health, Part A*. Vol. 51 (11), 930 – 937. DOI: [10.1080/10934529.2016.1191309](https://doi.org/10.1080/10934529.2016.1191309)
7. Hong Anh Duong, Minh Duc Le, **Kim Diem Mai Nguyen**, Peter C. Hauser, Hung Viet Pham, and Thanh Duc Mai (2015). In-house-made capillary electrophoresis instruments coupled with contactless conductivity detection as a simple and inexpensive solution for water analysis: a case study in Vietnam. *Environmental Science: Processes & Impacts*, Vol. 17 (11), 1941 – 1951. DOI: [10.1039/C5EM00362H](https://doi.org/10.1039/C5EM00362H)
  8. Duong Hong Anh and **Nguyen Kim Diem Mai** (2015). Study on the effects of some major ions to the analyzing of as (III) in groundwater by means of capillary electrophoresis using contactless conductivity detector with electrokinetic injection and the solutions. *Journal of Analytical Sciences – Vietnam Analytical Sciences Society* (ISSN: 0868-3224). Vol. 20 (2), 14 – 19. (In Vietnamese).

#### LIST OF PRESENTATIONS

1. **Mai Kim Diem Nguyen**, Tsuyoshi Imai, Takaya Higuchi, Ariyo Kanno, Koichi Yamamoto, and Masahiko Sekine. Application of Taguchi method in the investigation of the carbon dioxide removal process using water absorption innovated with the water-film-forming-unit. Water and Environmental Technology Conference 2017, Sapporo, Hokkaido, Japan. July 22<sup>nd</sup> – 23<sup>rd</sup>, 2017. (Oral and poster presentation)
2. **Mai Kim Diem Nguyen**, Tsuyoshi Imai, Wataru Yoshida, Takaya Higuchi, Ariyo Kanno, Koichi Yamamoto, and Masahiko Sekine. Removal of carbon dioxide from the mixed gas by using water absorption process advanced with the forming of fine bubbles. Water and Environmental Technology Conference 2016, Tokyo, Japan. August 27<sup>th</sup> – 28<sup>th</sup>, 2016. (Oral and poster presentation)
3. Thanh-Loc Thi Dang, Tsuyoshi Imai, Satoshi Nishihara, **Kim Diem Mai Nguyen**, Takaya Higuchi, Ariyo Kanno, Koichi Yamamoto, and Masahiko Sekine. Effect of pressure cycling on inactivation of *Enterococcus* sp. And *Escherichia coli* in seawater using pressurized carbon dioxide. Water and Environmental Technology Conference 2016, Tokyo, Japan. August 27<sup>th</sup> – 28<sup>th</sup>, 2016. (Co-author)

4. **Mai Kim Diem Nguyen**, Tsuyoshi Imai, Wataru Yoshida, and Loc Thi Thanh Dang. Carbon dioxide removal from the mixed gas by using water scrubbing enhanced with the microbubbles combined with normal bubbles generator. Poster presentation at Yamaguchi University, Yamaguchi, Japan. December 25<sup>th</sup>, 2015. (Poster presentation)
5. **Mai Kim Diem Nguyen**, Tsuyoshi Imai, Wataru Yoshida, Loc Thi Thanh Dang, Takaya Higuchi, Ariyo Kanno, Koichi Yamamoto, and Masahiko Sekine. Removal of carbon dioxide from the mixed gas by using water absorption in the apparatus outfitted with the liquid-film-forming device. Poster presentation at Yamaguchi University, Yamaguchi, Japan. December 22<sup>nd</sup>, 2016. (Poster presentation)